

Line strengths of early-type galaxies.¹

Ricardo L.C. Ogando,^{2,3} Marcio A.G. Maia,² Paulo S. Pellegrini,² and Luiz N. da Costa²

ABSTRACT

In this paper we present measurements of velocity dispersions and Lick indices for 509 galaxies in the local Universe, based on high signal-to-noise, long slit spectra obtained with the 1.52 m ESO telescope at La Silla. The conversion of our measurements into the Lick/IDS system was carried out following the general prescription of Worthey & Ottaviani (1997). Comparisons of our measurements with those of other authors show, in general, good agreement. We also examine the dependence between these indices (e.g., H β , Mg₂, Fe5270 and NaD) and the central velocity dispersion (σ_0), and we find that they are consistent with those previously reported in the literature. Benefiting from the relatively large size of the sample, we are able to investigate the dependence of these relations on morphology and environment, here represented by the local galaxy density. We find that for metallic lines these relations show no significant dependence on environment or morphology, except in the case of NaD, which shows distinct behavior for E and S0. On the other hand, the H β -log σ_0 shows a significant difference as a function of the local density of galaxies, which we interpret as being caused by the truncation of star formation in high density environments. Comparing our results with those obtained by other authors we find a few discrepancies, adding to the ongoing debate about the nature of these relations. Finally, we report that the scatter of the Mg indices versus σ_0 relations correlate with H β , suggesting that age may contribute to the scatter. Furthermore, this scatter shows no significant dependence on morphology or environment. Our results are consistent with the currently downsizing model, where low mass galaxies have an extended star formation history, except for those located in high density regions.

Subject headings: galaxies: formation — galaxies: elliptical and lenticular — galaxies: stellar content

¹Partly based on observations at European Southern Observatory (ESO) at the 1.52m telescope under the ESO-ON agreement.

²Observatório Nacional (ON/MCT), Rua General José Cristiano, 77, Rio de Janeiro 20921-400 - RJ, Brazil; maia@on.br, pssp@on.br, ldacosta@on.br

³Instituto de Física, Universidade Federal do Rio de Janeiro, (RJ), Brazil; ogando@if.ufrj.br

1. Introduction

Efforts to understand how early-type galaxies formed and evolved have shown the importance of determining a group of fundamental parameters and investigate their relations. For instance, the study of their central velocity dispersions (σ_0), luminosities (L) and characteristic sizes like the effective radius (r_e), which reflect the influence of both dark and baryonic matter, provided in the last decades a deeper understanding of the structural and kinematic properties of this class of galaxies. Moreover, relations among these parameters such as those referred as the Faber-Jackson (Faber & Jackson 1976) and the Fundamental Plane (Djorgovski & Davis 1987; Dressler et al. 1987) proved to be important tools to study galaxy formation and evolution. In addition, their chemical enrichment can be addressed by means of colors or absorption line features of key elements such as Mg, Fe and H Balmer lines. These can be compared to predictions of theoretical evolutionary single stellar population (SSP) models (e.g., Worthey 1994; Thomas et al. 2003), which summarize galaxies stellar content properties, such as age and metallicity, along with distinct elements abundance ratios. In practice, line strengths have some advantages over colors because they are less affected by dust effects and are useful in breaking the so called age-metallicity degeneracy, which prevents us from delivering a straight interpretation of galaxy light.

A particularly good example of the insight provided by line strengths analysis, as well as the difficulties involved, can be seen from the analysis of the well known $Mg_2 - \sigma_0$ relation (e.g., Gorgas et al. 1990; Bender, Burstein & Faber 1993; Bernardi et al. 1998). This is usually interpreted as a mass-metallicity relation, since more massive galaxies are, in principle, able to keep larger amounts of enriched gas blown out in supernovae events, thus increasing the metallicity of the material from which new stellar generations are formed. By the same token, this class of objects should have an extended history of star formation, as predicted by both traditional scenarios of galaxy formation: the monolithic dissipative collapse (Larson 1974) and the hierarchical clustering (Kauffmann et al. 1993), implying that the mass-metallicity relation should also be subject to age. Indeed, while this is, to some extent, true for early-type galaxies in general (Trager et al. 2000a), in the case of massive objects, observational evidences conflict with predictions, because they are essentially old (Kuntschner 2000) and had a short star formation time scale, as indicated by the super-solar α/Fe ratio (Worthey et al. 1992; Thomas et al. 2005). On the other hand, low mass objects have an extended star formation history, which is currently known as downsizing (Cowie et al. 1996), or yet anti-hierarchical, since in the hierarchical clustering scenario they should be the first galaxies to appear and therefore be the oldest. Part of the answer to that inconsistency might be related to the details of the baryonic matter interactions, in the form of dissipation and galactic winds, driven by supernovae or active galactic nuclei (e.g., Pipino & Matteucci 2004; De Lucia et al. 2006).

While the $Mg_2 - \sigma_0$ relation has proven to be extremely useful, the measurement of other line indices can provide additional information such as age, formation time-scale, and abundance, that may help discriminate among competing models of galaxy formation. The main goal of the present paper is to provide measurements for 10 Lick indices for a representative sample of nearby

early-type galaxies in order to characterize their dominant stellar population. For that purpose we use photometric and spectroscopic data for a subset of nearby early-type galaxies drawn from the ENEAR sample (da Costa et al. 2000) as well as new higher S/N spectroscopic data. These data are used to investigate the dependence of the index– $\log \sigma_0$ on morphology (E and S0) and environment.

The present sample complements those recently available at intermediate redshifts such as the NOAO Fundamental Plane Survey (e.g., Nelan et al. 2005) and the SDSS, now a standard within $z=0.3$ (e.g., Bernardi et al. 2005). While existing low redshift samples (e.g., Thomas et al. 2005; Sánchez-Blázquez et al. 2006) are relatively small compared to those at intermediate redshifts, they have the advantage of having higher quality spectroscopic data and more reliable morphological and structural information.

This paper is organized as follows: in § 2 we describe the sample selection and the observations and in § 3, the data reduction. In § 4 we present the velocity dispersion measurements. The methodology used to compute line indices and the results of their comparison with those available in the literature are presented in § 5. In § 6 we analyze the index– $\log \sigma_0$ relations and their dependence on galaxy morphology and environment. Finally, in § 7 we present a summary of our conclusions.

2. The Sample and Observations

The sample discussed here consists of objects extracted from the ENEAR catalog (da Costa et al. 2000). This survey contains a database of photometric (Alonso et al. 2003) and spectroscopic (Wegner et al. 2003) parameters for a magnitude limited ($m_B \leq 14.5$) sample of early-type galaxies which is considered representative of the nearby universe ($v_r < 7000 \text{ km s}^{-1}$). Several global parameters are available in this database such as magnitudes (m_R), the effective radius, mean surface brightness (μ_e) within r_e , characteristic diameter (D_n), and the central velocity dispersion.

This sample includes objects residing in different environments such as the general field, groups and clusters. As an additional criteria we excluded objects with $|b| \lesssim 15^\circ$ to avoid the galactic plane, and also objects with $\delta \gtrsim 30^\circ$ due to the observational constraints. The observed list consists of 115 E, 131 E/S0 and 263 S0, giving a total of 509 galaxies, whose physical properties (L, r_e, σ_0) are fairly representative of the parent sample. In this paper we group, for analysis purposes, the galaxies E and E/S0 in the general class of E galaxies. These morphological types were revised based on visual inspection in two bands using images available in the Digital Sky Survey (Lasker et al. 1990). In Table 1 we display the catalog of observed galaxies, including some information about their physical properties. The columns in this catalog refer to: (1) object name; (2) and (3) are for (J2000.0) equatorial coordinates; (4) morphological type T ; (5) apparent B -band magnitude m_B ; (6) the heliocentric radial velocity v_r and respective error in km s^{-1} ; (7) the logarithm of σ_0 and its associated error in km s^{-1} from our determinations (see § 4); (8) the logarithm of r_e in units of

kpc, based on the data of Alonso et al. (2003) and the $D_n - \sigma$ distances given by Bernardi et al. (2002). Finally, in column (9), the number of companions N_c as defined in § 6.1 is presented. To give an idea of the global sample characteristics, the v_r , m_B , M_B and σ_0 distributions are displayed in panels of Figure 1.

The line strengths presented in this paper are based on long-slit spectra collected using the Boller & Chivens spectrograph mounted on the 1.52 m telescope at the La Silla site of the European Southern Observatory, during several runs between November 1993 and November 2002. Our observations were carried out with a $4.1'' \times 2.5''$ slit centered on the galaxy nucleus using a TV guider. For the vast majority of the objects the spectrograph was rotated to allow the slit to be oriented along the galaxy's major axis. For some galaxies, observations were also done along the minor axis, and for a few of them the slit was oriented in an intermediate position. Typical exposure time was 10 minutes in the beginning of the survey, and 30 minutes at a later phase. More than one frame per object was frequently obtained, in particular, for a set of ~ 140 bright galaxies of the ENEAR sample selected to study metallicity gradients.

The various instrumental setups used are described in Table 2. The spectra were considered acceptable for the present analysis only if they had $S/N > 20$. The S/N was determined in the continuum range from 5860 Å to 5875 Å as the ratio between the average and the *rms* of the signal in that region. In Figure 2 we display the distribution of S/N for the observed galaxies. The typical resolutions are 3 Å and 6 Å (FWHM) as discussed below.

Dome flats and bias were taken on a nightly basis. The dark current was found to be negligible after all, and its correction was not applied. After each science target exposure, at the same position of the sky that the object was observed, arc lamps (He-Ar or He-Ar-Fe-Ne) were exposed for wavelength calibration. In addition, we observed radial velocity standard stars and stars in common with Lick/IDS system, which are mainly in the F to K spectral type range, with luminosity classes ranging from I to V. To determine the velocity dispersion of galaxies we restricted the sample of stars to G and K giants. Besides the calibration to the Lick/IDS system, all those standards allowed calibrations among different setups.

3. Data Reduction

We followed standard procedures to reduce CCD spectra using **IRAF**. The science frames were subtracted by an average bias frame and divided by a normalized average flat-field frame. The 2-D images had cosmic rays hits in the surroundings of the spectrum removed with the task **imedit**. Those hits reaching the frame in the region next to the spectrum were not removed to avoid the introduction of artificial features. We also decided to discard the equivalent widths of lines which had cosmic rays within their definition range.

The extraction of 1-D spectrum was made with the task **apall** setting the aperture to obtain most of the galaxy's light along the slit as possible. This means that the aperture size typically

reached a radial distance from the galaxy’s center where the intensity is $\approx 5\%$ of the peak value of the light profile. With this procedure we intended to obtain spectra containing as much information as possible of the galaxy as a whole, and not just from its central region.

Arc lamps observed after each object frame were used to provide wavelength solutions and spectra linearization. We adopted a 5-7th order Legendre polynomial and the final fits used ~ 20 and 50 lines with typical $rms \sim 0.02$ and 0.08 \AA , for the 1200 l mm^{-1} and 600 l mm^{-1} gratings, respectively. The wavelength solution was verified by checking that the sky lines (e.g., [O I] $\lambda 5577 \text{ \AA}$) were located at their expected rest wavelength. The spectral resolution is $\sim 3 \text{ \AA}$ or $\sim 6 \text{ \AA}$ depending on the grating used (see Table 2). No flux calibration was applied to the spectra.

4. Measurement of v_r and σ_0

Radial velocity and velocity dispersions were measured for each spectrum using the cross-correlation technique (Tonry & Davis 1979). In particular, we used the RVSAO package (Kurtz & Mink 1998) to obtain v_r by cross-correlating galaxy spectra with several templates. The velocity and error adopted was provided by the best template (largest correlation coefficient). Typical error for the v_r measurement is $\sim 20 \text{ km s}^{-1}$.

For the measurement of σ_0 we generated a series of templates for each run/grating, combining stellar spectra of G and K giants since they represent the absorption features present in early-type galaxy spectra quite well. We used the wavelength interval from 4500 \AA to 6000 \AA , which is common to all the setups, to determine σ_0 . Although this range encompasses the H β and NaD lines, which are suspected of providing poor fits, we tested different ranges, excluding one or both of them, finding no significant difference.

Another issue addressed in our procedure is the fact that the velocity dispersion varies with galactocentric radius. Global apertures, like the ones we are using, do not sample systematically a characteristic size of the galaxy like e.g., some fraction of r_e , or some fixed size at the galaxy’s referential frame. To avoid this bias, we followed the usual σ_0 aperture correction method, considering the galaxy at some fiducial distance (Coma cluster) and using a standard metric aperture. Following the prescription of Jørgensen, Franx & Kjærgaard (1995), the aperture correction is given by the equation:

$$\log(\sigma_{norm}) = \log(\sigma_{ab}) - \alpha \log(r_{ab}/r_{norm}) \quad (1)$$

where α is the average gradient of $\log \sigma$, r_{ab} and r_{norm} are the sizes of circular and normalized apertures, respectively. The r_{ab} radius is given by $1.025[lc/\pi]^{1/2}$, where l is the slit width and, c is the effective length of the rectangular aperture to simulate a circular one. We choose a metric aperture of 1.19 kpc (Davies et al. 1987) and $\alpha = -0.04$ (Jørgensen, Franx & Kjærgaard 1995).

For galaxies with multiple observations, we calculated an average value for σ_0 in two steps, first including all measurements, then a final value is computed discarding individual σ_0 greater

than two times the *rms* limits from the average. The typical σ_0 error is $\sim 17 \text{ km s}^{-1}$. Also, for the low resolution ($\sim 6 \text{ \AA}$) configurations, we had to avoid σ_0 determinations below 160 km s^{-1} , as given by their high resolution counterpart, because low resolution measurements of low σ_0 galaxies tend to overestimate it.

To check the quality of our σ_0 measurements, we performed a comparison with galaxies in common with Trager et al. (1998), Denicoló et al. (2005) and Sánchez-Blázquez et al. (2006). We also compare these new measurements with those in the original ENEAR paper presented by Wegner et al. (2003). The results are presented in Figure 3 and Table 3, where we show the number of galaxies in common with each author, the mean offset $\langle \delta\sigma_0 \rangle$, its *rms*, and the *t* value given by the Student *t* test, where $t > 1.96$ means that the offset is significant at 95% confidence level. In general, we have a good agreement with Sánchez-Blázquez et al. (2006) who observed with instrumental resolutions similar to ours. The small difference we find with Denicoló et al. (2005) is probably caused by their lower instrumental resolution of 6 \AA . Trager et al. (1998) measurements also shows good agreement over the entire range of σ_0 . Most of the data they present, came from Davies et al. (1987), who used an instrumental resolution up to 85 km s^{-1} . Finally, we compare our measurements with those of the ENEAR catalog (Wegner et al. 2003), since we use a slightly different procedure to calculate σ_0 . The agreement is good, although the *t* value indicates that the offset is significant at the 95% confidence level, but not at 90% level. It is worth mentioning that our sample includes new spectra with better *S/N* ratio, as compared to the data presented in Wegner et al. (2003).

5. Absorption Line Measurements

The formal connection between observational data and stellar population models was initiated by Burstein et al. (1984) and Faber et al. (1985) who established the so-called Lick/IDS system, where central bandpass and flanking continua were defined for several absorption lines. To measure these indices for galaxies, several procedures and calibrations are required and in this section we describe them and also apply several tests to evaluate their quality. Later in this paper, we study the relations of these indices with σ_0 . We postpone to future papers the determination of the global stellar population parameters such as age, [Z/H] and α/Fe (Ogando et al. 2008a), as well as their radial gradient (Ogando et al. 2008b, in preparation).

5.1. Indices Definitions

The equivalent widths W were measured for two kinds of features: atomic absorption lines (W_a , expressed in \AA) and molecular bands (W_m , in magnitudes). Their general expressions are

given by the equations below:

$$W_a = \left(1 - \frac{\int_{\lambda_1}^{\lambda_2} F(\lambda) d\lambda}{\int_{\lambda_1}^{\lambda_2} C(\lambda) d\lambda} \right) (\lambda_2 - \lambda_1) \quad (2)$$

$$W_m = -2.5 \log \left(\frac{\int_{\lambda_1}^{\lambda_2} F(\lambda) d\lambda}{\int_{\lambda_1}^{\lambda_2} C(\lambda) d\lambda} \right) \quad (3)$$

where $F(\lambda)$ is the line flux, $C(\lambda)$ is the continuum flux, and λ_1 and λ_2 are the wavelengths defining the interval within which $F(\lambda)$ and $C(\lambda)$ are calculated.

Statistical errors in the indices W_a and W_m were calculated, respectively, according to the following expressions:

$$\epsilon_{W_a} = \left[\left(\frac{1}{\int_{\lambda_1}^{\lambda_2} C(\lambda) d\lambda} \right)^2 \epsilon_F^2 + \left(\frac{\int_{\lambda_1}^{\lambda_2} F(\lambda) d\lambda}{(\int_{\lambda_1}^{\lambda_2} C(\lambda) d\lambda)^2} \right)^2 \epsilon_C^2 \right]^{\frac{1}{2}} (\lambda_2 - \lambda_1) \quad (4)$$

$$\epsilon_{W_m} = 2.5 \left[\left(\frac{1}{\int_{\lambda_1}^{\lambda_2} C(\lambda) d\lambda} \right)^2 \epsilon_C^2 + \left(\frac{1}{\int_{\lambda_1}^{\lambda_2} F(\lambda) d\lambda} \right)^2 \epsilon_F^2 \right]^{\frac{1}{2}} \quad (5)$$

where ϵ_F and ϵ_C are the *rms* values for the central and continuum features of the line measured. We have determined, for each galaxy, all the set of Lick indices within the observed spectral range. However, to define the final set of indices considered we took into account two conditions: a common spectral coverage to all observing setups and the variation of the fractional error of a given index with S/N . The different sensitivity functions produced by the combination of CCD and grating resulted in better determination of some indices than others. In particular, the blue indices measurements are poor, as they are in a region of low detector and grating efficiency. In Table 4 we list the indices measured with their passband and pseudo-continua definitions. We also include the [OIII] $\lambda 5007$ line definition as given by González (1993), although it is not defined in the Lick system. This index is used to identify and discard undesired emission contaminated spectra, as discussed below.

In Figure 4 we show, as an example, the spectra for NGC 7507 as observed with each instrumental setup. Note that the spectrum shape in configuration 1 is quite different from the others. In order to verify the impact that this may have using spectra that have not been flux calibrated we have used a sub-sample of galaxies for which flux calibration is available. We have then compared the line index measurements carried out in both subsets. We find that for the molecular indices Mg₁ and Mg₂ there is indeed a significant difference (as estimated from a Student *t* test). This is not unexpected since the continua definition for these indices is far from the central passband. In the next section we discuss this issue and the procedure to remove this effect.

5.2. Indices Calibrations

5.2.1. Correction to the Lick Resolution

Since we have a higher resolution than that of the Lick/IDS system, before calculating indices, we degrade our spectra in resolution to match that of the Lick/IDS system by convolving the spectra with a gaussian function with an appropriate width, as described by Worthey & Ottaviani (1997). In order to determine our resolution we fitted gaussian functions to lines of the wavelength calibration arc lamps. This procedure allowed us to estimate the resolution variation along the entire wavelength range. Figure 5 shows the measured FWHM for several lines for the two gratings used. For comparison, we plot the Lick resolution curve described by Worthey & Ottaviani (1997). It is important to consider this effect since some of the indices (e.g.: Mg_b, Fe5270, Fe5335) are very sensitive to resolution. An **IRAF** task named **lickeqv** was created to carry out the degradation and also measure equivalent widths.

Despite the conversion of our observed spectra to the Lick/IDS resolution, this is not enough to fully transform our data to that system. Small zero-point residuals still persisted. Offsets were, then calculated for each of the instrumental setups described in Table 2 using the same group of 21 stars of spectral types F to K and luminosity classes from I to V. This is true except for setup 1, which had only 9 stars in common with the others setups. In this case, we estimated the offset relative to setups 2 and 3, which had already been corrected to the Lick system. The choice of a homogeneous set of stars is important since variations in the offset amongst setups are produced by the use of different samples of stars. This is probably associated to internal systematic uncertainties in the Lick system. Spectra of M stars were available but were not included because of their non-monotonic behavior with resolution degradation.

The offsets computed as described above were applied to the indices calculated for galaxies, after the corrections described in the next two sections, as a last step to perform the transformation to the Lick system. Afterwards, as a final verification, we looked for any residual offset in the galaxies line strength measurements between setups. Only Mg₁ and Mg₂ have shown a significant offset between setup 1 and the others. As mentioned in § 5.2, this is probably related to the lack of flux calibration. This offset was taken into account and the results show that we ended up with a homogenous system of line strength measurements that is appropriate for stellar population analysis.

5.2.2. Correction for Velocity Dispersions

The stellar velocity dispersion in a galaxy causes a spillover of line flux outside the narrow central bandpass, as it was defined originally for stars. To compensate this effect we measured line strengths in artificially broadened spectra of G and K giants. We simulate velocity dispersions in the range 50-500 km s⁻¹ with steps of 30 km s⁻¹. This was done using a modified version of

the **gauss** task of **IRAF** package, where the gaussian dispersion is expressed in pixels, so that the transformation to km s^{-1} can be done by the relation:

$$\sigma(\text{km s}^{-1}) = c \frac{\delta\lambda}{\lambda} \sigma(\text{pixels}) \quad (6)$$

where c is the velocity of light, and λ is a reference wavelength (5400 Å). The values of the spectral dispersions are ~ 1 Å and ~ 2 Å for the 1200 1 mm^{-1} and 600 1 mm^{-1} gratings, respectively.

Measurements of indices in stellar spectra artificially broadened permit the calibration of a relation between the broadening effect on the indices, $F(I)$, and σ . For atomic indices the relation is $F(I) = I(0)/I(\sigma)$, while for molecular indices it is $F(I) = I(0)-I(\sigma)$, where $I(\sigma)$ is the index strength at a given σ and $I(0)$ is the index measured in the original spectrum. Functions $F(I)$ for each index and grating were generated from 3rd order polynomial fits to these relations for a group of stars of types G to K according to the expression:

$$F(I) = \sum_{i=0}^3 A_i (\log \sigma)^i \quad (7)$$

In Figure 6 we display these functions for each measured index for both gratings of 1200 1 mm^{-1} and 600 1 mm^{-1} . Qualitatively, this correction agrees well with others presented in the literature (e.g., Trager et al. 1998; Kuntschner 2000). For example, the amount of correction is very small for broad indices like Mg₂, but large for narrow indices like Fe5270 and Fe5335, reaching $\approx 30\%$ for galaxies with 300 km s^{-1} . Another point is that the H β index is very sensitive to the choice of stellar spectral type into the definition of $F(I)$, as already pointed out by Kuntschner (2000), producing sometimes values of $F(I)$ smaller than 1. The causes for this behavior are that the H β itself fades very quickly as the temperature gets lower, and a TiO band head ($\approx 4851\text{\AA}$) starts to appear in low temperatures stars (Schiavon et al. 2002). For this reason, in the particular case of the H β index, some of the lowest temperature stars are not included in the fit. Quantitatively, the average difference of $F(I)$ at the arbitrary value of $\sigma = 300 \text{ km s}^{-1}$ is about $1\pm 3\%$ for the indices in common with Trager et al. (1998), with the exception of Mg₁ and Mg₂. For the Mg indices they use a multiplicative factor instead of an additive one, thus not allowing a comparison.

5.2.3. Correction by Aperture

The indices calculated as described above do not refer to a fixed metric aperture or to some fraction of r_e , implying that we sample differently the galaxies, as described in § 3. Since the distribution of chemical elements inside the galaxy is not homogeneous, we need to correct them to some fiducial aperture in a similar way to what was done for σ_0 in § 4. Here, we also consider an average gradient, this time for line strengths, which are all measured in magnitudes, even in the case of atomic indices, so that they are converted from Å (I) to magnitudes (I') according to the equation:

$$I' = -2.5 \log \left(1 - \frac{I}{\Delta\lambda} \right) \quad (8)$$

where $\Delta\lambda$ is the central passband of the index. Then we derived a fiducial aperture corrected index (I'_{norm}) given by:

$$I'_{norm} = I'_{ab} - \beta \log \left(\frac{r_{ab}}{r_{norm}} \right) \quad (9)$$

where r_{ab} and r_{norm} have the same meaning as in equation (1), and β is the average radial gradient for each index, which is presented in Table 5. The parameter β is the angular coefficient of a straight line fitted to the $I'(r)$ profile as a function of $\log(r/r_e^*)$, where r_e^* is the galaxy's effective radius corrected for its ellipticity. A full description of this parameter and its determination will be presented in Ogando et al. 2008b.

5.2.4. Emission Contamination

Early-type galaxies may contain some amount of ionized gas and young stars, which may lead to the presence of emission lines and contamination of their old population spectra (e.g., Macchetto et al. 1996). In these cases, some line indices may be significantly affected by these emission features, in particular $H\beta$ and Fe5015 (by the [O III] $\lambda 5007$ line). Indeed, even if the emission is not strong, it may fill partially the $H\beta$ line, resulting in a smaller value for its measured equivalent width and as a consequence, causing ages to be overestimated when using SPP models (Trager et al. 2000a). A possible way to correct for the $H\beta$ contamination can be accomplished if we can infer the contribution from another emission line. For the case of $H\beta$, González (1993) derived a relation between the emission contamination in this line and the [OIII] $\lambda 5007$ equivalent width, established by the emission-free stellar spectra fit to those galaxies in his sample. He found that the amount of emission contamination in $H\beta$ is given by $\Delta H\beta = 0.6 \times [\text{OIII}] \lambda 5007$. However this correction has a considerable uncertainty and should be taken as a statistical approach since the $H\beta/[\text{OIII}] \lambda 5007$ ratio varies considerably from galaxy to galaxy.

Another possible way to deal with the emission contamination in the $H\beta$ index is to infer it through the intensity of $H\alpha$ line (e.g., Nelan et al. 2005; Denicoló et al. 2005). However, due to the different spectral coverage associated to the several instrumental setups used, we are able to measure $H\alpha$ for only one third of the sample. Thus, instead of using these statistical corrections, we decided to exclude from the analysis galaxies with measurable emission of [OIII] $\lambda 5007$ at a detection level larger than twice its rms error. This condition affects 18 galaxies, or about 4% of the sample, which is a smaller fraction than that of 12% found by Nelan et al. (2005) for galaxies selected on the basis of red sequence criteria which may include some early-type spirals, since no explicit morphological segregation was imposed. The galaxies with detected emission are predominantly S0 (11 galaxies), and they are distributed evenly among the distinct environments. We illustrate the impact of this rejection criteria on the distribution of [OIII] $\lambda 5007$ and $H\beta$ intensities in Figure 7, where we note that even galaxies with positive $H\beta$ indices are excluded from the sample, showing how subtle the emission contamination can be.

5.3. Internal Comparison

For objects with several observations, the final value for an index was computed by: 1) applying to each available measurement all the calibrations and corrections mentioned above; 2) computing the mean of all measurements; 3) discarding outliers with values 2σ above the average; 4) re-computing the mean one more time. The final values for the indices of all the 509 galaxies are presented in Table 6, including those with emission lines which are not included in the analysis below.

Besides the statistical error determination described in § 5.1 we need to take into account other sources of uncertainties as, for example, those related to wavelength calibration, sky background subtraction, position angle of the slit over the galaxy, the fraction of galactocentric radius encompassed by the slit. Multiple observations ($N > 2$) are available for 91 galaxies ($\approx 18\%$) of our sample, and they are used to estimate a more representative error for our line strengths. We calculated for each line index an average of the fractional error combining the individual determinations. In Table 7 we present the statistics of this averaging process and it can be noted that, in general, the errors derived from multiple observations reach 5-10% of the index value, while errors from individual measurements are typically 1-3% of the index value. In Figure 8 we display measurements of indices for galaxies with more than 10 observations in order to show the range of their fluctuations. Thus, based on the statistics shown in Table 7 we claim that, in general, our errors are less than 10% of the index value.

5.4. Comparison with other Authors

To evaluate the overall quality of our data and calibrations, we have compared our measurements of line indices with those from measurements reported in the literature by other authors of samples having a significant number of overlaps with ours. The results of these comparisons are shown in Table 8 and Figures 9 to 13. Table 8 gives: in column (1) the reference; in column (2) the number of galaxies in common N_{gal} ; in column (3) the mean difference $\langle \delta I \rangle$ and its *rms*; and in column (4) the *t* value of the Student test. We remind that for $t > 1.96$, the differences are considered significant at a 95% confidence level.

Figure 9 shows the comparison with Trager et al. (1998), which includes the original Lick/IDS data. Despite of the lower quality of the data, we find from Table 8 that the agreement is very good. The same is true regarding the comparison with Trager et al. (2000a) (Figure 10) which reports data of better quality obtained by González (1993). The only exception is the Fe5270 index. More recently, new data have been presented by Denicoló et al. (2005) and Sánchez-Blázquez et al. (2006). Comparison with their measurements are shown in Figures 11 and 12. We find that in general the agreement is good, except for the Fe indices measured by Denicoló et al. (2005). In the case of Sánchez-Blázquez et al. (2006) only the Fe5015 presents a more discrepant result. Finally, in Figure 13 we compare our measurements of the Mg₂ index with those presented earlier

in Wegner et al. (2003) for ≈ 400 galaxies in common, but occasionally using new spectra with better S/N . We note that in the present paper we use a slightly different method to estimate the pseudo-continuum on each side of the band trying to correct for the local inclination of the spectra. The quantitative results are given in Table 8, from where we find that the agreement is excellent.

We also mention that in the last years large surveys similar to the one being reported here have been conducted (e.g., Nelan et al. 2005; Colless et al. 2001) but unfortunately the number of objects in common is very small (< 3) to allow a comparison.

In summary, based on the results presented above, we conclude that, in general, our measurements of line index are in good agreement with those available in the literature. Occasionally, some significant discrepancies are detected for a particular index, but this does not seem to reflect a systematic problem as it varies from author to author. Instead, they probably reflect different effects that may affect the measurement such as differences in the region of the galaxy sampled (e.g. different position angle and/or radial extent), lack of a suitable set of stars used to calibrate the Lick system by some authors, and the details of the procedure adopted for estimating the correction due to velocity dispersion and resolution.

6. Indices, Mass, Velocity Dispersion and Environment

A connection between dynamical and chemical properties of early-type galaxies may be established through relations between the strength of line indices and their velocity dispersions or masses, as for example the well known $Mg_2 - \sigma_0$ relation. Since our data constitute one of the largest samples of early-type galaxies with good spectral quality and resolution at $z \approx 0$ we investigate not only this but similar relations for other lines taking into account different morphologies and environments. In order to do that, we first define environment and mass estimators for our galaxies as described below.

6.1. Characterizing the Galaxy Environment

Although early-type galaxies are found more frequently in clusters and groups of galaxies, their relative quantity to other morphological types depend essentially on the local density of galaxies. This behavior is translated in the well known “morphology-density” relation (e.g., Dressler 1980; Maia & da Costa 1990). Taking this into account, we decided to characterize the environment for a galaxy estimating the number of companions brighter than a fixed absolute magnitude, within a given “box” size. This is equivalent to calculate the density of objects, being more representative of the local environment around an object than just classifying it as a field, group and cluster galaxy.

In order to estimate the number of neighbors (N_c) for each galaxy in our sample, we used the catalog of galaxies available in the HyperLeda database (Paturel et al. 2003), which has a larger

sky coverage than the Southern Sky Redshift Survey (da Costa et al. 1998), for example. Although the former represents a compilation, it is considered complete down to $m_B \approx 15.5$. A galaxy from this catalog contributes to the neighborhood counts of a given galaxy in our sample, if it satisfies the following criteria: (i) the difference between their radial velocities is $< 750 \text{ km s}^{-1}$, (ii) their projected separation is $< 500 \text{ kpc}$, (iii) the HyperLeda galaxy has $M_B < -16.0$. It should be mentioned that there is not any strong bias of N_c with distance as can be seen in Figure 14. The distribution of N_c for our sample divided by morphological type is displayed in Figure 15. We note that this density indicator has a wide dynamical range making it sensitive to variations from the external to central regions of clusters and to the mean cluster density. This can be seen in Figure 15 where we indicate in the plot the position occupied by a galaxy in the central part of the Fornax cluster (medium density) and from one in the central part of the Virgo cluster (high density). This indicates that this classification scheme is more meaningful than the usual field/group/cluster one, as used by Bernardi et al. (1998), for instance.

The median value for the N_c distribution in the volume considered is 10 galaxies and the lower and upper quartiles are LQ=4 and UQ=22 galaxies, respectively. Taking these values into account, we divided the sample in 3 intervals of densities: low density (LD; $N_c \leq 4$), median density (MD; $4 < N_c < 22$), and high density (HD; $N_c \geq 22$). Our main goal in splitting the sample in this way is to compare the two extreme environments, LD and HD, using about the same number of objects in each one of them, so that we can avoid misleading statistical inferences. Among the 509 galaxies of our sample, only two galaxies were considered isolated ($N_c = 0$) according to the prescribed criteria. Examining N_c for 11 galaxies in common with the isolated sample of Reda et al. (2004), only three have $N_c > 2$. Among them, NGC 1132, that is the galaxy with the greatest N_c (11 companions), has an associated extended x-ray emission typical of groups of galaxies. Indeed this galaxy is considered a “fossil group” by Mulchaey & Zabludoff (1999), and if we inspect DSS images, it is possible to see fainter galaxies around this object. We also note that among the criteria adopted by Reda et al. (2004) there is one that excludes companions 2 magnitudes fainter than that of the target object, what could explain this case.

6.2. Galaxy Mass Estimators

The mass of a galaxy is one of its fundamental parameters and its determination may follow different recipes. The most common estimator is the central velocity dispersion σ_0 which, in fact, probes the gravitational potential. Another mass estimator comes from the consideration that the object is in dynamical equilibrium, satisfying the virial theorem. Thus, the mass M_e in units of M_\odot is given according to Burstein et al. (1997) by the expression:

$$\log M_e = \log(\sigma_0^2 r_e) + 5.67 \quad (10)$$

where r_e is the galaxy effective radii in units of kpc.

In both cases it is implicit that the contribution by rotation to the object’s dynamical support

is assumed to be negligible. Another point of concern is related to the conversion of r_e in arc seconds to kpc which needs a reliable determination of the galaxy distance (D). Considering just the redshift to calculate D , we may incur in error due to the peculiar motion of galaxies. Thus, we adopted D given by $D_n - \sigma$ relation (Bernardi et al. 2002) to calculate r_e in kpc.

Since in the next section we discuss the relations between indices and mass for the sample divided in different morphologies and environments, it is interesting to previously inspect the differences in the mass distribution of these particular subsets. We show in Figure 16 these distributions using both estimators described above, according to distinct morphological type. In Table 9 we present mean values, dispersion, skewness, and kurtosis for these estimators. Also, in Table 10 we show the probability that the samples of E and S0 galaxies have the same parent population as given by the Kolmogorov-Smirnov (KS) test. For both mass estimators, these samples have very different distributions, where the mass distribution of E galaxies is skewed towards higher masses as compared to the one for S0s. We investigate below if this behavior implies in different index– $\log \sigma_0$ relations for distinct morphologies.

We also use the environment definitions described above to divide the mass distribution of E and S0 galaxies, as shown respectively in Figures 17 and 18. These plots, which reflect the morphology-density relation, stress that the most massive Es are located in high density environments, but S0s do not follow this trend, having similar mass distribution in all environments.

It is noticeable in Figure 17 and also from the computed values of kurtosis and skewness in Table 10, that the mass distribution of E galaxies in HD is less peaked and more concentrated towards the high mass end of the distribution than those in LD environment. For the S0s, such trend occurs more mildly and, in particular, for $\log M_e$, the similarities between the shape parameters and the higher KS probability (40%) indicate that S0s have almost the same mass distributions in different environments.

This observed mass distribution of E galaxies is expected by hierarchical clustering models, where higher mass objects are formed in denser regions (Lemson & Kauffmann 1999), and most of them turn out to be Es in numerical simulations (Springel et al. 2001). On the other hand, this result can be interpreted as an evolutionary difference if E are the product of a faster and older process of growth of spheroids through dissipationless mergers or coherent collapse, while lenticulars may be formed at least partially, from stripping of spirals by strong two-body gravitational interactions (Dressler et al. 1997). We should take this fact into account when interpreting the index– $\log \sigma_0$ relations in the next section.

6.3. Index– $\log \sigma_0$ Relations

The first well established relation between an index and σ_0 was set for the Mg₂ index (e.g., Terlevich et al 1981; Dressler et al. 1987; Bender, Burstein & Faber 1993; Bernardi et al. 1998), which is generally interpreted as a relationship between mass and metallicity. However, there is

some debate about the true nature of this relation, which might be influenced by stellar ages or variations in abundances ratios, for instance that of $[\alpha/\text{Fe}]$. In particular, for a given mass, the small scatter of the $\text{Mg}_2 - \log \sigma_0$ relation has also been attributed to a “conspiracy” between metallicity and age (Trager et al. 2000b), in the sense that older galaxies are less rich in metals. Thus, it is important to investigate the index– $\log \sigma_0$ relations for other elements, whose slopes and scatter should be sensitive to different chemical composition variations.

In the discussion below, we present all of our measured indices (I) in magnitudes (I'), using the transformation given by equation (8), in order to permit the comparison with other authors. The $I' - \log \sigma_0$ relations for 10 measured indices, separating galaxies by morphology (E and S0), are shown in Figure 19. The lines in the Figure represent the best fit, $I' = A + B \log \sigma_0$, to the data. The parameters of the fits and their associated errors are presented in Table 11, which also gives the number of galaxies (N_{gal}) used in the fit, the Spearman rank r_s coefficient and the t parameter, which tests the null hypothesis ($B = 0$). We remind that a value of $t > 1.96$ means that the slope (B) is significantly different from zero. We stress that our data were obtained using a long slit and each spectrum represents a light-weighted measurement, reflecting the mean stellar population contributing to most of the galaxy’s light.

From Figure 19 and Table 11 we find that, in general, there is a significant correlation between the metallic indices and σ_0 , as indicated by the rank coefficient r_s , which is specially strong for the Mg and NaD lines. The Fe lines, on the other hand, tend to have a moderate correlation with σ_0 . The only exception is the Fe5709' index which, in agreement with Clemens et al. (2006), shows no correlation. This behavior is probably due to the weak dependence of this Lick index on Fe abundance, as discussed by Korn et al. (2005). We point out that, in contrast to our result and the one reported by Nelan et al. (2005), Clemens et al. (2006) also finds no correlation for the Fe5270' index.

The NaD' line shows a correlation with σ_0 as significant as that of the Mg lines (see also Clemens et al. 2006), but its known dependence on interstellar absorption hampers a reliable interpretation. While S0s may be affected, one should not expect a strong contribution from the ISM in a “dust-free” object like an E galaxy.

Finally, Figure 19 shows that the Balmer line H β' is the only one that decreases with increasing σ_0 (anti-correlates). This result is consistent with several previous works (e.g., Trager et al. 1998; Denicoló et al. 2005; Sánchez-Blázquez et al. 2006; Clemens et al. 2006).

In order to verify possible differences of the $I' - \sigma_0$ relation between E and S0 galaxies, we compare in Figure 20 the linear fit coefficients (Table 11) obtained for these two sub-samples. From this figure, taking into account the coefficients errors, the metallic indices do not differ by more than 1.5σ . Interestingly, the most discrepant index is the NaD' line, whose behavior may be caused by the influence of the more conspicuous interstellar medium expected for the lenticulars. This can also be seen on the slightly higher H β' values for low mass S0, indicating that this gas reservoir can be used to fuel star formation.

Similarly, we examine the possible influence of the environment on the relations defined above, using the definitions of § 6.1, classifying galaxies in regions of low, medium and high density of objects (LD, MD and HD). Figure 21 shows the results and the parameters for the fits are listed in Table 12. As can be seen, there are no significant differences between metallic $I' - \log \sigma_0$ relations for LD and HD environments, in agreement with several previous works, except for $H\beta'$. Galaxies in LD environments display a steeper relation than the ones in HD, possibly indicating that the latter have, on average, older stellar populations. Furthermore, a less steep relation in high density regions, is an indication of a truncated star formation history at the low mass end. Possible mechanisms responsible for this could be harassment (Moore et al. 1998) or gas stripping (Gunn & Gott 1972), both of which keep the morphology intact.

A comparison of our results with those available in the literature for nearby samples is shown in Figure 22, where we plot the coefficients computed in different environments. This is done despite the distinct selection criteria of each work, their reduction and analysis procedures, and density estimator. In the comparison we include the following authors: 1) Bernardi et al. (1998) who analyzed the Mg_2 index for field, group and cluster galaxies. Their linear fits for each environment are very similar, thus we show only their cluster fit; 2) Kuntschner (2000) who analyzed data for 11 E and 11 S0 galaxies of the Fornax cluster, considered here equivalent to our HD definition; 3) Kuntschner et al. (2001) who analyzed 72 galaxies in groups and clusters; 4) Denicoló et al. (2005) who analyzed results for 84 galaxies with indices measured at $r_e/8$, distributed in the field and in groups, including 8 isolated galaxies; 5) Sánchez-Blázquez et al. (2006) who analyzed $I' - \log \sigma_0$ relations for a sample of 98 objects divided in two environments defined by low (field, group and Virgo cluster) and high galaxy density (central region of Coma cluster).

Figure 22 shows that within the uncertainties, our $I' - \log \sigma_0$ relations do not depend on environment. This is in agreement with the findings of Bernardi et al. (1998) and Denicoló et al. (2005). In contrast, Sánchez-Blázquez et al. (2006) reported a significant difference, and attributed it to a variation of chemical abundance ratios. These conflicting results may originate from the σ_0 ranges considered by the authors, sometimes by the sparse sampling of low σ_0 objects, by poor spectral resolution, or by the methodology in obtaining and analyzing the data.

We also compare our results with deeper samples. For instance, Bernardi et al. (2003) find no dependence of the $Mg_2 - \sigma_0$ and $H\beta' - \sigma_0$ relations on environment using the SDSS data. By contrast, Clemens et al. (2006) using data from the same survey, report “small, but very significant trends with environments”. A potential problem with analyses based on the SDSS is the adopted morphological classification, which is based exclusively on color properties. That may lead to a mixture of populations, including bulges of early spirals, which may follow different star formation histories (Trager 2004). Since they reside in low-density regions, this may introduce a false dependence on environment.

The weaker correlation of Fe indices with velocity dispersion, as compared to those for α representatives (Mg) and the anti-correlation of $H\beta'$, which is not very sensitive to α/Fe ratio

(Korn et al. 2005), suggests a variation of the α/Fe ratio with σ_0 . This abundance ratio is associated to a short star formation history (Trager et al. 2000a; Thomas et al. 2005), which taken together with their inferred old luminosity-weighted ages and metal rich content, are conflicting with the predictions from hierarchical clustering models and give support to the so-called downsizing scenario (Cowie et al. 1996), as observed by recent works (e.g., Denicoló et al. 2005; Thomas et al. 2005; Sánchez-Blázquez et al. 2006). Theoretical efforts to explain these apparent inconsistencies are based on the use of active galactic nuclei feedback to regulate the star formation history (Scannapieco et al. 2005; De Lucia et al. 2006), also separating the stellar population birth time from the galaxy mass assembly time (De Lucia et al. 2006). Nevertheless, while no specific abundance ratio prediction is made, forming the bulk of stars before mass assembly leads to subsequent “dry-mergers”, currently a popular scenario for the origin of bright E galaxies (Bernardi et al. 2007).

Regarding the scatter of the $I' - \log \sigma_0$ relation, although relatively small, specially in the case of the Mg_2 line, it can not be explained solely by the uncertainties. As we have seen, the α/Fe ratio and age also contribute to the slope of this relation, and one might wonder if the scatter can also be driven by age, an usual claim in the literature (e.g., Terlevich & Forbes 2002; Sánchez-Blázquez et al. 2006), or by variations of abundance ratios (e.g., Sánchez-Blázquez et al. 2006).

Following the discussion made by Sánchez-Blázquez et al. (2006) we tested for possible age effects on the scatter of the different $I' - \log \sigma_0$ relations by measuring the correlation of the residuals ($\delta I'$) of the least-square fits to the relations versus the $H\beta'$ index, which is an age-sensitive indicator. The plots of the $\delta I' - H\beta'$ relations are shown in the Figure 23 for the sample divided by morphology, while the correlation parameters are listed in Table 13 which contains the results of the Spearman and t tests. Apparently, there is no dependence of the scatter correlation on morphology (Table 13). The lines that show a significant anti-correlation of the residuals with $H\beta'$ are those of Mg and NaD' . Differently, the Fe (except for $\text{Fe}5015'$) residuals do not show any dependence on $H\beta'$. The fact that the scatter of distinct metallic lines behave differently with $H\beta'$ suggests that not only age has an effect on the scatter of the $I' - \log \sigma_0$ relation, but it may also be affected by the $[\alpha/\text{Fe}]$ ratio as suggested by Sánchez-Blázquez et al. (2006). The $\text{Fe}5015'$ index, according to the line formation calculations of Korn et al. (2005), is more sensitive to the chemical abundances of Ti and Mg than to that of Fe, where in fact, $\text{Fe}5015'$ anti-correlates with the abundance of Mg, what could explains its odd behavior amidst the Fe lines.

The results of the $\delta I' - H\beta'$ relations according to the environments are shown in Figure 24 and in Table 14. The Mg and Na indices, that follow the α elements, give distinct answers, but Mg indices still tend to anti-correlate while the NaD' index shows no correlation at all, a result that is shared by the Fe indices. In general, we find that those correlations do not vary significantly between LD and HD environment, except for the $\text{Fe}5015'$ and the Mgb index. Similar analysis was carried out by Sánchez-Blázquez et al. (2006), who also found that Mg and Fe lines scatter with $H\beta'$ behave differently, attributing it to α/Fe variations. However, they find that the residuals of

Fe lines with $H\beta'$ correlate in LD regions, but not in HD. On the other hand, Kuntschner et al. (2002) compared the scatter of the $Mgb-\sigma_0$ relation in low density regions and the Fornax cluster and found no difference between those environments. We also note that the scatter increases for galaxies with large $H\beta'$, which are the low mass objects. This result points towards the scenario of downsizing (Cowie et al. 1996), where low mass galaxies have an extended star formation history.

7. Summary

In this work we present the measurements of velocity dispersion and Lick indices obtained from high $S/N (> 20)$, long-slit spectra for 509 early-type galaxies, drawn from the ENEAR survey (da Costa et al. 2000), considered a fair representation of the present-day early-type population, having fairly similar distributions of apparent magnitude, radial velocity, morphology and velocity dispersion to the ENEAR sample as a whole. This sample is one of the largest of its kind currently available in the nearby Universe ($z < 0.002$), and complements the much larger and higher redshift ($z > 0.005$) data from the SDSS (Bernardi et al. 2003; Clemens et al. 2006). While the latter has a large number of objects which is unmatched for statistical studies, it suffers from the uncertainties of color-based morphological classification, the limitations inherited to fiber-based measurements and the need of spectra stacking, given the typical low S/N .

We find that our measurements of velocity dispersion and line strength indices are, in general, in good agreement with those available in the literature. A few discrepant cases exist, but these vary from line to line and from author to author, showing no systematic behavior. These data are used in this and forthcoming papers to study the chemical evolution of early-type galaxies. In the present paper we use different line indices-velocity dispersion relations to probe the properties of early-type galaxies. The relatively large sample allows us to split it, both by morphological types and different galaxy density regimes, without compromising the statistical significance of the sub-samples considered. We emphasize that our densities are estimated locally, therefore more representative than the broad categories such as field/groups/clusters normally used in some studies.

The main findings of this paper are:

1. Our new measurements of velocity dispersion and Mg_2 are robust, agreeing with those obtained by Wegner et al. (2003) using a different methodology.
2. Our indices' measurements show small offsets when compared to those of other authors (Trager et al. 1998, 2000a; Wegner et al. 2003; Denicoló et al. 2005; Sánchez-Blázquez et al. 2006), but with comparable scatter, consistent with the error estimates. Furthermore, several more subtle effects such as the placement of the slit, the aperture size and the calibration procedure adopted may affect the measurements.
3. Independent of the mass estimator used we find that E galaxies in high density regimes are on average more massive than those located in low-density regions. This is in agreement with

the conclusions of Clemens et al. (2006). In addition, we find that E are more massive than S0 galaxies, a fact that has been used as an argument in favor of the hierarchical growth of elliptical galaxies.

4. As well-known, we find that all the Mg indices show a relatively strong increase with σ_0 while the Fe indices depend only mildly on it. These correlations are interpreted by many authors (e.g., Bernardi et al. 1998) as driven mainly by metallicity in a coeval population, while others believe that age also plays an important role in defining this relation and its scatter (Trager et al. 2000a; Sánchez-Blázquez et al. 2006).
5. The observed distinct dependence of Mg and Fe on velocity dispersion, along with the anti-correlation with velocity dispersion of the $H\beta'$ index, which has a low sensitivity to α/Fe ratio, suggests that the chemical abundance ratio of Mg/Fe also varies with mass, as pointed out by several authors (e.g., Trager et al. 2000a; Kuntschner et al. 2002; Thomas et al. 2005; Sánchez-Blázquez et al. 2006).
6. In general, the metallic $I' - \sigma_0$ relations show no dependence on morphology or local density of galaxies. The exception is the NaD', where the low-mass lenticulars show stronger line indices than ellipticals with comparable σ_0 . The $H\beta' - \sigma_0$ also shows a weak dependence on both morphology and local density. This result contrasts with the findings of Sánchez-Blázquez et al. (2006), based on a considerably smaller sample, and claims by Clemens et al. (2006) using the SDSS data.
7. The $H\beta'$ index decreases with σ_0 which suggests, along with the metallic lines, that the last episode of star formation for massive galaxies took place early in the galaxies history. Comparing this relation in high and low-density regions we find that the slope of the relation is significantly flatter in high-density regions indicating that the star formation of low mass galaxies has been interrupted by some interaction like harassment (Moore et al. 1998) or gas stripping (Gunn & Gott 1972).
8. The residuals of Mg- σ_0 relation show correlation with $H\beta'$, decreasing for larger values of $H\beta'$. This dependence may indicate that variations in age contribute to the amplitude of the scatter of the Mg- σ_0 relation, specially in the case of low mass objects. No such correlation is seen for Fe, which may be a hint for Mg/Fe variation taking part in the scatter.

The fact that massive galaxies have on average high values of Mg, low values of $H\beta'$, and relatively high Mg/Fe ratio, can be interpreted as evidence that massive elliptical galaxies are metal-rich and that the last burst of star formation was brief and took place in an early phase of their history. The data also shows that low mass early-type galaxies are younger, metal poorer and have an extended star formation history, except those in high density regions, where their star formation has been truncated, probably due to interactions with the intracluster medium. Taken together, these evidences favor the currently popular downsizing model for the formation of early-type galaxies.

It should be pointed out that interpreting the relations between metallic indices and σ_0 as a mass-metallicity relation for a population of coeval objects is not strictly correct and will be explored in a future paper, where we use evolutionary synthesis models to take into account the effects of age and abundance ratios (Ogando et al. 2008a).

Finally, as demonstrated in Ogando et al. (2005), an alternative way to constraint models for the formation of early-type galaxies is to use the dependence of metallicity with the galactocentric radius, since the existence of steep gradients indicate a quick formation, as expected in monolithic-like models. In a forthcoming paper (Ogando et al. 2008b), we use high-quality data for a sub-sample of the galaxies presented here to measure these gradients, extending our previous work.

R.L.C.O. acknowledges CNPq Fellowship 141420/2002-2; M.A.G.M. CNPq grants 301366/86-1, 472301/04-7 and 308855/06-0; P.S.P. CNPq grant 301373/86-8.

REFERENCES

- Alonso, M.V., Bernardi, M., da Costa, L.N., Wegner, G., Willmer, C.N.A., Pellegrini, P.S., & Maia, M.A.G. 2003, AJ, 125, 2307
- Bender, R., Burstein, D., & Faber, S.M. 1993, ApJ, 411, 153
- Bernardi, M., Renzini, A., da Costa, L.N., Wegner, G., Alonso, M.V., Pellegrini, P.S., Rit , C., & Willmer, C.N.A. 1998, ApJ, 508, L143
- Bernardi, M., Alonso, M.V., da Costa, L.N., Willmer, C.N.A. Wegner, G., Pellegrini, P.S., Rit , C. & Maia, M.A.G. 2002, AJ, 123, 2159
- Bernardi, M., Sheth, R.K., Annis, J., et al. 2003, AJ, 125, 1817
- Bernardi, M., Sheth, R.K., Annis, J., et al. 2003, AJ, 125, 1882
- Bernardi, M. Sheth, R.K., Nichol, R.C., Schneider, D.P. & Brinkmann, J. 2005 AJ, 129, 61
- Bernardi, M., Hyde, J.B., Sheth, R.K., Miller, C.J., & Nichol, R.C. 2007, AJ, 133, 1741
- Burstein, D., Faber, S.M., Gaskell, C.M. & Krumm, N. 1984, ApJ, 287, 586
- Burstein, D., Bender, R., Faber, S.M., & Nolthenius, R. 1997, AJ, 114, 1365
- Clemens, M.S., Bressan, A., Nikolic, B., Alexander, P., Annibali, F. & Rampazzo, R. 2006, MNRAS, 370, 702
- Colless, M., Dalton, G., Maddox, S., et al. 2001, MNRAS, 328, 1039
- Cowie, L.L., Songaila, A., Hu, E.M., & Cohen, J.G. 1996, AJ, 112, 839

- da Costa, L.N., Willmer, C.N.A., Pellegrini, P.S., et al. 1998, AJ, 116, 1
- da Costa, L.N., Bernardi, M., Alonso, M.V., Wegner, G., Willmer, C.N.A., Pellegrini, P.S., Rit , C., & Maia, M.A.G. 2000, AJ, 120, 95
- Davies, R.L., Burstein, D., Dressler, A., Faber, S.M., Lynden-Bell, D., Terlevich, R.J., & Wegner, G. 1987, ApJS, 64, 581
- De Lucia, G., Springel, V., White, S.D.M., et al. 2006, MNRAS, 366, 499
- Denicol , G., Terlevich, R., Terlevich, E., Forbes, D.A., Terlevich, A., & Carrasco, L. 2005, MNRAS, 356, 1440
- Djorgovski, S. & Davis, M. 1987, AJ, 313, 59
- Dressler, A. 1980, ApJ, 236, 351
- Dressler, A., Lynden-Bell, D., Burstein, D., Davies, R.L., Faber, S.M., Terlevich, R., & Wegner, G. 1987, ApJ, 313, 42
- Dressler, A., Oemler, A., Warrick, J.C., Smail, I., Ellis, R.S., Barger, A., Butcher, H., Poggianti, B.M. & Sharples, R.M. 1997, ApJ, 490, 577
- Faber, S.M., & Jackson, R.E. 1976, ApJ, 204, 668
- Faber, S.M., Friel, E.D., Burstein, D., & Gaskell, C.M. 1985, ApJS, 57, 711
- Gonz lez, J.J. 1993, PhD Thesis, University of California, Santa Cruz, USA
- Gorgas, J., Efstathiou, G., & Arag n-Salamanca, A. 1990, MNRAS, 245, 217
- Gunn, J.E. & Gott, J.R.I. 1972, ApJ, 176, 1
- J rgensen, I., Franx, M., Kj rgaard, P. 1995, MNRAS, 276, 1341
- Kauffmann, G., White, S.D.M., & Guiderdoni, B. 1993, MNRAS, 264, 201
- Korn, A.J., Maraston, C., & Thomas, D. 2005, A&A, 438, 685
- Kuntschner, H. 2000, MNRAS, 315, 184
- Kuntschner, H., Lucey, J.R., Smith, R.J., Hudson, M.J., & Davies, R.L. 2001, MNRAS, 323, 615
- Kuntschner, H., Smith, R.J., Colless, M., et al. 2002, MNRAS, 337, 172
- Kurtz, M.J., & Mink, D.J. 1998, PASP, 110, 934
- Larson, R.B. 1974, MNRAS, 166, 585

- Lasker, B.M., Sturch, C.R., McLean, B.J., Russell, J.L., Jenkner, H., Shara, M.M. 1990, AJ, 99, 2019
- Lemson, G., & Kauffmann, G. 1999, MNRAS, 302, 111
- Macchetto, F., Pastoriza, M., Caon, N., et al. 1996, A&AS, 120, 463
- Maia, M.A.G., & da Costa, L.A.N. 1990, ApJ, 352, 457
- Moore, B., Lake, G., & Katz, N. 1998, ApJ, 495, 139
- Mulchaey, J.S., & Zabludoff, A.I. 1999, ApJ, 514, 133
- Nelan, J.E., Smith, R.J., Hudson, M.J., Wegner, G.A., Lucey, J.R., Moore, S.A.W., Quinney, S.J. & Suntzeff, N.B., ApJ, 632, 137
- Ogando, R.L.C., Maia, M.A.G., Chiappini, C., Pellegrini, P.S., Schiavon, R., & da Costa, L.N. 2005, ApJ, 632, L61
- Ogando, R.L.C., Maia, M.A.G., Pellegrini, P.S., & da Costa, L.N. 2008, ApJ, in press
- Paturel, G., Petit, C., Prugniel, P., et al. 2003, A&A, 412, 45
- Pipino, A. & Matteucci, F. 2004, MNRAS, 347, 968
- Reda, F.M., Forbes, D.A., Beasley, M.A., O'Sullivan, E.J., & Goudfrooij, P. 2004, MNRAS, 354, 851
- Sánchez-Blázquez, P., Gorgas, J., Cardiel, N., & González, J.J. 2006, A&A, 457, 787
- Scannapieco, E., Silk, J., & Bouwens, R. 2005, ApJ, 635, L13
- Schiavon, R.P., Faber, S.M., Castilho, B.V., et al. 2002, ApJ, 580, 850
- Springel, V., White, S.D.M., Tormen, G., & Kauffmann, G. 2001, MNRAS, 328, 726
- Terlevich, R., Davies, R.L., Faber, S.M., Burstein, D. 1981, MNRAS, 196, 381
- Terlevich, A.I. & Forbes, D.A. 2002, MNRAS, 330, 547
- Thomas, D., Maraston, C., & Bender, R. 2003, MNRAS, 339, 897
- Thomas, D., Maraston, C., Bender, R. & Oliveira, C.M. ApJ, 621, 673
- Tonry, J., & Davis, M. 1979, AJ, 84, 1511
- Trager, S.C., Worthey, G., Faber, S.M., Burstein, D., González, J.J. 1998, ApJS, 116, 1
- Trager, S.C., Faber, S.M., Worthey, G., González, J.J. 2000a, AJ, 119, 1645

- Trager, S.C., Faber, S.M., Worthey, G., González, J.J. 2000b, AJ, 120, 165
- Trager, S.C. 2004, in Origin and Evolution of the Elements, ed. A. McWilliam & M. Rauch, 388
- Wegner, G., Bernardi, M., Willmer, C.N.A., da Costa, L.N., Alonso, M.V., Pellegrini, P., Maia, M.A.G., Chaves, O.L., & Rit  , C. 2003, AJ, 126, 2268
- Worthey, G., Faber, S.M., & Gonzalez, J.J. 1992, ApJ, 398, 69
- Worthey, G. 1994, ApJS, 95, 107
- Worthey, G., & Ottaviani, D.L. 1997, ApJS, 111, 377

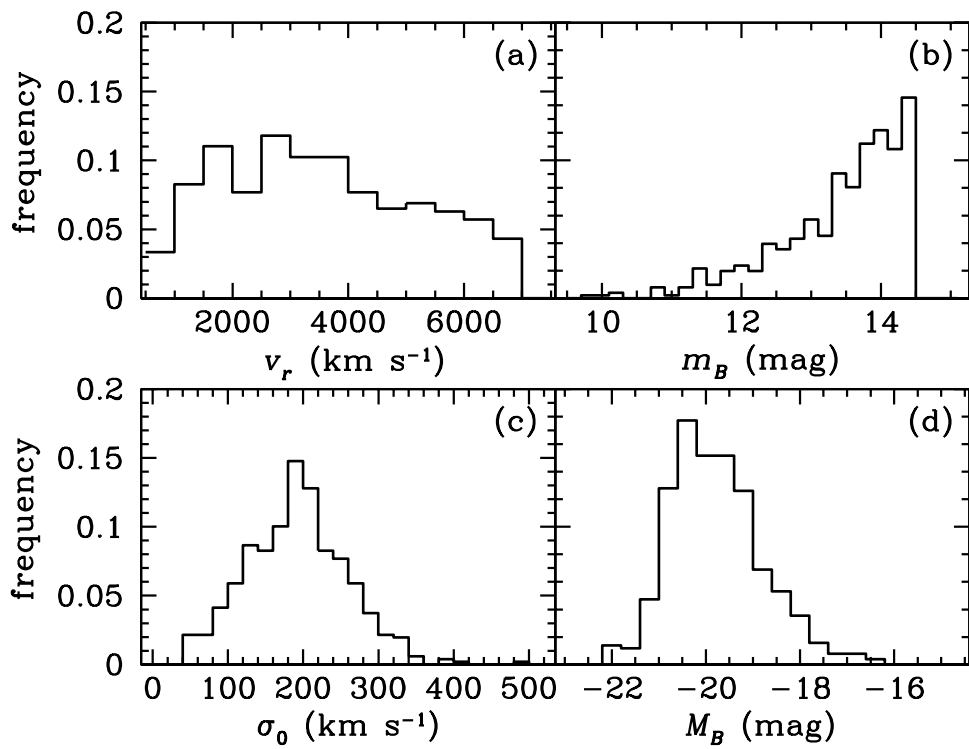


Fig. 1.— Distributions of v_r , m_B , σ_0 and M_B for the galaxies of our sample.

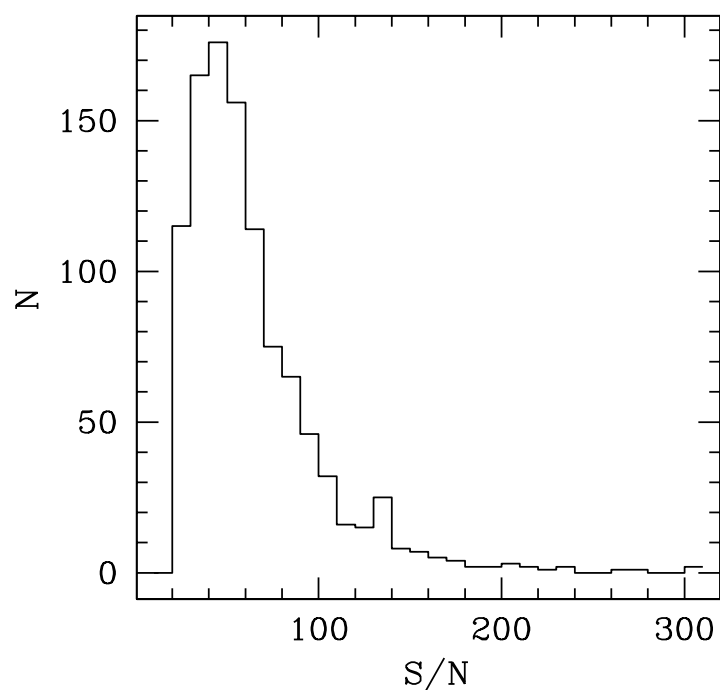


Fig. 2.— Distribution of S/N for the galaxies of our sample.

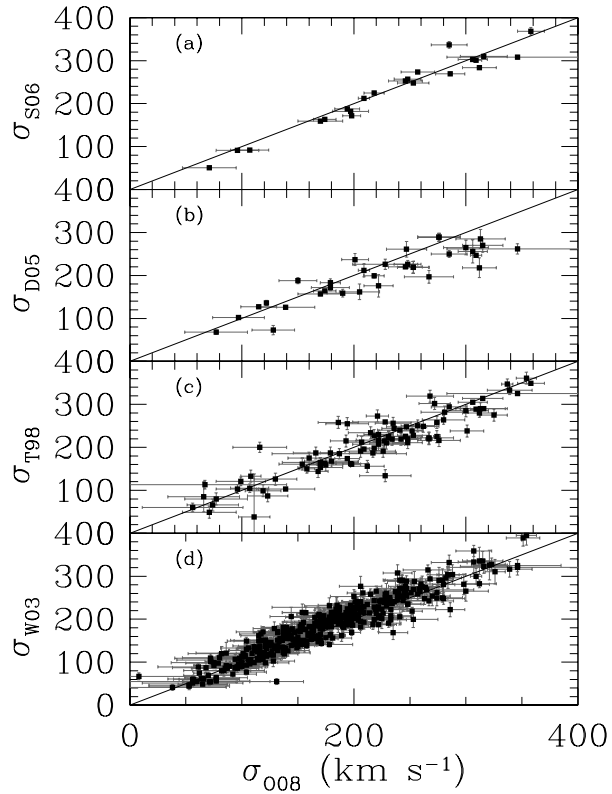


Fig. 3.— Comparison between our measurements of σ_0 (σ_{008}) and those values by Sánchez-Blázquez et al. (2006) (panel a); Denicoló et al. (2005) (panel b); Trager et al. (1998) (panel c) and Wegner et al. (2003) (panel d).

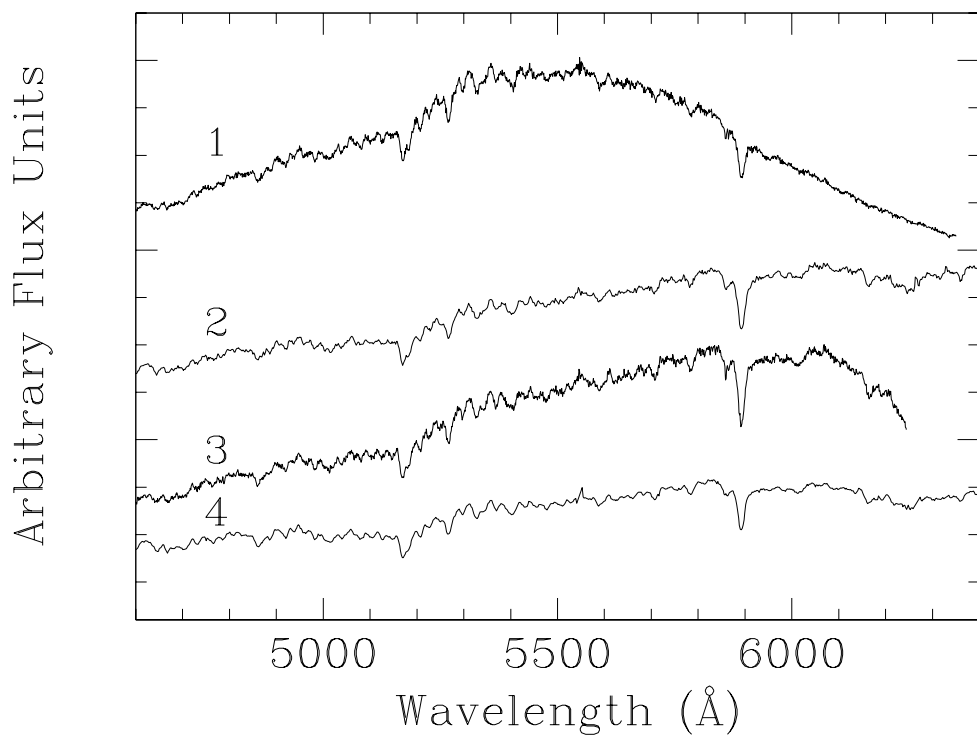


Fig. 4.— The galaxy NGC 7507 is taken as an example of the typical spectra in each of the setups mentioned in Table 4. The setup identification number is shown at the left side of each spectrum. No flux calibration was applied.

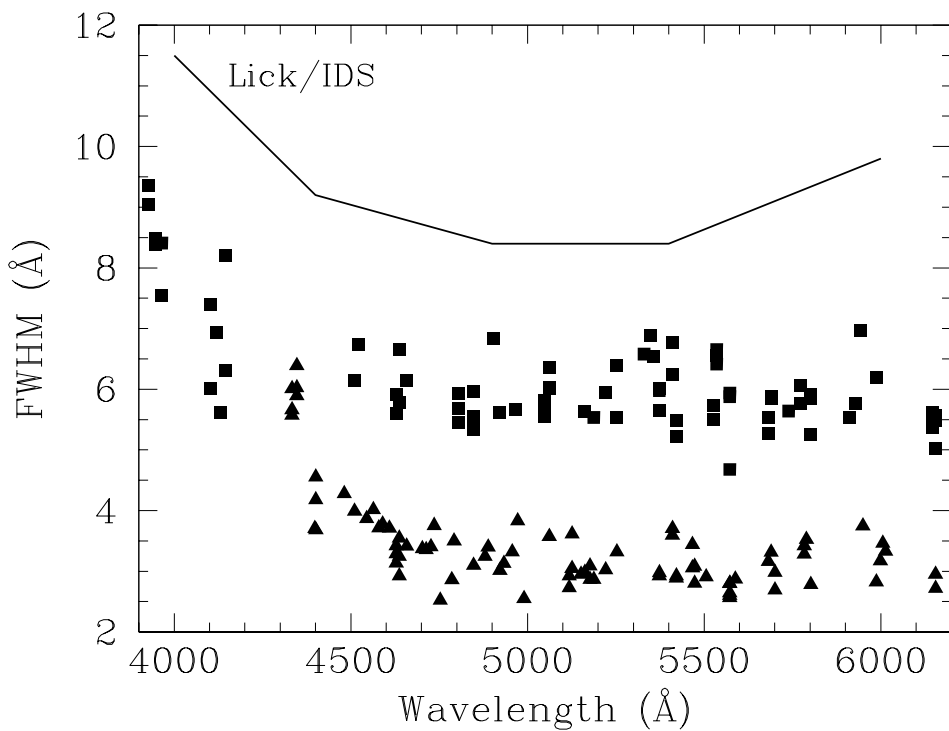


Fig. 5.— Measurements of the FWHM for lines in arc lamp spectra for 1200 l mm^{-1} (triangles) and 600 l mm^{-1} (squares) gratings. It is also shown the Lick/IDS resolution as given by Worthey & Ottaviani (1997) (continuous line).

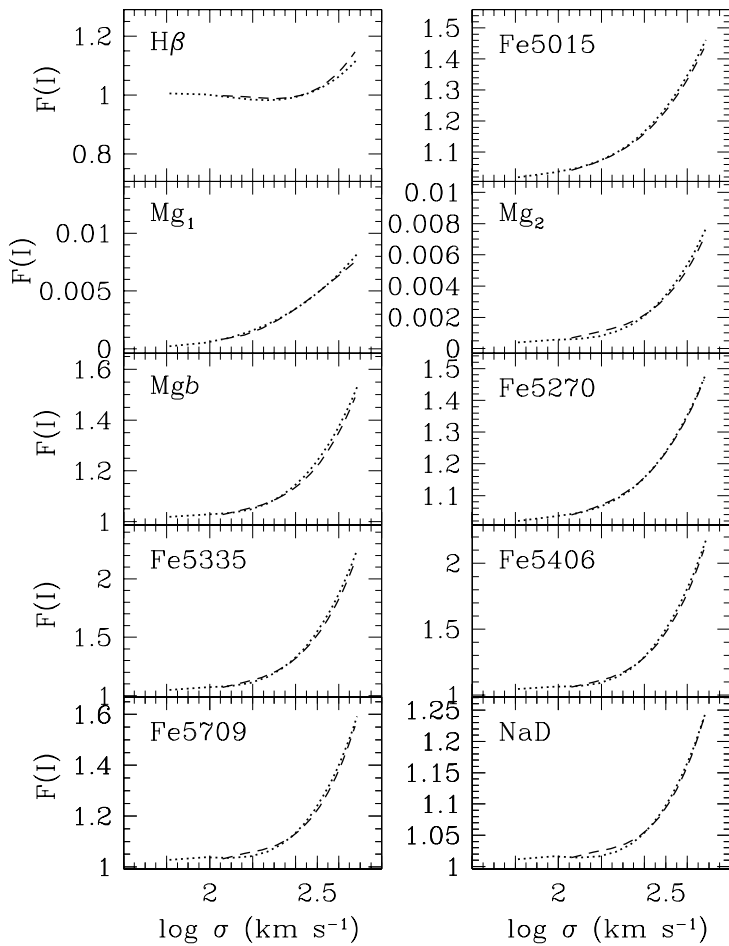


Fig. 6.— Correction factor $F(I)$ for the velocity dispersion. We show the 3rd order fits for the grating of 1200 l mm^{-1} (dotted line) and 600 l mm^{-1} (dashed line).

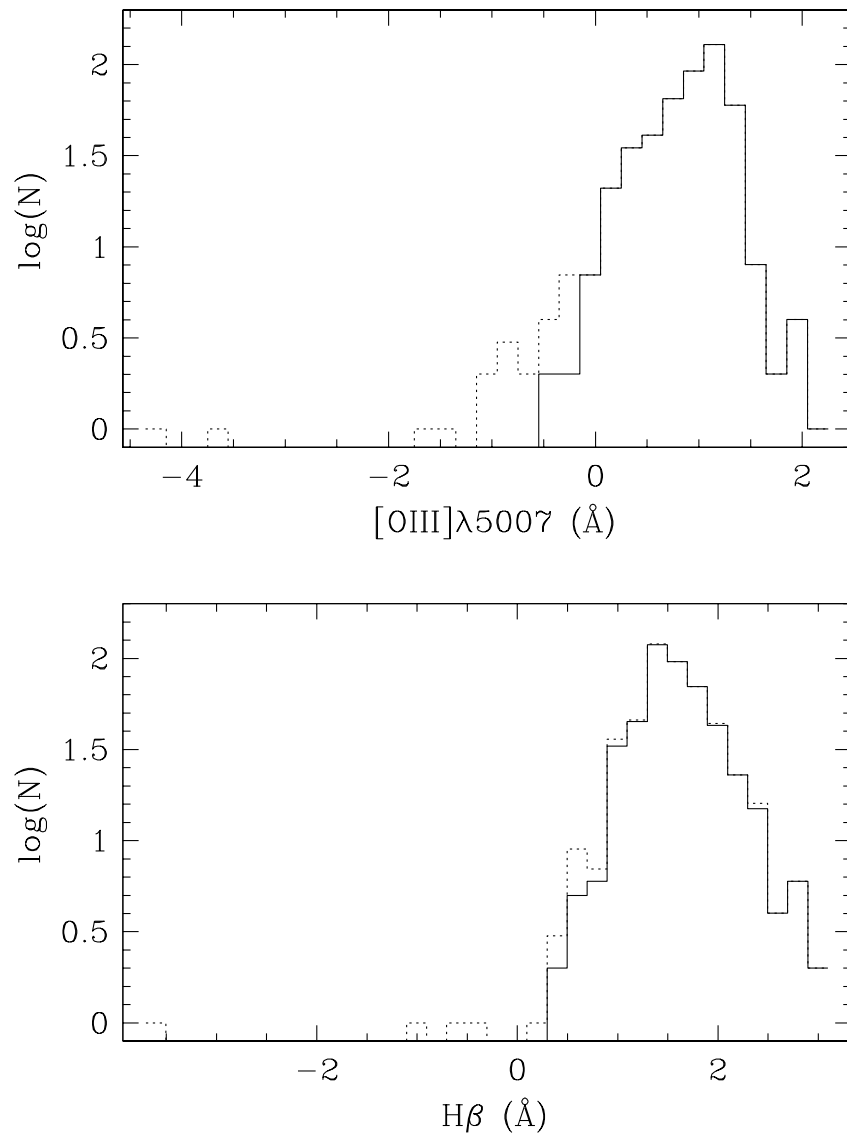


Fig. 7.— Distribution of $[\text{OIII}]\lambda 5007$ (top panel) and $H\beta$ (bottom panel) before (dotted line) and after (solid line) discarding galaxies with detected emission.

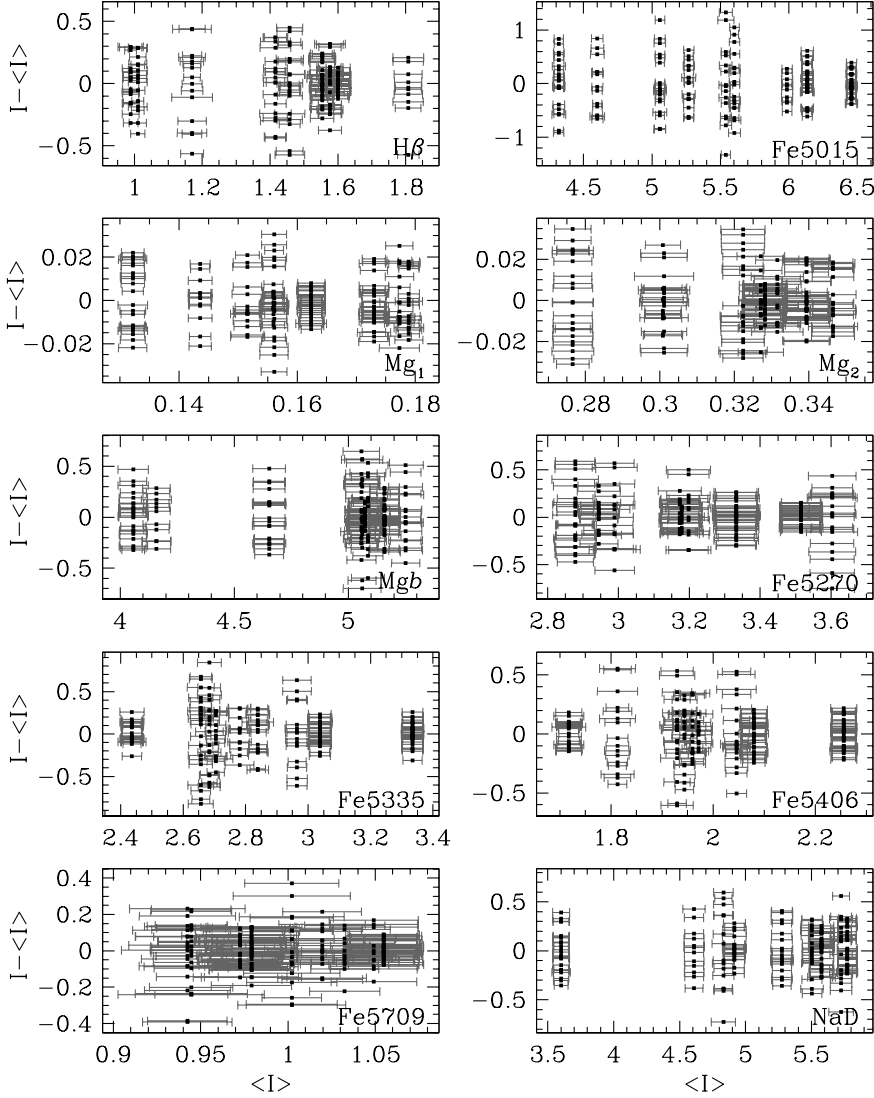


Fig. 8.— Scattering of line indices for galaxies with more than ten observations. The panels show the fractional errors ($I - \langle I \rangle$) for the various line indices versus the average line index ($\langle I \rangle$). The horizontal error bars indicate the error of each individual measure.

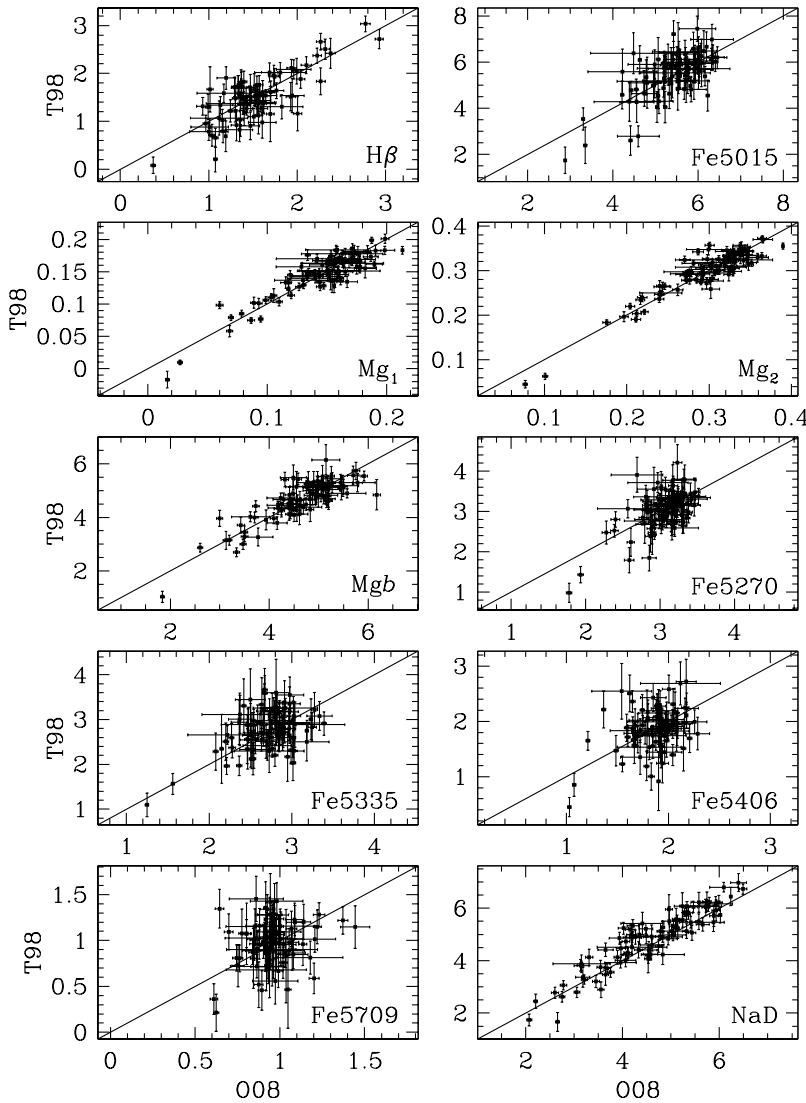


Fig. 9.— Comparison between galaxies indices measured by Trager et al. (1998) and our results (O08).

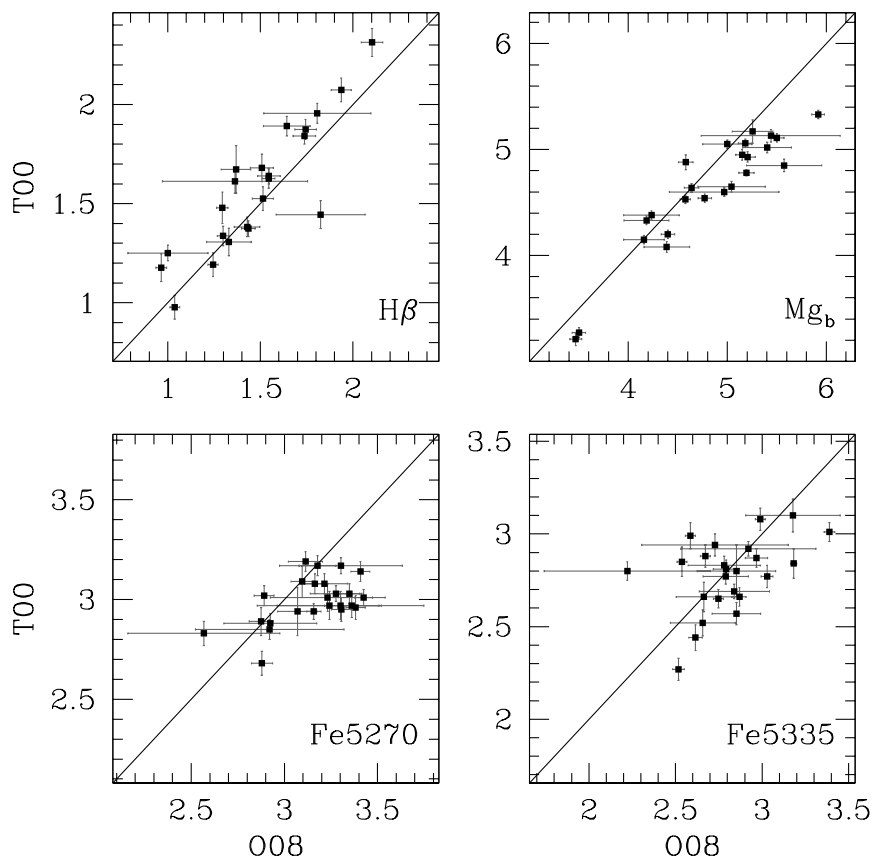


Fig. 10.— Comparison between galaxies indices measured by Trager et al. (2000a) and our results (O08).

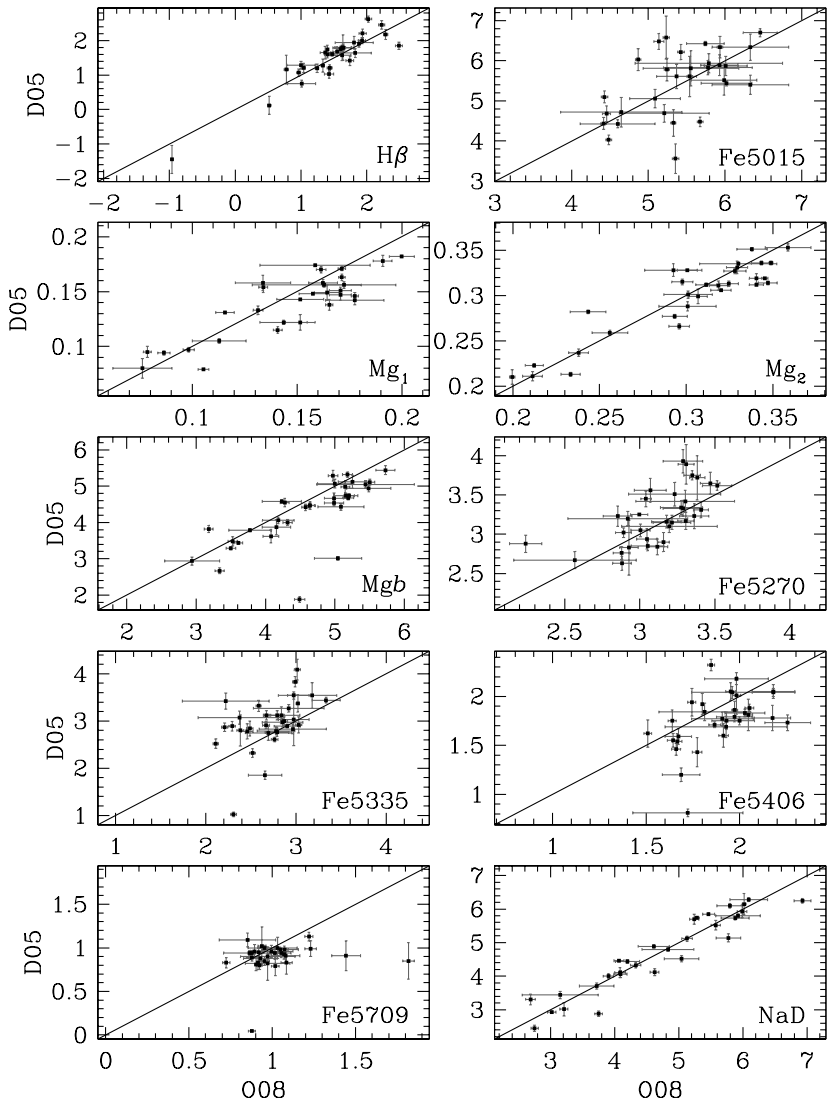


Fig. 11.— Comparison between galaxies indices measured by Denicoló et al. (2005) and our results (O08).

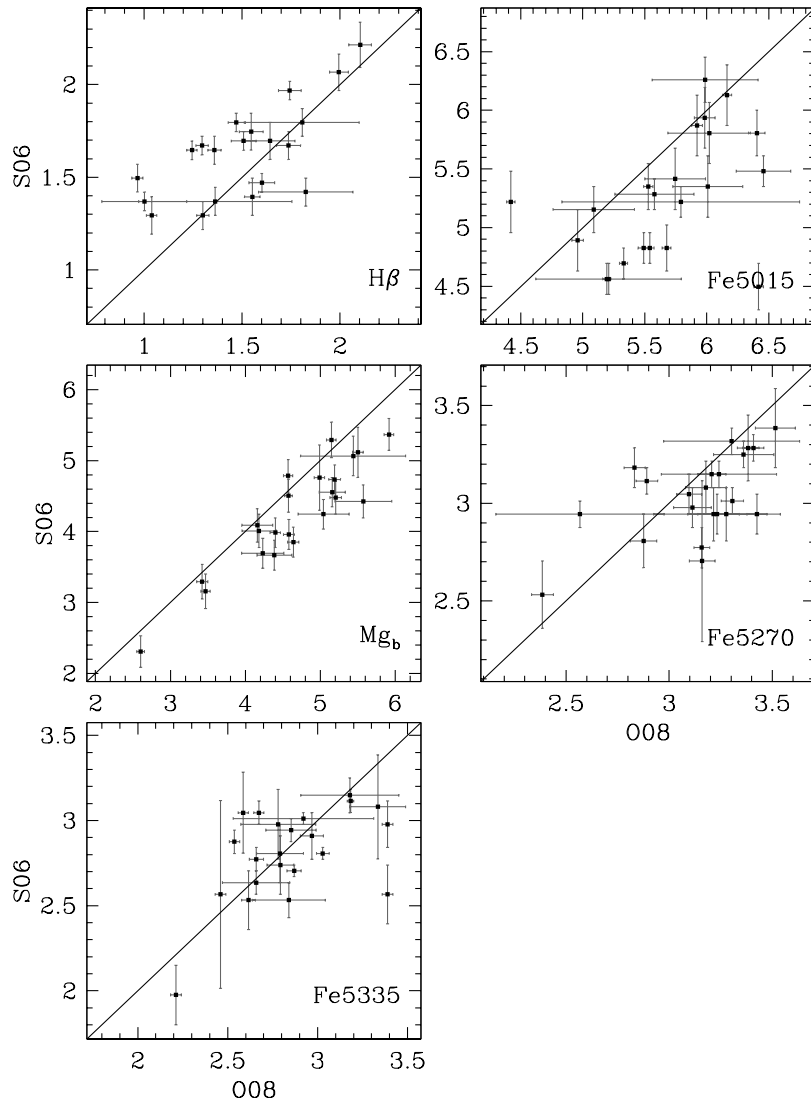


Fig. 12.— Comparison between galaxies indices measured by Sánchez-Blázquez et al. (2006) and our results (O08).

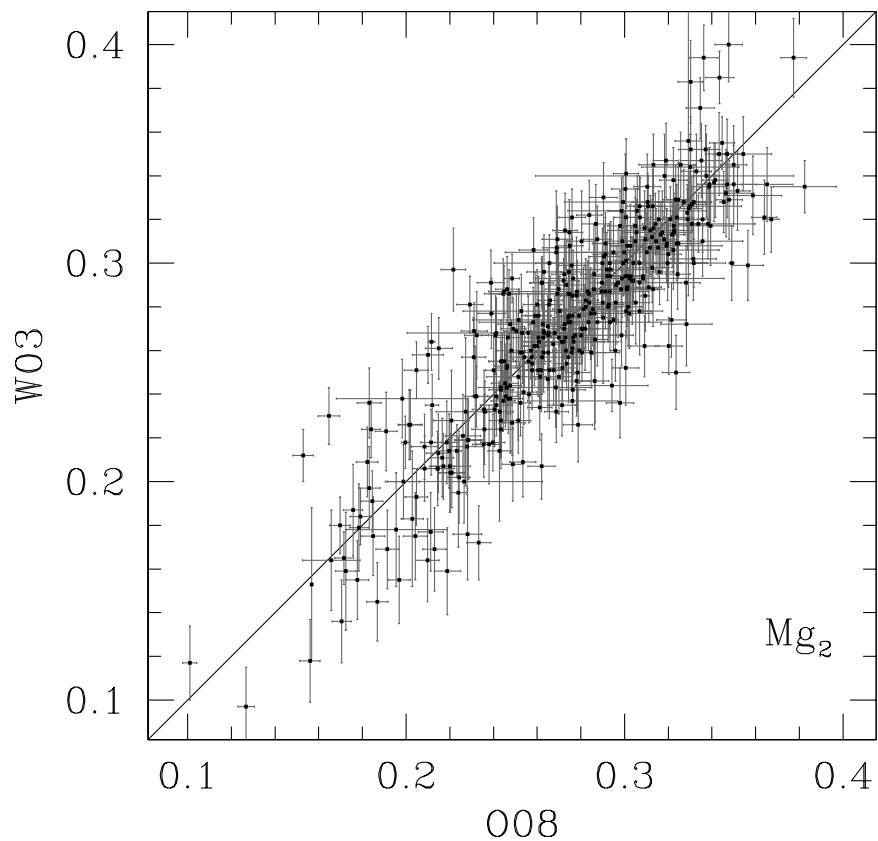


Fig. 13.— Comparison between Mg_2 index measured by Wegner et al. (2003) and our results (O08).

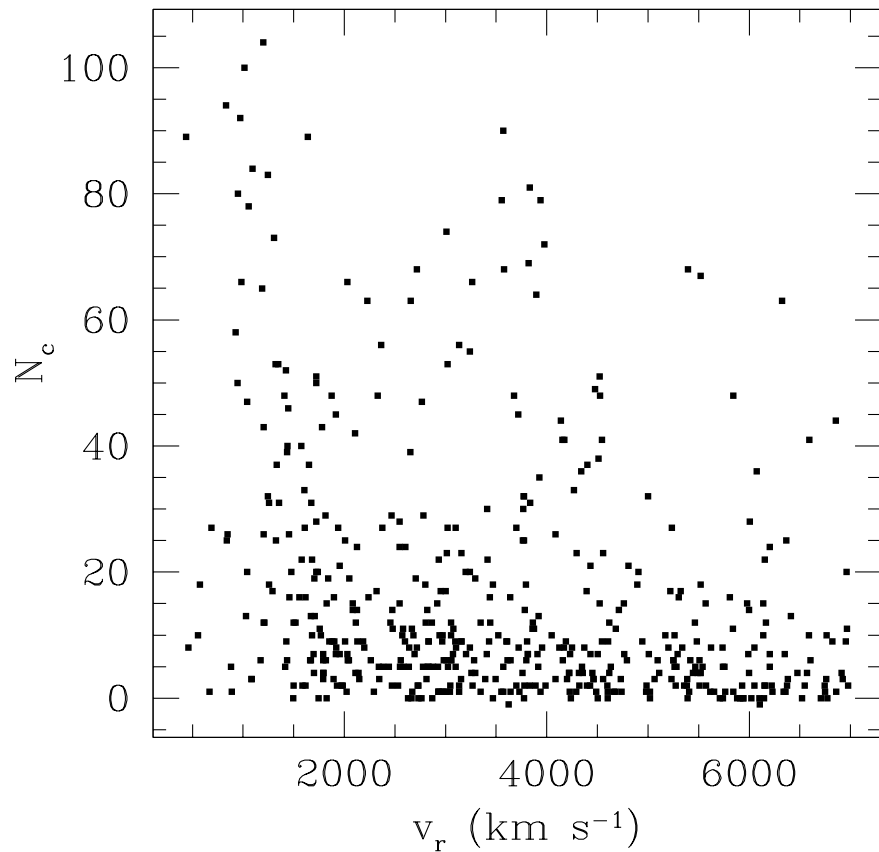


Fig. 14.— Number of companions (N_c) for the galaxies of our sample versus the radial velocity v_r . The concentration of galaxies around v_r 1000 km s⁻¹ is related to the Virgo cluster.

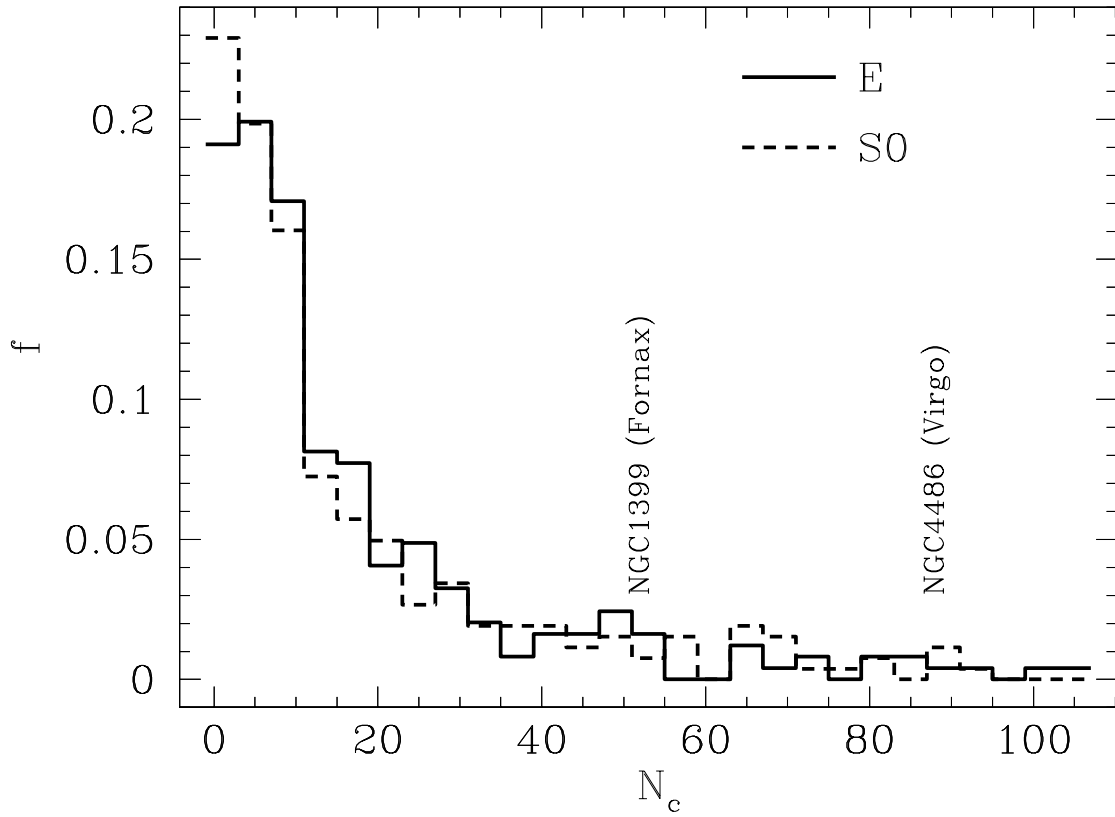


Fig. 15.— Frequency distribution of the number of companions (N_c) according to morphological type, E (continuous line) and S0 (dashed line). Two galaxies in clusters of different richness, NGC 1399 in Fornax and NGC 4486 in Virgo, indicate the sensitivity of the N_c determination method to distinct density regimes.

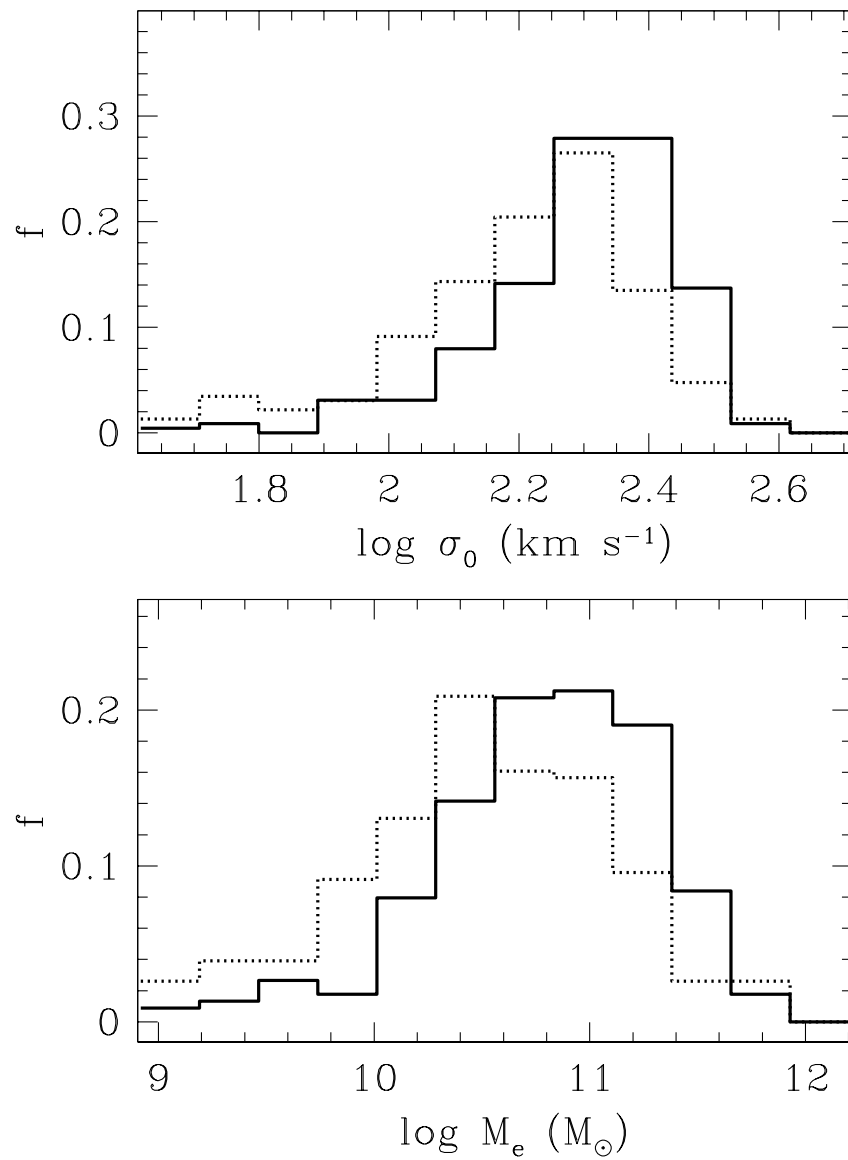


Fig. 16.— Frequency distribution of mass estimators for E (continuous line) and S0 (dotted lines).

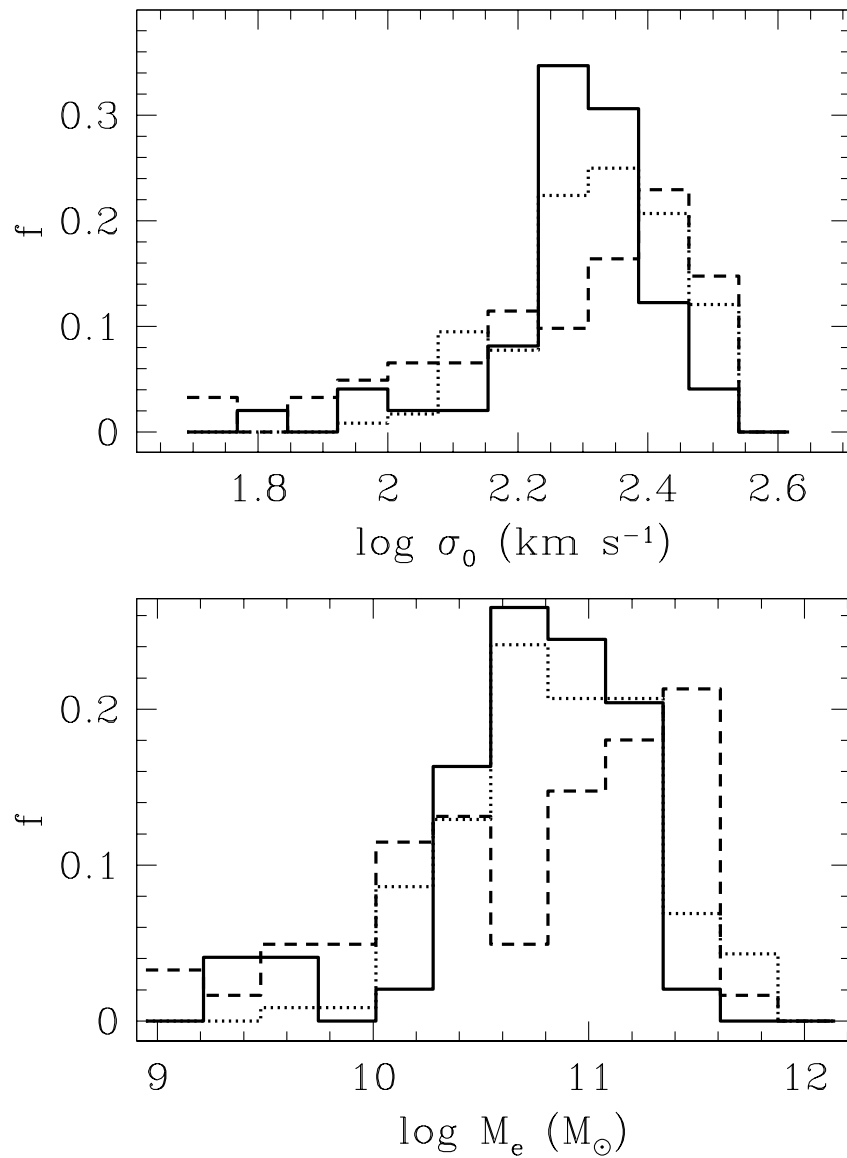


Fig. 17.— Frequency distribution of mass estimators for E galaxies in different environments: LD (continuous), MD (dotted), and HD (dashed).

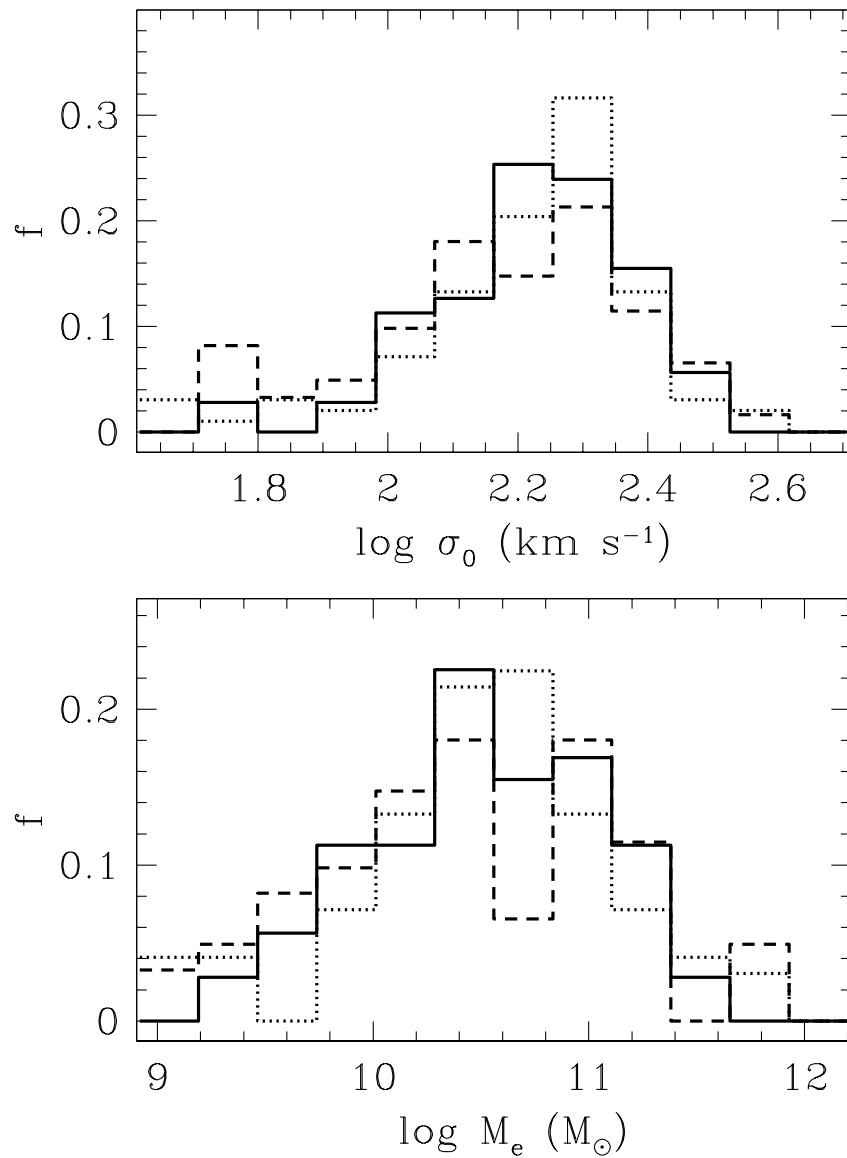


Fig. 18.— Frequency distribution of mass estimators for S0 galaxies in different environments: LD (continuous), MD (dotted), and HD (dashed).

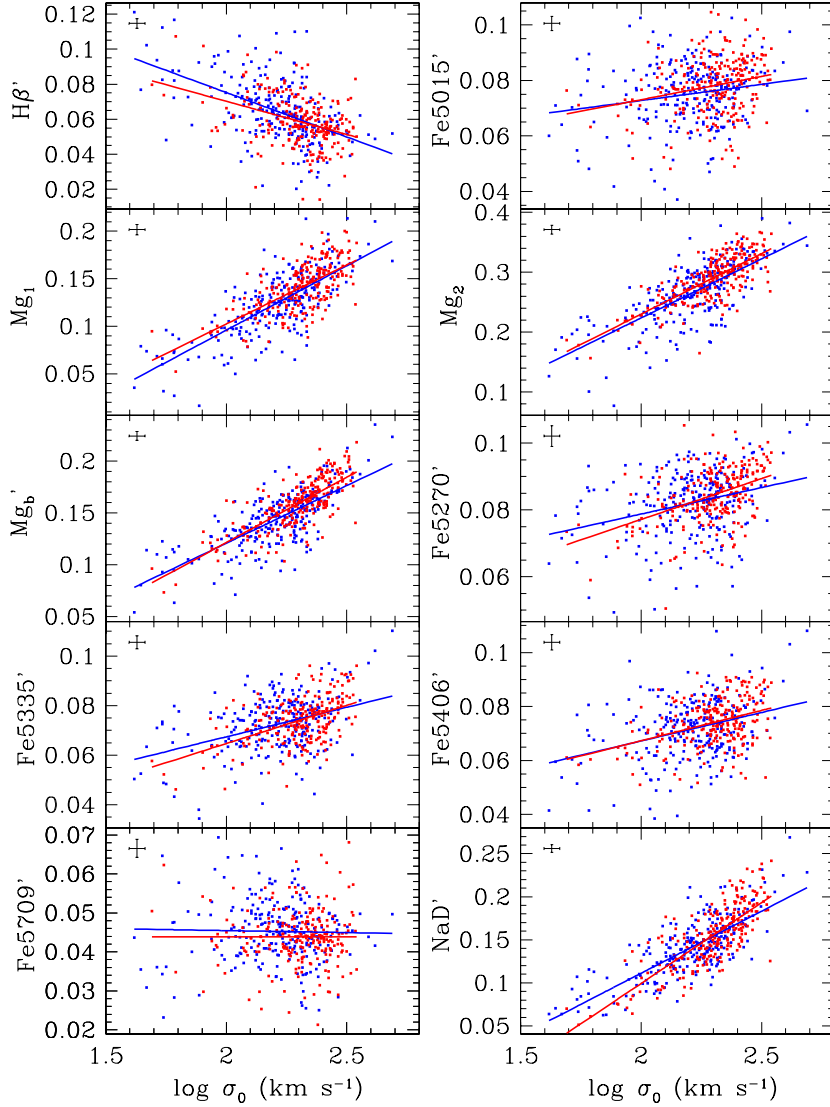


Fig. 19.— Index– $\log \sigma_0$ relations for E (red dots) and S0 (blue dots) galaxies. The ordinary least-square linear fits to the data are shown as continuous lines with the same colors as the related dots. Mean error bars are indicated in the upper left corner of each panel and indices are expressed in magnitudes.

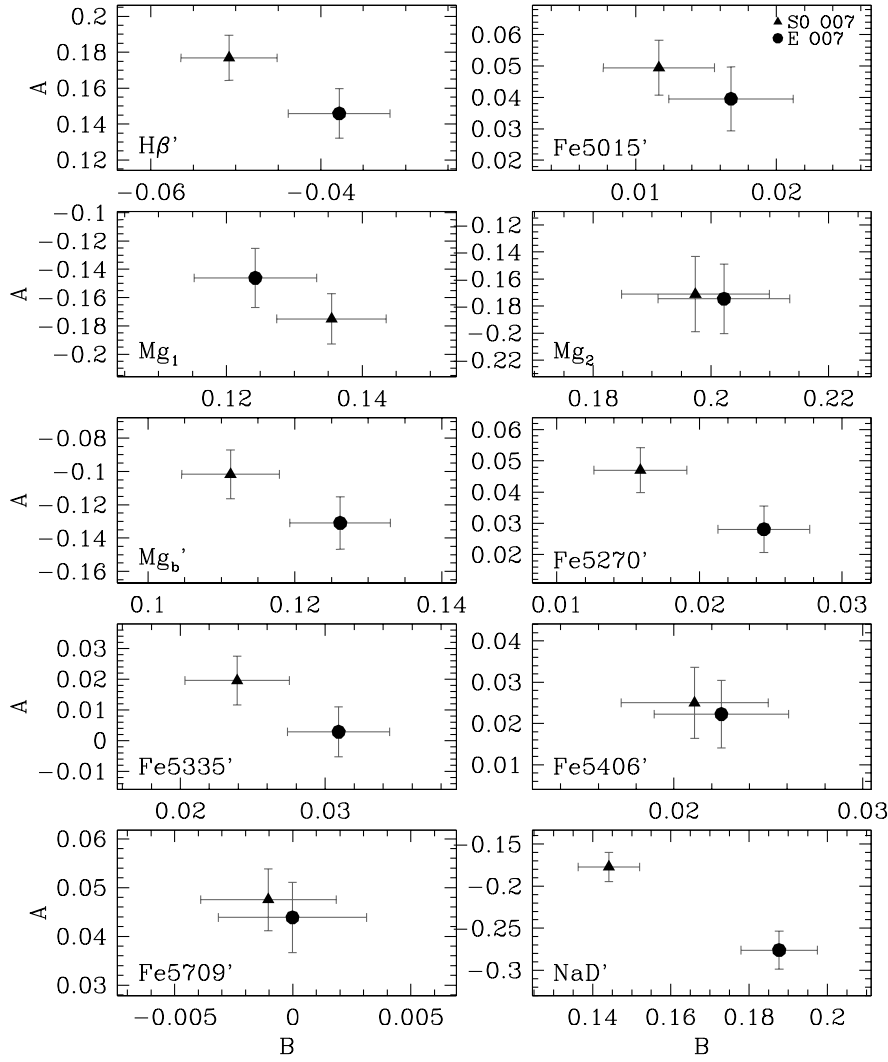


Fig. 20.— Index–log σ_0 linear fits ($I' = A + B \log \sigma_0$) coefficients for E (circle) and S0 (triangle) galaxies.

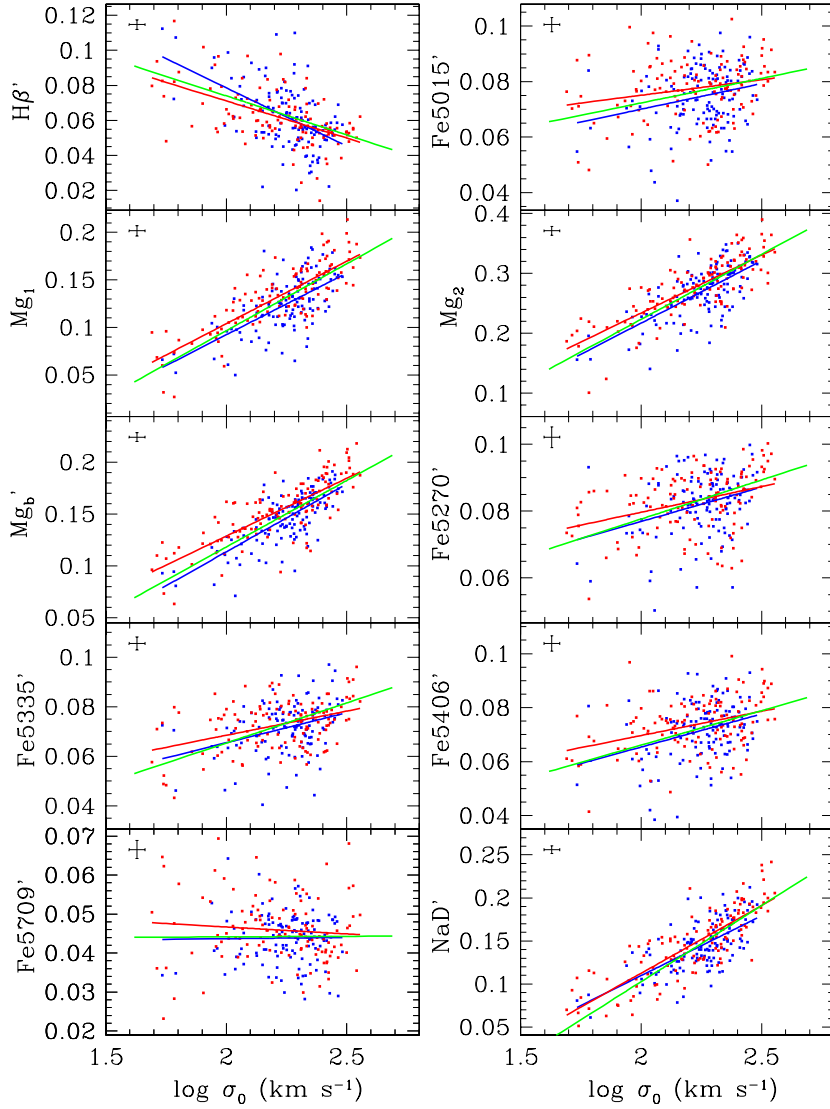


Fig. 21.— Index– $\log \sigma_0$ relations for galaxies in LD (blue dots) and HD (red dots) environments. The ordinary least-square linear fits to the data are shown as continuous lines with the same colors as the related dots. MD points were omitted for clarity, but its fit is shown as a green line. Mean error bars are indicated in the upper left corner of each panel and indices are expressed in magnitudes.

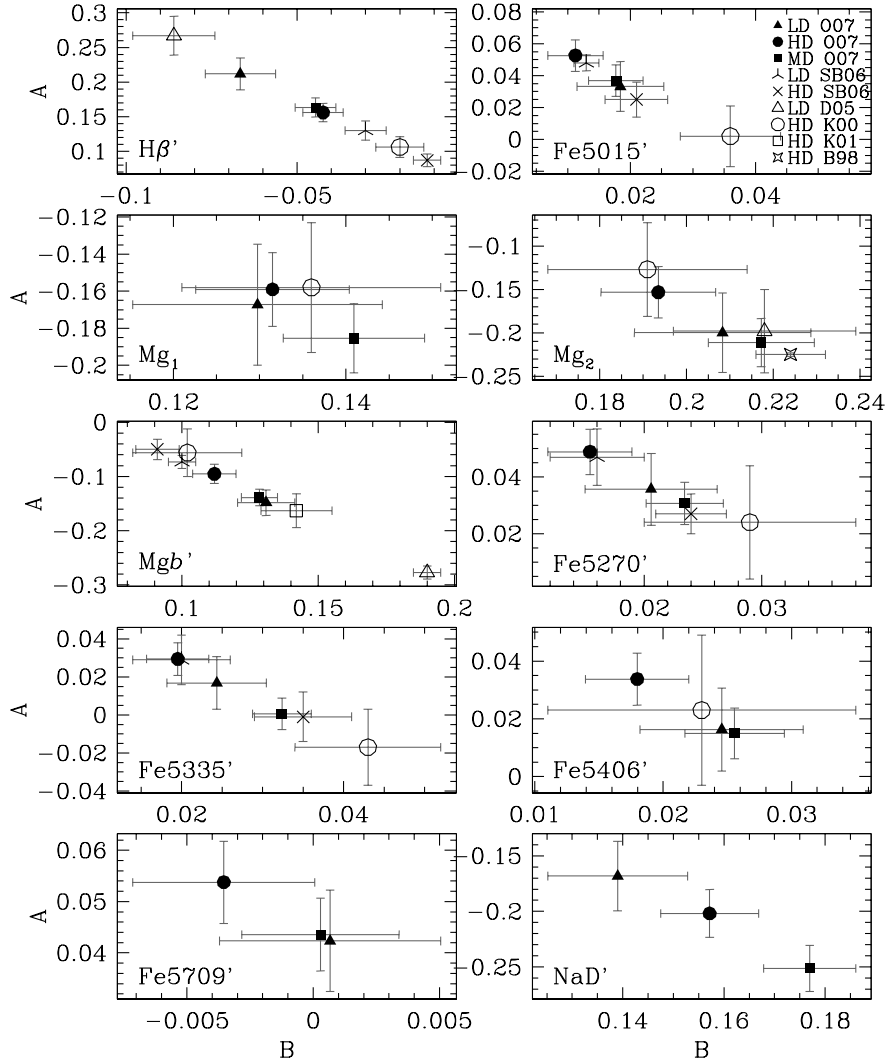


Fig. 22.— Index - $\log \sigma_0$ linear fits ($I' = A + B \log \sigma_0$) coefficients for galaxies in LD (filled triangle), MD (filled square), and HD (filled circle) environments. The other symbols displayed are SB06 - Sánchez-Blázquez et al. (2006); D05 - Denicoló et al. (2005); K00 - Kuntschner (2000); K01 - Kuntschner et al. (2001); and B98 - Bernardi et al. (1998). For those samples characterized as being made of galaxies of “isolated” or “cluster” regions, we added a LD or HD to the reference code.

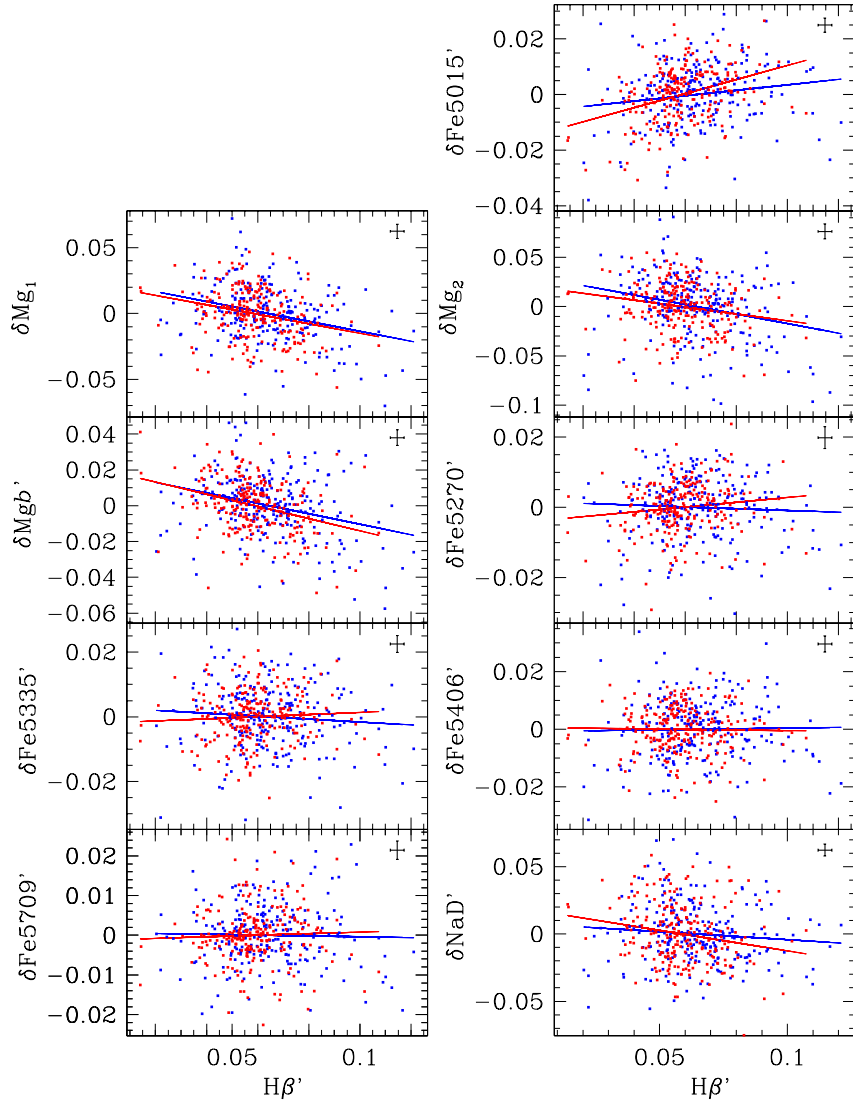


Fig. 23.— Residuals of the index– $\log \sigma_0$ relation versus $H\beta'$ for E (red dots) and S0 (blue dots) galaxies. In the upper right corner we display the mean error bar.

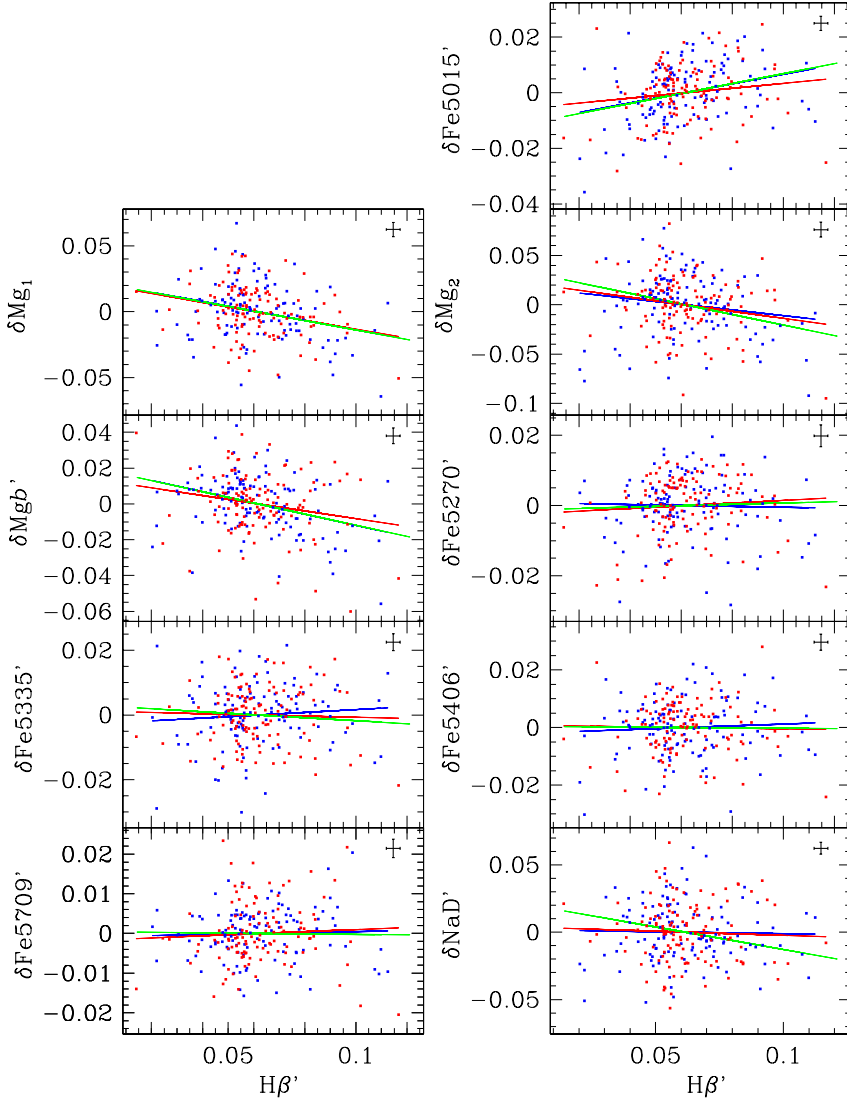


Fig. 24.— Residuals of index–log σ_0 relation versus $H\beta'$ for galaxies in LD (blue dots) and HD (red dots) environments. Related fits are also shown as continuous lines. MD points were omitted for clarity, but its fit is shown as a green line. In the upper right corner we display the mean error bar.

Table 1. Sample of Galaxies.

Name (1)	α (2000) (2)	δ (2000) (3)	T (4)	m_B (5)	v_r (km s $^{-1}$) (6)	$\log \sigma_0$ (km s $^{-1}$) (7)	$\log r_e$ (kpc) (8)	N_c (9)
NGC 7832	00 06 28.5	-03 42 58	-3	13.50	6247±12	2.340±0.096	0.725	6
NGC 0050	00 14 44.7	-07 20 44	-3	12.50	5548±15	2.413±0.020	0.750	6
NGC 0113	00 26 54.7	-02 30 05	-3	14.00	4458±19	2.185±0.046	0.356	9
NGC 0125	00 28 50.4	+02 50 23	-2	13.83	5288±18	2.064±0.094	0.539	11
NGC 0155	00 34 40.1	-10 46 01	-3	14.00	6291±21	2.250±0.051	0.700	11
ESO 242G014	00 34 32.5	-43 39 22	-2	14.00	5940±14	2.017±0.066	0.562	1
NGC 0163	00 35 59.8	-10 07 19	-3	13.50	6028±21	2.301±0.043	0.782	16
NGC 0179	00 37 46.4	-17 51 01	-5	13.90	6004±20	2.393±0.022	...	1
NGC 0193	00 39 18.3	+03 19 53	-3	14.30	4414±15	2.286±0.028	0.840	18
MCG -01-03-018	00 50 27.6	-05 51 32	-3	13.50	5763±23	2.279±0.043	0.631	2
NGC 0273	00 50 48.5	-06 53 10	-2	13.50	4855±21	2.371±0.023	0.287	2
NGC 0277	00 51 17.2	-08 35 50	-2	14.00	4322±26	2.228±0.003	0.663	5
MCG -01-03-049	00 58 11.0	-08 13 01	-3	14.50	4599±19	2.248±0.035	0.291	3
IC 1609	00 59 47.4	-40 19 56	-2	14.30	7016±25	2.255±0.021	0.640	3
NGC 0349	01 01 50.8	-06 48 01	-3	14.00	5986±18	1.875±0.089	...	8
IC 1628	01 08 47.2	-28 34 55	-3	14.40	5704±28	2.288±0.039	0.561	9
NGC 0430	01 12 59.4	-00 15 08	-5	13.60	5319±21	2.400±0.017	0.455	18
NGC 0442	01 14 38.5	-01 01 14	-2	14.50	5588±16	2.267±0.009	1.429	16
NGC 0448	01 15 15.9	-01 37 30	-2	13.20	1931±19	2.064±0.053	0.051	3
IC 0090	01 16 30.6	-07 58 39	-3	14.50	5666±21	2.320±0.032	0.417	3
NGC 0474	01 20 06.8	+03 25 00	-2	12.51	2383±18	2.279±0.031	1.034	6
NGC 0502	01 22 55.4	+09 02 54	-2	13.80	2568±21	2.137±0.042	0.180	16
NGC 0516	01 24 08.3	+09 33 05	-2	14.30	2451±18	1.724±0.225	0.026	13
NGC 0533	01 25 31.5	+01 45 35	-5	13.44	5538±27	2.428±0.033	1.097	19
NGC 0541	01 25 44.4	-01 22 42	-2	14.00	5414±21	2.338±0.029	0.886	69
NGC 0547	01 26 48.0	-01 20 38	-5	13.40	5572±16	2.474±0.032	0.787	68
NGC 0584	01 31 20.9	-06 52 06	-3	12.50	1895±19	2.338±0.018	0.328	10
NGC 0599	01 32 53.8	-12 11 29	-3	14.00	5527±21	2.210±0.038	0.775	5
NGC 0596	01 32 52.1	-07 01 57	-3	12.00	1883±17	2.230±0.079	0.320	10
UGC 01169	01 38 47.0	+01 04 19	-2	14.20	5032±23	2.250±0.048	0.083	3
NGC 0641	01 38 39.4	-42 31 35	-5	13.00	6433±31	2.387±0.037	0.744	14
NGC 0636	01 39 06.6	-07 30 47	-3	13.00	1909±11	2.294±0.034	0.336	9
ESO 244G045	01 38 58.4	-46 34 30	-3	14.00	6610±19	2.255±0.033	0.650	7
IC 1729	01 47 55.5	-26 53 29	-3	13.00	1519±25	2.173±0.006	0.483	3
NGC 0682	01 49 04.5	-14 58 30	-3	14.00	5602±19	2.253±0.030	0.392	2
NGC 0686	01 48 56.4	-23 47 55	-2	14.00	4681±11	2.326±0.030	0.439	2
IC 0164	01 49 08.4	-03 54 18	-3	14.00	5281±20	2.314±0.006	0.548	7
UGC 01325	01 51 37.2	+08 15 25	-5	14.20	5534±23	2.352±0.026	...	5
NGC 0720	01 53 24.0	-13 44 21	-3	12.00	1782±21	2.393±0.031	0.457	5
NGC 0731	01 54 56.2	-09 00 39	-5	14.00	3914±19	2.185±0.033	0.250	3
NGC 0770	01 59 13.2	+18 57 18	-5	14.20	2530±19	1.875±0.178	-0.344	3
NGC 0774	01 59 35.0	+14 00 30	-3	14.40	4620±19	2.276±0.029	0.789	6
NGC 0790	02 01 21.6	-05 22 16	-2	14.00	5328±23	2.236±0.039	0.674	9
NGC 0809	02 04 19.0	-08 44 08	-2	14.50	5367±18	2.155±0.043	0.289	4

Table 1—Continued

Name (1)	α (2000) (2)	δ (2000) (3)	T (4)	m_B (5)	v_r (km s $^{-1}$) (6)	$\log \sigma_0$ (km s $^{-1}$) (7)	$\log r_e$ (kpc) (8)	N_c (9)
NGC 0822	02 06 39.3	−41 09 27	−5	14.10	5430±19	2.236±0.034	0.407	7
NGC 0821	02 08 21.1	+10 59 44	−3	12.59	1750±10	2.320±0.010	0.661	1
NGC 0830	02 08 58.8	−07 46 05	−3	14.50	3891±28	2.086±0.066	0.428	12
NGC 0842	02 09 49.3	−07 46 57	−2	14.50	3857±19	2.176±0.039	0.383	12
NGC 0862	02 13 02.9	−42 02 00	−3	14.10	5395±18	2.182±0.043	0.285	3
NGC 0875	02 17 05.0	+01 14 39	−3	14.20	6471±11	2.262±0.021	0.575	4
NGC 0883	02 19 05.3	−06 47 31	−3	13.50	5443±19	2.435±0.022	0.620	5
MCG -02-07-002	02 21 47.4	−10 01 24	−3	14.50	5233±21	2.330±0.024	0.224	4
NGC 0936	02 27 37.6	−01 09 17	−2	11.28	1450±22	2.336±0.040	0.351	10
NGC 0940	02 29 27.5	+31 38 24	−2	13.40	5190±23	2.279±0.035	...	11
IC 0232	02 31 11.4	+01 15 57	−2	14.20	6396±20	2.297±0.026	0.611	26
NGC 0968	02 34 06.3	+34 28 47	−5	13.80	3589±23	2.246±0.033	0.708	10
NGC 0969	02 34 08.0	+32 56 51	−2	13.50	4508±25	2.236±0.041	0.637	16
NGC 0978A	02 34 47.1	+32 50 45	−3	13.30	4746±24	2.394±0.024	...	16
ESO 545G042	02 39 29.3	−19 50 32	−2	14.20	4681±21	2.086±0.060	0.960	2
NGC 1052	02 41 04.9	−08 15 22	−5	12.50	1493±37	2.346±0.025	0.400	9
IC 1858	02 49 08.5	−31 17 24	−2	13.70	6082±21	2.188±0.048	0.814	37
IC 1860	02 49 34.6	−31 11 25	−5	12.90	6917±28	2.387±0.031	1.046	45
NGC 1132	02 52 51.6	−01 16 33	−2	13.90	7009±21	2.303±0.025	1.131	12
IC 1864	02 53 39.6	−34 11 49	−5	14.00	4590±24	2.286±0.037	0.413	10
NGC 1162	02 58 56.0	−12 23 56	−5	14.00	3936±46	2.272±0.020	0.541	8
NGC 1172	03 01 36.1	−14 50 13	−2	13.50	1594±20	1.826±0.320	0.667	7
NGC 1199	03 03 38.5	−15 36 50	−3	13.00	2726±15	2.346±0.043	0.585	9
NGC 1200	03 03 54.6	−11 59 32	−2	14.00	4063±26	2.305±0.082	0.754	11
NGC 1201	03 04 08.3	−26 04 03	−2	11.84	1686±11	2.253±0.030	0.118	11
NGC 1209	03 06 03.1	−15 36 42	−5	13.00	2658±28	2.360±0.028	0.429	9
ESO 417G021	03 13 16.0	−31 39 08	−3	14.10	4190±30	2.303±0.033	0.266	7
NGC 1297	03 19 14.1	−19 06 04	−2	12.87	1586±12	2.057±0.077	0.645	23
NGC 1298	03 20 12.9	−02 06 44	−5	14.20	6547±27	2.220±0.038	0.594	3
NGC 1315	03 23 06.5	−21 22 34	−2	13.70	1615±23	1.886±0.143	0.215	28
NGC 1332	03 26 17.3	−21 20 09	−2	11.46	1600±14	2.528±0.006	0.586	34
NGC 1331	03 26 28.3	−21 21 22	−5	14.46	1210±20	1.778±0.319	0.021	44
NGC 1336	03 26 31.1	−35 42 52	−3	13.80	1451±20	1.924±0.155	0.378	47
NGC 1339	03 28 06.5	−32 17 10	−3	12.63	1335±21	2.188±0.056	0.116	38
NGC 1344	03 28 19.1	−31 04 05	−3	11.51	1208±17	2.276±0.007	0.324	27
NGC 1351	03 30 34.8	−34 51 12	−3	12.91	1730±19	2.158±0.064	0.315	51
ESO 548G033	03 32 28.4	−18 56 49	−2	14.10	1677±21	1.964±0.089	0.262	38
NGC 1366	03 33 53.3	−31 11 36	−2	13.13	1231±19	2.064±0.056	−0.109	32
NGC 1374	03 35 16.7	−35 13 35	−5	12.56	1325±21	2.220±0.049	0.251	54
ESO 358G025	03 35 33.4	−32 27 54	−2	14.10	1433±30	2.117±0.073	...	40
NGC 1379	03 36 03.3	−35 26 26	−5	12.33	1354±10	2.033±0.035	0.295	54
NGC 1380	03 36 26.9	−34 58 33	−2	11.36	1890±19	2.346±0.037	0.621	49
NGC 1381	03 36 31.5	−35 17 39	−2	12.60	1731±19	2.170±0.060	0.074	52
NGC 1389	03 37 11.8	−35 44 42	−2	12.65	956±19	2.137±0.067	0.068	51

Table 1—Continued

Name (1)	α (2000) (2)	δ (2000) (3)	T (4)	m_B (5)	v_r (km s $^{-1}$) (6)	$\log \sigma_0$ (km s $^{-1}$) (7)	$\log r_e$ (kpc) (8)	N_c (9)
NGC 1383	03 37 38.8	-18 20 19	-2	14.00	2001±21	2.176±0.059	0.308	28
NGC 1395	03 38 29.6	-23 01 40	-5	11.44	1734±17	2.438±0.003	0.607	29
NGC 1393	03 38 38.6	-18 25 40	-2	13.80	2151±17	2.013±0.121	0.211	25
NGC 1399	03 38 29.0	-35 26 58	-5	11.11	1448±22	2.530±0.025	0.604	53
NGC 1394	03 39 06.7	-18 17 36	-2	14.30	4234±58	2.262±0.012	0.121	5
NGC 1404	03 38 51.7	-35 35 36	-5	11.46	1954±26	2.438±0.005	0.450	46
NGC 1403	03 39 11.3	-22 23 18	-5	12.90	4272±46	2.230±0.013	0.482	2
NGC 1411	03 38 45.0	-44 06 00	-2	11.96	1031±16	2.176±0.047	...	14
NGC 1400	03 39 31.3	-18 41 19	-3	12.34	573±25	2.447±0.029	0.502	19
NGC 1407	03 40 12.4	-18 34 52	-3	11.06	1816±12	2.477±0.028	0.876	30
NGC 1412	03 40 29.0	-26 51 41	-2	13.90	1811±22	2.017±0.069	-0.095	11
NGC 1419	03 40 42.7	-37 30 42	-5	14.30	1593±20	2.097±0.043	0.014	41
NGC 1427	03 42 19.6	-35 23 36	-3	12.20	1451±23	2.230±0.010	0.334	49
UGC 02836	03 43 57.0	+39 17 42	-2	13.80	5007±31	2.204±0.051	...	3
NGC 1426	03 42 49.3	-22 06 37	-3	12.57	1461±17	2.225±0.023	0.428	41
NGC 1439	03 44 50.4	-21 55 21	-2	12.84	1689±11	2.199±0.019	0.342	32
ESO 358G059	03 45 03.4	-35 58 22	-5	14.10	1021±17	1.813±0.127	-0.102	48
NGC 1453	03 46 27.3	-03 58 10	-5	13.50	3962±23	2.455±0.024	0.689	14
NGC 1461	03 48 27.1	-16 23 30	-2	13.50	1472±20	2.303±0.039	0.468	17
IC 2006	03 54 28.4	-35 58 02	-3	12.53	1361±20	2.140±0.067	0.286	32
NGC 1521	04 08 19.0	-21 03 06	-3	12.66	4243±12	2.364±0.007	0.643	5
NGC 1527	04 08 24.4	-47 53 50	-2	11.96	1212±17	2.279±0.031	...	13
IC 2035	04 09 01.5	-45 31 04	-2	12.44	1494±13	2.061±0.033	-0.619	13
NGC 1537	04 13 41.0	-31 38 46	-3	11.88	1429±18	2.243±0.036	0.178	6
NGC 1549	04 15 45.1	-55 35 31	-5	11.13	1256±12	2.364±0.009	0.410	19
NGC 1553	04 16 10.4	-55 46 51	-2	10.73	1292±16	2.348±0.025	0.518	18
NGC 1550	04 19 38.3	+02 24 35	-5	14.00	3825±54	2.450±0.021	0.710	15
NGC 1567	04 21 08.7	-48 15 16	-3	14.00	4633±19	2.155±0.057	0.346	5
NGC 1574	04 21 59.1	-56 58 26	-2	11.56	1041±16	2.342±0.025	0.184	21
NGC 1596	04 27 37.8	-55 01 37	-2	12.16	1557±12	2.299±0.002	...	17
NGC 1595	04 28 21.8	-47 48 57	-5	13.66	4812±12	2.281±0.051	0.460	7
NGC 1600	04 31 39.9	-05 05 16	-3	13.50	4752±12	2.539±0.073	0.995	15
ESO 084G028	04 37 18.1	-62 34 59	-3	14.00	6369±20	2.274±0.031	0.624	8
NGC 1653	04 45 47.6	-02 23 29	-5	12.90	4363±30	2.369±0.011	0.592	6
MCG -02-13-009	04 48 12.7	-13 40 03	-3	14.50	5668±11	2.246±0.045	0.877	2
IC 0395	04 49 33.8	+00 15 14	-2	13.90	6322±24	2.294±0.042	0.454	2
NGC 1713	04 58 51.1	-00 29 30	-3	13.90	4465±40	2.288±0.041	0.881	22
NGC 1700	04 56 56.2	-04 52 03	-5	12.39	3946±18	2.391±0.026	0.474	6
ESO 486G019	05 03 16.5	-22 49 56	-2	14.30	4619±40	2.297±0.056	0.021	2
NGC 1930	05 25 56.6	-46 43 47	-3	13.10	4353±35	2.279±0.050	0.502	3
NGC 1979	05 34 01.2	-23 18 32	-3	12.85	1699±18	2.140±0.036	0.274	5
ESO 423G024	05 34 41.6	-29 13 59	-3	13.13	3971±28	2.230±0.013	0.252	2
NGC 1993	05 35 25.4	-17 48 56	-3	13.41	3144±34	2.170±0.039	0.414	3
NGC 2073	05 45 53.8	-22 00 00	-3	13.44	3026±19	2.155±0.051	0.322	2

Table 1—Continued

Name (1)	α (2000) (2)	δ (2000) (3)	T (4)	m_B (5)	v_r (km s $^{-1}$) (6)	$\log \sigma_0$ (km s $^{-1}$) (7)	$\log r_e$ (kpc) (8)	N_c (9)
NGC 2106	05 50 46.4	−21 34 03	−2	13.12	1969±17	2.104±0.061	0.375	8
NGC 2191	06 08 23.8	−52 30 40	−2	13.26	4512±29	2.286±0.028	0.172	1
ESO 425G014	06 13 02.7	−27 43 53	−2	13.62	2942±50	2.310±0.006	0.230	2
NGC 2211	06 18 30.5	−18 32 16	−2	13.70	2003±20	2.193±0.040	−0.069	3
ESO 489G035	06 18 59.3	−24 37 48	−3	13.55	2798±40	2.393±0.021	0.311	3
ESO 489G037	06 19 17.5	−24 27 56	−2	13.56	2761±18	2.121±0.053	0.069	3
ESO 425G019	06 21 26.2	−28 06 53	−3	13.38	6727±75	2.380±0.021	0.524	1
ESO 490G006	06 29 13.8	−26 29 45	−2	13.88	6792±22	2.274±0.035	0.966	1
NGC 2267	06 40 51.9	−32 28 54	−2	13.24	1545±18	2.182±0.043	0.463	1
NGC 2272	06 42 41.7	−27 27 31	−3	12.74	2134±69	2.230±0.020	0.386	15
ESO 491G006	06 53 02.3	−26 31 33	−3	13.58	2432±22	2.338±0.023	0.332	15
ESO 058G019	06 52 56.8	−71 45 45	−3	13.59	4247±22	2.111±0.060	0.634	1
NGC 2325	07 02 40.5	−28 41 50	−3	12.17	2185±22	2.358±0.042	0.846	10
ESO 428G011	07 15 31.2	−29 21 32	−5	13.31	2110±52	2.299±0.030	0.227	13
ESO 367G008	07 16 39.0	−35 22 25	−2	13.66	2790±24	2.348±0.025	0.725	4
IC 2200A	07 28 06.7	−62 21 45	−2	13.74	3286±19	2.083±0.063	0.048	9
ESO 208G021	07 33 56.6	−50 26 31	−3	12.01	1085±18	2.356±0.040	0.258	4
NGC 2502	07 55 52.2	−52 18 27	−2	13.09	1105±20	2.233±0.005	0.131	4
IC 0494	08 06 24.4	+01 02 10	−2	14.30	4607±20	2.025±0.092	0.350	4
UGC 04228	08 06 47.9	+05 18 29	−2	13.90	4481±18	2.204±0.049	0.349	3
ESO 124G014	08 09 12.3	−61 39 36	−3	14.09	3045±20	2.301±0.023	0.388	2
ESO 494G031	08 10 35.2	−22 42 32	−2	14.15	5444±22	2.415±0.024	0.863	1
MCG -02-22-008	08 23 36.5	−15 02 11	−2	14.50	4602±33	2.250±0.048	0.710	1
IC 0513	08 33 05.3	−12 21 19	−2	14.50	5951±37	2.310±0.031	0.476	1
NGC 2663	08 45 08.2	−33 47 40	−2	11.85	2141±11	2.453±0.005	0.571	5
ESO 563G024	08 49 18.7	−19 00 17	−3	14.40	2750±19	2.104±0.061	0.387	8
NGC 2679	08 51 33.1	+30 51 56	−2	14.30	2080±19	1.973±0.099	0.340	2
UGC 04670	08 55 55.8	+13 13 43	−2	14.20	4159±20	2.121±0.064	0.462	4
NGC 2716	08 57 36.2	+03 05 26	−2	13.70	3687±19	2.167±0.055	0.607	7
NGC 2723	09 00 14.5	+03 10 42	−2	14.50	3868±18	2.158±0.054	0.445	7
NGC 2729	09 01 28.9	+03 43 12	−2	14.00	3881±19	2.137±0.059	0.564	8
NGC 2749	09 05 21.6	+18 18 52	−5	13.30	4240±22	2.364±0.029	0.699	10
IC 2437	09 05 32.8	−19 12 20	−2	13.94	5298±22	2.294±0.026	0.738	3
NGC 2765	09 07 36.6	+03 23 34	−2	13.30	3832±31	2.217±0.050	0.601	5
NGC 2822	09 13 49.8	−69 38 41	−2	11.64	1652±16	2.258±0.039	0.096	3
NGC 2865	09 23 30.8	−23 09 48	−2	12.65	2644±17	2.255±0.054	0.424	6
ESO 498G004	09 23 47.6	−25 38 13	−2	13.57	2568±20	2.093±0.053	0.763	6
ESO 498G006	09 24 52.5	−25 47 16	−2	14.25	2819±23	2.387±0.019	0.190	6
NGC 2888	09 26 19.7	−28 02 08	−2	13.54	2429±18	2.090±0.059	0.707	6
NGC 2891	09 26 56.7	−24 46 58	−3	13.56	2384±16	1.991±0.009	−0.112	4
ESO 126G014	09 28 26.4	−60 48 03	−2	13.41	2281±19	2.367±0.027	0.610	17
NGC 2911	09 33 46.5	+10 09 09	−2	13.82	3314±20	2.253±0.039	0.823	10
NGC 2918	09 35 44.5	+31 42 17	−5	13.60	6839±20	2.332±0.033	0.708	4
NGC 2945	09 37 41.0	−22 02 14	−2	13.49	4679±25	2.270±0.042	0.523	4

Table 1—Continued

Name (1)	α (2000) (2)	δ (2000) (3)	T (4)	m_B (5)	v_r (km s $^{-1}$) (6)	$\log \sigma_0$ (km s $^{-1}$) (7)	$\log r_e$ (kpc) (8)	N_c (9)
IC 0552	09 41 16.8	+10 38 43	-2	14.50	5851±19	2.288±0.036	0.485	17
IC 0555	09 41 57.1	+12 17 43	-2	14.40	6833±18	2.188±0.051	0.353	11
NGC 2974	09 42 33.3	-03 41 59	-5	12.80	1919±13	2.427±0.034	0.536	4
NGC 2984	09 43 40.4	+11 03 44	-2	14.30	6226±20	2.158±0.054	0.490	13
NGC 2983	09 43 40.8	-20 28 41	-2	13.07	2032±22	2.270±0.025	0.603	7
NGC 2986	09 44 16.3	-21 16 42	-5	11.86	2340±22	2.449±0.031	0.683	6
UGC 05226	09 46 03.7	+04 24 16	-5	14.00	5044±20	2.121±0.067	0.523	2
ESO 434G040	09 47 39.9	-30 56 57	-2	14.36	2525±28	2.182±0.030	0.042	9
NGC 3022	09 49 39.2	-05 10 01	-2	14.50	6240±27	2.338±0.018	0.977	8
NGC 3042	09 53 20.0	+00 41 58	-2	13.80	3856±17	2.196±0.047	0.280	1
ESO 499G013	09 53 16.7	-25 55 40	-2	14.20	3496±23	2.272±0.027	0.562	4
NGC 3051	09 53 58.7	-27 17 06	-2	13.05	2507±24	2.303±0.025	0.769	12
NGC 3056	09 54 33.0	-28 17 49	-2	12.87	964±15	1.792±0.034	-0.091	11
IC 2526	09 57 03.2	-32 15 19	-2	13.65	2763±18	2.215±0.043	0.242	20
NGC 3078	09 58 24.5	-26 55 34	-5	12.26	2580±20	2.479±0.021	0.454	12
NGC 3082	09 58 53.0	-30 21 23	-2	13.75	2864±18	2.320±0.032	0.393	13
NGC 3085	09 59 28.9	-19 29 36	-2	14.25	4005±17	2.230±0.041	0.123	9
NGC 3091	10 00 13.9	-19 38 14	-3	12.30	3804±23	2.496±0.030	0.741	10
NGC 3090	10 00 30.2	-02 58 19	-5	13.57	6154±23	2.371±0.029	0.832	23
NGC 3096	10 00 32.9	-19 39 45	-2	14.34	4230±19	2.017±0.090	0.611	9
NGC 3100	10 00 41.2	-31 39 45	-2	12.41	2642±20	2.286±0.035	0.601	17
NGC 3115	10 05 14.1	-07 43 07	-2	11.50	704±21	2.494±0.020	0.246	2
ESO 316G034	10 09 38.8	-39 56 16	-3	13.86	5368±26	2.365±0.022	0.757	3
NGC 3142	10 10 11.1	-08 29 46	-2	14.50	5420±10	2.149±0.060	0.447	2
IC 2552	10 10 46.4	-34 50 42	-2	13.68	3102±18	2.164±0.050	0.259	7
ESO 316G046	10 11 41.0	-37 55 32	-2	14.11	4654±19	2.185±0.051	0.461	10
ESO 500G018	10 14 54.2	-23 03 02	-2	14.22	3781±22	2.307±0.035	0.739	2
ESO 567G052	10 20 07.4	-21 41 42	-2	14.24	3582±23	2.137±0.056	0.694	11
NGC 3209	10 20 38.5	+25 30 15	-5	13.90	6278±20	2.453±0.024	0.932	3
NGC 3224	10 21 41.5	-34 41 45	-5	13.41	3058±18	2.124±0.058	0.238	24
ESO 317G021	10 23 08.0	-39 37 24	-3	13.85	2473±19	2.057±0.050	0.306	12
ESO 263G033	10 24 47.6	-43 57 51	-3	14.03	2885±19	2.134±0.037	0.240	13
ESO 436G027	10 28 53.8	-31 36 34	-2	12.99	4303±20	2.314±0.034	0.702	8
NGC 3273	10 30 29.2	-35 36 49	-2	13.76	2503±20	2.422±0.024	0.548	30
IC 2586	10 31 02.8	-28 43 08	-5	13.94	3664±29	2.494±0.015	0.725	49
IC 2587	10 31 12.0	-34 33 50	-2	13.64	2091±24	2.210±0.046	0.595	20
ESO 263G048	10 31 11.3	-46 15 02	-2	12.70	2899±22	2.354±0.030	0.610	10
ESO 501G003	10 31 48.2	-26 33 57	-3	14.03	4176±15	2.301±0.023	0.716	42
NGC 3282	10 32 22.5	-22 18 04	-2	14.25	3701±17	2.152±0.052	0.374	2
MCG -01-27-015	10 32 54.0	-06 29 00	-2	14.00	5065±10	2.328±0.018	1.173	4
MCG -01-27-018	10 33 13.6	-07 27 54	-2	14.50	5095±21	2.338±0.033	0.674	7
ESO 501G025	10 35 25.6	-26 39 27	-2	14.41	3831±20	2.061±0.063	0.593	70
NGC 3302	10 35 47.5	-32 21 33	-2	13.77	3864±23	2.375±0.025	0.770	8
NGC 3305	10 36 12.5	-27 09 46	-5	14.14	3984±23	2.307±0.027	0.454	73

Table 1—Continued

Name (1)	α (2000) (2)	δ (2000) (3)	T (4)	m_B (5)	v_r (km s $^{-1}$) (6)	$\log \sigma_0$ (km s $^{-1}$) (7)	$\log r_e$ (kpc) (8)	N_c (9)
NGC 3300	10 36 38.5	+14 10 19	-2	13.21	3079±18	2.134±0.054	0.368	6
NGC 3308	10 36 22.3	-27 26 16	-3	13.55	3574±19	2.314±0.029	0.678	80
NGC 3311	10 36 43.3	-27 31 41	-2	12.19	3924±33	2.228±0.046	1.307	82
ESO 437G015	10 36 58.0	-28 10 41	-2	13.81	2756±20	2.210±0.034	0.044	48
NGC 3316	10 37 37.4	-27 35 36	-2	13.92	3950±13	2.230±0.060	0.705	80
ESO 501G056	10 37 44.9	-26 37 48	-2	14.05	3580±24	2.265±0.023	0.512	69
ESO 437G021	10 38 10.9	-28 47 01	-2	14.26	3914±18	2.193±0.003	0.673	65
NGC 3325	10 39 20.3	-00 11 54	-5	14.00	5672±18	2.137±0.059	0.485	9
NGC 3335	10 39 34.5	-23 55 21	-2	14.02	3882±25	2.045±0.079	0.240	13
NGC 3332	10 40 28.7	+09 11 00	-2	13.70	5925±21	2.292±0.038	0.688	1
[R89] 461	10 40 24.6	-27 52 52	-2	0.00	4504±30	1.748±0.265	0.229	49
ESO 437G038	10 40 50.7	-27 57 53	-2	14.47	4493±20	2.246±0.036	0.426	50
ESO 437G045	10 41 59.4	-28 46 37	-2	14.26	3753±17	2.068±0.065	0.622	46
ESO 376G009	10 42 02.0	-33 14 43	-2	13.93	3067±18	2.127±0.058	0.132	7
IC 0642	10 48 08.5	+18 11 24	-2	14.00	6048±23	2.283±0.037	0.719	3
ESO 569G012	10 49 16.5	-19 38 11	-2	13.79	4207±21	2.225±0.035	0.441	4
NGC 3412	10 50 53.2	+13 24 46	-2	12.00	901±17	1.987±0.092	-0.189	26
NGC 3483	10 59 06.0	-28 28 35	-2	13.33	3576±16	2.201±0.016	0.374	2
NGC 3522	11 06 40.5	+20 05 08	-3	14.20	1240±18	1.833±0.159	0.082	13
MCG -03-28-037	11 07 13.3	-19 30 14	-2	13.00	3722±20	2.326±0.024	...	9
NGC 3546	11 09 46.4	-13 22 59	-2	14.50	4455±24	2.391±0.019	0.455	4
NGC 3557	11 09 57.5	-37 32 17	-3	11.76	3088±18	2.446±0.014	0.601	13
NGC 3564	11 10 35.8	-37 33 00	-2	13.57	2852±19	2.228±0.042	0.231	15
NGC 3585	11 13 16.9	-26 45 20	-5	10.90	1434±12	2.427±0.005	0.430	7
NGC 3591	11 14 03.0	-14 05 18	-2	14.50	5507±22	2.241±0.034	0.430	5
ESO 377G029	11 14 38.8	-33 54 21	-2	13.73	2942±19	2.301±0.033	0.253	6
NGC 3598	11 15 11.6	+17 15 49	-3	13.50	6176±37	2.320±0.014	0.613	1
NGC 3599	11 15 27.3	+18 06 46	-2	13.00	876±18	1.886±0.135	-0.103	27
NGC 3605	11 16 46.7	+18 01 04	-5	13.71	709±18	1.982±0.078	0.023	28
NGC 3617	11 17 50.7	-26 08 06	-2	13.71	2188±19	2.114±0.059	0.374	4
NGC 3615	11 18 06.8	+23 23 49	-5	14.00	6683±19	2.389±0.029	0.674	5
NGC 3636	11 20 25.3	-10 16 55	-5	13.50	1751±25	2.061±0.057	0.443	5
IC 2764	11 27 05.3	-28 58 43	-2	13.41	1689±34	1.940±0.114	0.344	7
NGC 3706	11 29 44.1	-36 23 33	-2	12.46	3055±30	2.489±0.014	...	11
NGC 3768	11 37 14.0	+17 50 24	-2	13.70	3473±19	2.243±0.045	0.667	19
NGC 3778	11 38 21.7	-50 43 01	-3	14.15	4349±19	2.310±0.031	0.493	5
NGC 3805	11 40 42.0	+20 20 35	-3	13.80	6629±19	2.386±0.029	0.951	42
NGC 3818	11 41 57.4	-06 09 21	-3	13.50	1698±22	2.288±0.024	0.497	8
NGC 3837	11 43 56.7	+19 53 42	-5	14.20	6407±29	2.270±0.040	0.836	64
NGC 3886	11 47 05.2	+19 50 16	-3	14.30	5896±21	2.360±0.031	0.638	49
ESO 378G020	11 47 16.7	-37 33 04	-2	13.84	3113±18	2.064±0.069	-0.071	12
NGC 3892	11 48 01.1	-10 57 43	-2	13.50	1797±17	2.107±0.042	0.483	8
NGC 3904	11 49 13.3	-29 16 35	-3	12.08	1714±12	2.356±0.015	0.357	14
NGC 3919	11 50 41.7	+20 00 54	-5	14.50	6195±20	2.386±0.028	0.658	16

Table 1—Continued

Name (1)	α (2000) (2)	δ (2000) (3)	T (4)	m_B (5)	v_r (km s $^{-1}$) (6)	$\log \sigma_0$ (km s $^{-1}$) (7)	$\log r_e$ (kpc) (8)	N_c (9)
NGC 3923	11 51 02.1	-28 48 23	-3	10.85	1824±36	2.441±0.029	0.657	16
NGC 3954	11 53 41.7	+20 53 01	-5	14.40	7021±21	2.225±0.047	0.485	21
NGC 3962	11 54 39.8	-13 58 23	-3	12.50	1818±17	2.394±0.022	0.530	7
ESO 440G037	11 59 17.5	-28 54 18	-3	14.40	2008±24	1.934±0.126	0.419	26
NGC 4033	12 00 34.8	-17 50 30	-3	13.05	1662±20	2.114±0.059	0.100	17
ESO 440G038	12 01 42.9	-31 42 12	-2	13.68	2304±10	1.748±0.084	0.225	18
NGC 4078	12 04 47.8	+10 35 45	-2	13.90	2592±19	2.299±0.032	0.321	7
NGC 4191	12 13 50.1	+07 12 01	-2	13.90	2667±19	2.117±0.062	0.331	40
NGC 4215	12 15 54.7	+06 24 07	-2	13.04	2047±19	2.143±0.042	0.089	67
NGC 4233	12 17 06.6	+07 37 23	-3	13.41	2347±22	2.342±0.027	0.838	49
NGC 4239	12 17 14.7	+16 31 55	-2	13.50	904±19	1.748±0.256	0.117	59
NGC 4240	12 17 24.3	-09 57 07	-3	14.50	1990±17	2.000±0.017	-0.025	3
NGC 4261	12 19 22.8	+05 49 36	-5	11.84	2227±21	2.486±0.018	0.714	64
NGC 4270	12 19 48.7	+05 27 52	-2	13.26	2364±19	2.064±0.082	0.301	57
NGC 4318	12 22 43.5	+08 11 55	-5	14.40	1259±18	1.949±0.088	-0.098	84
NGC 4339	12 23 34.4	+06 04 55	-5	12.83	1309±17	2.076±0.055	0.180	74
IC 3289	12 24 57.1	-26 01 49	-2	14.33	3336±19	2.255±0.039	0.426	5
NGC 4374	12 25 03.7	+12 53 15	-5	10.82	1051±19	2.490±0.007	0.519	101
NGC 4373	12 25 18.6	-39 45 37	-2	11.85	3436±20	2.358±0.022	0.518	17
NGC 4379	12 25 14.8	+15 36 27	-2	12.77	1085±17	2.121±0.044	0.315	79
NGC 4373A	12 25 37.6	-39 19 12	-2	13.37	2996±19	2.265±0.038	0.718	23
NGC 4404	12 26 16.2	-07 40 50	-3	14.50	5585±20	2.314±0.029	0.486	3
NGC 4417	12 26 50.5	+09 35 02	-2	12.43	854±11	2.176±0.025	-0.034	95
NGC 4472	12 29 46.5	+07 59 58	-5	9.84	962±12	2.500±0.028	0.729	93
NGC 4474	12 29 53.4	+14 04 06	-2	12.95	1644±18	2.017±0.073	0.424	90
NGC 4486	12 30 49.7	+12 23 24	-5	10.30	1306±43	2.549±0.011	1.051	89
NGC 4489	12 30 52.3	+16 45 31	-2	13.20	987±18	1.851±0.126	-0.219	67
NGC 4515	12 33 04.5	+16 15 55	-5	13.30	996±18	1.914±0.120	-0.025	81
NGC 4546	12 35 29.5	-03 47 37	-2	11.50	1092±18	2.364±0.020	0.199	21
NGC 4550	12 35 30.9	+12 13 17	-2	12.73	465±17	2.107±0.060	-0.164	90
NGC 4551	12 35 38.2	+12 15 56	-5	13.27	1205±22	1.996±0.087	-0.067	105
NGC 4553	12 36 08.1	-39 26 19	-2	13.57	3145±18	2.146±0.053	0.462	28
ESO 574G012	12 36 24.4	-19 23 42	-3	14.30	6653±20	2.037±0.124	0.885	1
UGC 07813	12 39 01.1	+00 21 56	-5	14.40	6957±20	2.393±0.019	1.085	10
NGC 4603C	12 40 43.6	-40 45 45	-2	14.42	3123±19	2.000±0.090	0.216	57
ESO 322G051	12 40 53.9	-41 36 22	-2	14.22	3247±21	2.367±0.031	0.500	56
NGC 4612	12 41 32.9	+07 18 55	-2	12.59	1783±17	1.886±0.105	-0.167	44
NGC 4645A	12 43 05.4	-41 21 32	-2	13.71	3306±20	2.230±0.044	0.647	67
NGC 4645B	12 43 31.5	-41 21 43	-2	13.68	2727±18	2.279±0.037	0.267	69
NGC 4649	12 43 40.3	+11 32 58	-5	10.30	1159±20	2.554±0.014	0.704	85
NGC 4645	12 44 09.8	-41 45 01	-3	13.08	2657±19	2.396±0.020	0.355	64
NGC 4685	12 47 11.7	+19 27 49	-2	13.80	6789±20	2.190±0.050	0.424	2
NGC 4683	12 47 42.6	-41 31 40	-2	14.28	3592±21	2.111±0.063	0.419	91
ESO 507G014	12 48 20.5	-26 27 51	-2	13.92	3336±17	2.100±0.061	0.280	20

Table 1—Continued

Name (1)	α (2000) (2)	δ (2000) (3)	T (4)	m_B (5)	v_r (km s $^{-1}$) (6)	$\log \sigma_0$ (km s $^{-1}$) (7)	$\log r_e$ (kpc) (8)	N_c (9)
NGC 4694	12 48 15.1	+10 59 07	-2	12.64	1202±24	1.820±0.172	0.283	66
NGC 4697	12 48 35.9	-05 48 02	-3	11.50	1278±12	2.297±0.017	0.398	33
NGC 4696	12 48 49.8	-41 18 39	-2	11.47	3011±22	2.444±0.015	1.376	75
NGC 4714	12 50 19.3	-13 19 29	-3	14.50	4280±22	2.318±0.028	0.854	24
ESO 507G021	12 50 29.0	-26 50 31	-2	13.51	3238±18	2.294±0.034	0.634	22
ESO 507G024	12 51 27.1	-26 48 24	-2	13.96	3405±19	2.013±0.081	0.382	23
ESO 507G025	12 51 32.0	-26 27 06	-5	12.73	3278±21	2.316±0.024	...	21
ESO 507G027	12 51 37.9	-26 07 00	-2	13.77	3198±22	2.233±0.029	0.225	21
NGC 4739	12 51 37.2	-08 24 37	-3	14.50	3787±22	2.121±0.053	0.399	33
NGC 4730	12 52 30.0	-41 08 48	-2	14.16	2131±20	2.346±0.019	0.545	43
NGC 4742	12 51 48.1	-10 27 18	-2	13.00	1314±16	2.029±0.064	...	26
NGC 4756	12 52 52.7	-15 24 48	-3	13.50	4083±20	2.305±0.025	0.924	27
NGC 4760	12 53 07.3	-10 29 40	-3	13.50	4555±24	2.418±0.023	0.902	24
NGC 4767	12 53 53.3	-39 42 52	-3	12.88	3022±20	2.286±0.026	0.533	54
IC 3896	12 56 44.0	-50 20 43	-3	11.42	2064±20	2.382±0.018	0.429	7
NGC 4825	12 57 12.3	-13 39 54	-3	13.00	4490±24	2.378±0.023	0.860	24
NGC 4830	12 57 27.6	-19 41 30	-3	12.94	3388±14	2.307±0.094	0.535	4
NGC 4855	12 59 18.5	-13 13 52	-3	14.50	4808±19	2.301±0.029	0.567	22
MCG -01-33-074	13 02 06.1	-07 42 07	-2	14.50	3443±18	2.029±0.085	...	13
ESO 443G039	13 03 03.3	-30 47 30	-2	14.00	3043±18	2.086±0.072	0.209	18
NGC 4933A	13 03 57.4	-11 29 49	-3	13.50	3191±19	2.149±0.044	...	10
NGC 4936	13 04 16.4	-30 31 29	-5	12.02	3268±26	2.446±0.017	...	17
ESO 443G053	13 04 31.3	-30 10 04	-5	14.12	3847±23	2.267±0.040	0.420	19
NGC 4958	13 05 48.9	-08 01 14	-2	12.50	1494±13	2.230±0.008	-0.091	27
IC 4180	13 06 56.1	-23 55 01	-2	13.86	2972±18	1.857±0.151	0.158	16
ESO 508G008	13 07 28.6	-27 23 19	-2	14.27	5938±13	2.267±0.077	0.477	1
NGC 4989	13 09 16.1	-05 23 48	-2	14.50	3115±17	2.292±0.024	...	6
NGC 4993	13 09 47.3	-23 23 04	-3	13.60	3003±18	2.212±0.045	0.546	18
NGC 4997	13 09 51.7	-16 30 59	-3	14.00	2376±18	2.079±0.048	0.178	28
ESO 323G092	13 12 15.7	-39 56 19	-5	14.40	3207±18	2.121±0.044	0.410	8
NGC 5011	13 12 51.9	-43 05 48	-5	12.40	3159±20	2.393±0.019	0.535	24
NGC 5017	13 12 54.5	-16 46 00	-5	14.50	2546±18	2.204±0.049	0.336	29
NGC 5028	13 13 45.9	-13 02 33	-3	14.50	6600±20	2.509±0.016	1.033	11
NGC 5044	13 15 24.0	-16 23 09	-3	12.50	2782±23	2.332±0.039	1.019	30
NGC 5048	13 16 08.3	-28 24 37	-3	14.00	4424±23	2.228±0.049	...	3
NGC 5049	13 15 59.4	-16 23 52	-2	14.50	3023±19	2.204±0.031	0.218	28
ESO 382G034	13 18 02.2	-36 56 59	-2	13.81	3416±18	1.973±0.099	0.186	8
NGC 5061	13 18 04.9	-26 50 10	-5	11.44	2082±19	2.354±0.021	0.179	16
NGC 5062	13 18 23.4	-35 27 28	-2	13.45	3320±19	2.545±0.018	0.882	7
ESO 576G030	13 18 59.2	-18 35 15	-2	14.26	2581±23	2.004±0.086	0.128	28
NGC 5077	13 19 31.7	-12 39 26	-5	12.50	2806±21	2.512±0.016	0.635	13
NGC 5087	13 20 25.3	-20 36 37	-5	12.22	1858±11	2.545±0.013	0.498	20
NGC 5102	13 21 57.8	-36 37 47	-2	10.00	459±20	1.869±0.118	-0.429	9
NGC 5111	13 22 51.0	-12 57 39	-3	13.50	5516±21	2.412±0.018	0.992	5

Table 1—Continued

Name (1)	α (2000) (2)	δ (2000) (3)	T (4)	m_B (5)	v_r (km s $^{-1}$) (6)	$\log \sigma_0$ (km s $^{-1}$) (7)	$\log r_e$ (kpc) (8)	N_c (9)
ESO 576G076	13 30 43.2	−22 25 15	−2	14.12	1664±23	2.083±0.070	...	14
NGC 5193	13 31 53.6	−33 14 07	−5	12.95	3755±16	2.301±0.021	0.491	28
NGC 5203	13 32 13.5	−08 47 13	−3	14.50	6730±21	2.346±0.036	0.566	3
NGC 5206	13 33 43.9	−48 09 04	−2	11.62	550±18	1.580±0.355	0.463	11
IC 4296	13 36 38.9	−33 57 59	−5	11.78	3772±13	2.539±0.046	0.935	26
MCG −01-35-007	13 37 30.0	−08 12 45	−2	14.50	2867±17	2.185±0.033	0.237	1
IC 4310	13 38 57.1	−25 50 43	−2	13.51	2516±17	2.210±0.046	0.310	3
MCG −05-32-074	13 45 21.5	−30 01 04	−2	14.39	4414±19	2.207±0.008	0.286	38
ESO 509G108	13 47 12.2	−24 22 21	−2	14.49	5969±19	2.365±0.031	0.540	3
ESO 445G028	13 47 18.8	−29 48 39	−5	14.30	4503±24	2.342±0.012	0.539	39
IC 4329	13 49 05.3	−30 17 45	−2	12.22	4542±33	2.425±0.035	1.265	42
ESO 445G049	13 49 10.0	−31 09 54	−2	13.80	5056±26	2.241±0.052	0.777	33
NGC 5304	13 50 01.7	−30 34 40	−2	13.85	3758±22	2.238±0.045	0.875	26
NGC 5330	13 52 59.7	−28 28 10	−2	14.00	4763±10	2.149±0.033	0.323	8
NGC 5343	13 54 11.8	−07 35 18	−5	14.50	2640±19	2.190±0.032	0.283	6
ESO 510G009	13 54 18.8	−26 52 19	−2	14.16	6002±22	2.507±0.021	0.720	5
ESO 445G075	13 54 54.9	−28 22 06	−2	14.16	2544±19	1.929±0.131	0.503	5
ESO 384G013	13 55 42.0	−33 43 34	−2	14.23	3786±19	1.898±0.136	...	31
IC 4350	13 57 14.0	−25 14 43	−2	13.96	6200±18	2.393±0.029	0.706	3
ESO 384G019	13 57 39.8	−34 13 06	−2	13.92	4264±18	2.083±0.057	0.329	34
UGC 08872	13 57 18.7	+15 27 29	−2	14.50	5534±18	2.196±0.055	0.583	3
ESO 384G021	13 57 57.6	−34 00 30	−2	14.40	4380±17	1.857±0.160	0.349	37
ESO 221G020	13 58 23.4	−48 28 29	−5	13.25	2805±19	2.117±0.035	−0.083	19
ESO 384G023	13 58 29.8	−34 14 32	−2	14.48	3933±18	1.914±0.135	0.288	36
NGC 5397	14 01 10.2	−33 56 40	−2	14.05	4110±27	2.405±0.018	0.715	45
NGC 5424	14 02 56.3	+09 25 14	−2	14.30	6031±19	2.286±0.030	0.587	29
NGC 5419	14 03 38.6	−33 58 41	−2	12.03	4185±21	2.487±0.022	1.111	42
ESO 510G054	14 04 03.5	−26 12 52	−3	14.40	6095±21	2.228±0.044	0.470	9
IC 4374	14 07 30.5	−27 01 02	−2	13.87	6561±29	2.389±0.039	1.075	11
ESO 510G071	14 07 41.1	−25 07 02	−2	14.37	6526±20	2.378±0.030	0.563	5
NGC 5493	14 11 29.5	−05 02 40	−2	14.00	2693±25	2.301±0.013	0.167	12
NGC 5507	14 13 20.0	−03 08 58	−2	14.20	1844±17	2.314±0.025	0.245	10
NGC 5516	14 15 54.9	−48 06 55	−3	13.01	4123±20	2.025±0.085	1.137	9
ESO 221G037	14 18 11.3	−48 00 38	−2	13.15	4424±20	2.250±0.044	0.288	8
ESO 579G017	14 19 11.0	−20 46 40	−2	14.10	6396±22	1.903±0.150	0.268	3
IC 0999	14 19 32.9	+17 52 33	−3	14.50	5756±19	2.146±0.047	0.314	6
NGC 5576	14 21 04.2	+03 16 14	−5	12.16	1516±37	2.253±0.021	0.090	13
NGC 5583	14 21 41.1	+13 13 53	−5	14.20	5018±18	2.061±0.076	0.334	2
IC 4421	14 28 31.5	−37 34 59	−5	13.91	3699±14	2.365±0.034	0.360	3
NGC 5628	14 28 26.0	+17 55 31	−5	14.50	5773±21	2.305±0.035	0.567	1
UGC 09288	14 28 58.6	+13 51 42	−2	14.40	5282±12	2.083±0.048	0.415	6
NGC 5626	14 29 48.7	−29 44 56	−2	14.01	6963±19	2.267±0.038	0.833	5
NGC 5638	14 29 40.5	+03 14 04	−3	12.67	1704±18	2.230±0.048	0.394	20
ESO 447G030	14 39 47.0	−32 40 04	−2	13.62	3005±17	2.149±0.052	0.178	2

Table 1—Continued

Name	α (2000)	δ (2000)	T	m_B	v_r (km s $^{-1}$)	$\log \sigma_0$ (km s $^{-1}$)	$\log r_e$ (kpc)	N_c
(1)	(2)	(3)	(4)	(5)	(6)	(7)	(8)	(9)
ESO 447G031	14 40 55.8	-32 22 31	-2	14.08	3066±18	1.785±0.201	0.142	2
NGC 5726	14 42 56.2	-18 26 37	-2	14.13	3426±20	2.140±0.048	0.889	10
ESO 512G019	14 43 36.5	-24 28 00	-2	13.31	3566±19	2.305±0.025	...	6
NGC 5761	14 49 08.3	-20 22 38	-5	13.88	4173±18	2.176±0.107	0.439	9
NGC 5770	14 53 15.2	+03 57 37	-2	13.30	1502±17	2.000±0.090	0.128	21
ESO 386G038	14 56 20.0	-37 28 40	-2	14.43	6256±24	2.076±0.080	0.812	2
NGC 5791	14 58 46.0	-19 16 03	-3	13.15	3350±11	2.417±0.015	0.594	13
NGC 5796	14 59 24.1	-16 37 27	-5	13.50	3023±18	2.410±0.025	0.418	11
NGC 5813	15 01 11.2	+01 42 08	-2	12.09	1979±12	2.394±0.021	0.670	22
NGC 5831	15 04 07.2	+01 13 15	-5	13.05	1673±21	2.241±0.024	0.295	23
NGC 5846	15 06 29.4	+01 36 25	-3	11.76	1788±20	2.403±0.023	0.822	21
NGC 5858	15 08 49.2	-11 12 28	-2	14.50	2105±19	2.220±0.030	0.000	5
NGC 5869	15 09 49.3	+00 28 13	-5	13.50	2127±20	2.312±0.037	0.636	15
ESO 387G016	15 16 42.3	-36 48 06	-2	14.43	4279±20	2.250±0.033	0.342	2
NGC 5898	15 18 13.3	-24 05 49	-5	12.63	2129±25	2.367±0.025	0.539	10
NGC 5903	15 18 36.3	-24 04 06	-3	12.37	2599±15	2.330±0.024	0.730	11
NGC 5928	15 26 02.6	+18 04 28	-2	13.80	4516±18	2.272±0.038	0.918	2
NGC 6017	15 57 15.3	+05 59 54	-2	13.80	1802±15	2.064±0.018	-0.062	4
NGC 6172	16 22 10.3	-01 30 55	-2	14.40	5036±13	2.086±0.004	-0.003	1
ESO 137G024	16 25 50.5	-60 45 07	-2	13.69	5264±23	2.431±0.025	0.730	28
ESO 137G036	16 36 54.0	-61 01 41	-2	13.95	5479±21	2.182±0.049	...	13
ESO 137G044	16 50 56.0	-61 48 54	-2	13.68	4637±26	2.637±0.016	...	13
NGC 6364	17 24 27.6	+29 23 26	-2	14.40	6874±20	2.217±0.064	0.707	2
UGC 10864	17 28 19.5	+14 10 03	-2	14.30	2971±20	1.991±0.088	-0.203	2
NGC 6375	17 29 21.8	+16 12 25	-5	14.50	6165±20	2.301±0.039	0.744	3
ESO 139G005	17 34 19.8	-60 52 14	-5	14.12	4747±20	2.146±0.061	0.542	12
NGC 6442	17 46 51.2	+20 45 34	-5	14.50	6358±22	2.326±0.037	0.788	2
NGC 6495	17 54 50.7	+18 19 38	-5	13.80	3203±18	2.267±0.038	0.566	10
UGC 11082	18 00 05.4	+26 22 01	-2	14.40	4739±21	2.314±0.038	0.544	4
NGC 6548	18 05 59.1	+18 35 12	-2	13.10	2209±23	2.223±0.044	0.785	9
NGC 6577	18 12 00.0	+21 28 00	-5	13.40	5198±21	2.456±0.019	0.695	9
NGC 6587	18 13 50.7	+18 49 36	-2	14.30	3100±22	2.487±0.019	0.962	8
ESO 182G007	18 16 49.5	-57 13 50	-3	13.87	5124±19	2.212±0.041	0.394	5
NGC 6614	18 25 07.8	-63 14 51	-3	13.80	4319±22	2.358±0.022	0.690	7
IC 4704	18 27 53.8	-71 36 35	-2	12.61	3642±12	2.425±0.048	...	7
IC 4731	18 38 43.1	-62 56 34	-2	13.84	4517±35	2.223±0.049	0.314	52
NGC 6673	18 45 07.0	-62 17 48	-2	12.69	1171±18	2.152±0.009	...	7
ESO 141G003	18 46 55.6	-57 41 39	-5	14.02	6116±23	2.382±0.023	0.611	0
NGC 6684	18 48 57.5	-65 10 26	-2	11.34	862±18	2.045±0.075	...	6
NGC 6706	18 56 51.4	-63 09 58	-3	13.88	3865±21	2.260±0.032	0.754	32
IC 4796	18 56 28.0	-54 12 52	-2	13.48	3108±17	2.061±0.070	0.154	10
NGC 6721	19 00 50.5	-57 45 28	-5	13.23	4444±31	2.415±0.024	0.720	4
NGC 6725	19 01 56.3	-53 51 53	-2	13.41	3625±19	2.083±0.051	0.425	10
ESO 231G017	19 04 45.9	-47 50 52	-2	13.54	2768±19	2.158±0.043	-0.097	1

Table 1—Continued

Name (1)	α (2000) (2)	δ (2000) (3)	T (4)	m_B (5)	v_r (km s $^{-1}$) (6)	$\log \sigma_0$ (km s $^{-1}$) (7)	$\log r_e$ (kpc) (8)	N_c (9)
ESO 282G010	19 05 54.2	−43 43 23	−5	14.24	5773±23	2.356±0.024	0.968	6
ESO 282G024	19 13 31.3	−47 03 40	−5	13.37	5518±24	2.459±0.018	0.894	7
ESO 282G028	19 14 34.0	−46 35 41	−5	13.73	5264±23	2.365±0.022	0.753	7
ESO 283G020	19 51 26.9	−44 50 37	−3	13.99	5737±20	2.262±0.030	0.693	1
ESO 142G049	19 52 55.8	−60 59 02	−3	14.40	3988±20	2.318±0.036	0.687	3
IC 4913	19 56 47.6	−37 19 45	−2	13.98	3629±19	2.097±0.064	0.357	0
NGC 6841	19 57 49.2	−31 48 35	−3	13.44	5872±36	2.423±0.064	0.749	2
IC 4931	20 00 50.2	−38 34 30	−5	12.82	6035±43	2.453±0.015	0.906	15
NGC 6850	20 03 29.9	−54 50 45	−2	14.35	4973±20	2.212±0.038	...	21
NGC 6851	20 03 33.6	−48 17 02	−3	12.87	3126±18	2.352±0.019	0.404	9
IC 4943	20 06 28.3	−48 22 27	−5	14.42	2969±19	2.127±0.128	0.492	10
NGC 6849	20 06 16.3	−40 11 52	−3	13.80	6071±26	2.403±0.036	1.044	1
NGC 6861	20 07 19.2	−48 22 12	−2	12.36	2829±17	2.690±0.037	0.745	10
NGC 6868	20 09 53.8	−48 22 45	−3	12.09	2947±18	2.446±0.027	0.561	11
IC 1317	20 23 15.4	+00 39 48	−2	14.50	3789±30	1.857±0.029	−0.309	3
NGC 6903	20 23 45.0	−19 19 29	−2	12.91	3318±22	2.272±0.121	0.502	3
NGC 6909	20 27 38.7	−47 01 34	−3	13.04	2755±20	2.076±0.011	0.288	6
NGC 6924	20 33 19.0	−25 28 26	−2	13.90	6068±19	2.307±0.052	0.871	3
ESO 341G013	20 47 09.3	−38 05 21	−2	14.40	6930±18	2.161±0.053	0.622	4
NGC 6958	20 48 42.9	−37 59 46	−3	12.47	2741±17	2.286±0.030	0.328	1
ESO 107G004	21 03 29.0	−67 10 49	−5	13.06	3158±19	2.086±0.050	...	2
ESO 235G049	21 04 41.1	−48 11 20	−5	13.70	5259±21	2.447±0.015	0.601	18
ESO 235G051	21 05 36.0	−51 56 49	−2	14.40	2300±11	1.756±0.119	0.000	2
ESO 286G049	21 06 47.9	−47 11 14	−5	13.70	5346±17	2.378±0.018	0.562	17
ESO 286G050	21 06 41.4	−42 33 20	−3	13.80	2646±26	1.806±0.080	0.000	2
NGC 7014	21 07 52.6	−47 10 40	−5	13.51	4893±12	2.509±0.020	0.842	19
NGC 7029	21 11 52.4	−49 16 58	−3	12.95	2839±10	2.362±0.065	0.394	6
NGC 7049	21 19 18.0	−48 33 50	−2	12.06	2259±19	2.420±0.033	0.578	7
NGC 7075	21 31 32.5	−38 37 03	−3	13.90	5493±22	2.378±0.025	0.614	6
NGC 7079	21 32 35.1	−44 04 00	−2	12.76	2684±16	2.199±0.034	0.234	11
NGC 7097	21 40 13.4	−42 32 23	−5	12.78	2616±19	2.367±0.032	0.345	10
NGC 7144	21 52 42.9	−48 15 16	−2	11.88	2021±19	2.274±0.009	0.581	8
NGC 7145	21 53 20.2	−47 52 57	−5	12.34	1967±10	2.173±0.009	0.436	8
ESO 466G026	21 58 43.4	−28 28 02	−5	13.80	6213±21	2.350±0.021	0.882	25
NGC 7173	22 02 03.7	−31 58 25	−5	13.31	2611±17	2.316±0.028	0.260	25
NGC 7176	22 02 08.7	−31 59 25	−3	13.16	2570±17	2.384±0.026	0.367	25
NGC 7185	22 02 56.2	−20 28 17	−2	14.11	1800±14	1.973±0.056	0.368	7
IC 5157	22 03 26.9	−34 56 28	−3	13.20	4461±17	2.350±0.032	0.744	5
NGC 7196	22 05 54.7	−50 07 11	−5	12.81	2923±19	2.519±0.034	0.635	6
NGC 7192	22 06 50.0	−64 18 57	−5	12.47	2978±13	2.307±0.002	0.556	7
ESO 467G037	22 16 14.3	−27 24 08	−3	13.90	5511±22	2.441±0.018	0.640	10
MCG -01-57-004	22 23 36.0	−03 25 00	−2	14.50	2940±23	2.267±0.032	1.103	2
ESO 533G025	22 25 30.9	−25 38 44	−2	13.70	4518±19	2.093±0.053	0.537	8
IC 1445	22 25 30.3	−17 14 32	−2	14.00	2647±20	2.079±0.048	0.549	1

Table 1—Continued

Name	α (2000)	δ (2000)	T	m_B	v_r (km s $^{-1}$)	$\log \sigma_0$ (km s $^{-1}$)	$\log r_e$ (kpc)	N_c
(1)	(2)	(3)	(4)	(5)	(6)	(7)	(8)	(9)
NGC 7280	22 26 27.7	+16 08 57	-2	13.60	1841±15	2.025±0.012	0.299	1
NGC 7302	22 32 24.0	-14 07 00	-2	13.50	2686±16	2.176±0.047	0.247	1
NGC 7351	22 41 18.0	-04 27 00	-2	13.50	864±20	1.857±0.125	0.484	2
NGC 7359	22 44 47.5	-23 41 13	-2	13.80	3270±15	2.164±0.015	0.100	5
NGC 7365	22 45 09.8	-19 57 07	-5	12.90	3047±18	2.037±0.052	0.341	7
NGC 7391	22 50 36.5	-01 32 34	-5	13.70	3074±19	2.344±0.019	...	3
NGC 7404	22 54 18.7	-39 18 55	-2	13.10	1909±16	1.845±0.119	0.042	17
IC 5267B	22 56 56.7	-43 45 39	-2	14.10	1737±22	1.724±0.225	0.015	12
IC 1459	22 57 10.5	-36 27 45	-5	11.24	1775±13	2.513±0.012	0.564	21
NGC 7454	23 01 06.7	+16 23 24	-3	13.60	2042±18	2.143±0.074	0.275	10
NGC 7458	23 01 28.3	+01 45 13	-5	13.90	5039±19	2.238±0.034	0.514	8
NGC 7507	23 12 07.6	-28 32 29	-3	11.56	1590±21	2.401±0.015	0.462	3
NGC 7562	23 15 57.4	+06 41 15	-5	13.24	3666±21	2.373±0.020	0.602	17
NGC 7576	23 17 22.8	-04 43 42	-2	14.50	3590±18	2.045±0.052	0.026	2
NGC 7600	23 18 53.9	-07 34 50	-5	13.50	3483±21	2.111±0.207	0.709	1
UGC 12515	23 19 51.3	+26 15 47	-2	14.10	5898±20	2.352±0.026	0.438	12
NGC 7619	23 20 14.7	+08 12 23	-3	12.78	3792±30	2.498±0.024	0.819	33
NGC 7626	23 20 42.4	+08 13 02	-5	12.90	3436±16	2.358±0.052	0.765	31
IC 1492	23 30 36.1	-03 02 25	-2	14.50	5289±22	2.348±0.026	0.736	6
IC 5328	23 33 17.0	-45 01 01	-3	12.21	3177±17	2.236±0.078	0.583	4
NGC 7778	23 53 20.1	+07 52 14	-5	13.80	5326±19	2.292±0.028	0.580	8
UGC 12840	23 54 29.4	+28 52 20	-2	14.30	6851±16	1.934±0.119	0.444	10
NGC 7785	23 55 19.1	+05 54 53	-2	13.22	3882±12	2.382±0.035	0.535	3
NGC 7796	23 58 59.8	-55 27 24	-3	12.58	3364±17	2.384±0.007	0.644	2
NGC 7805	00 01 26.6	+31 26 02	-5	14.30	4962±17	2.072±0.092	0.058	10

Table 2. Observing Setups

Setup	N_{gal}	Detector	Gain e $^{-}$ ADU $^{-1}$	Readout Noise e $^{-}$	Grating 1 mm $^{-1}$	Dispersion Å pixel $^{-1}$	Resolution Å	Spectral Range Å
(1)	(2)	(3)	(4)	(5)	(6)	(7)	(8)	(9)
1	73	CCD #24	2.9	8.0	600	0.93	3.0	4500–6300
2	43	CCD #39	1.2	5.5	600	1.91	6.0	3750–7300
3	348	CCD #39	1.2	5.5	1200	0.98	3.0	4300–6200
4	144	CCD #38	1.6	7.1	600	1.91	6.0	3750–8000

Note. — N_{gal} means the number of galaxies with one or more observations in that configuration. All CCDs have size 2048x2048 except #38 which is 2688x512. The spatial scale is 0.82''/pix, and the slit width 2.5''. Setup #1, used the second order dispersion of the 600 1 mm $^{-1}$ grating.

Table 3. Comparison between our σ_0 measurements with other authors.

Reference (1)	N_{gal} (2)	$\langle \delta\sigma_0 \rangle$ (3)	t (4)
Sánchez-Blázquez et al. (2006)	20	-3±17	0.13
Denicoló et al. (2005)	27	-16±32	0.89
Trager et al. (1998)	75	-7±31	0.60
Wegner et al. (2003)	432	+9±21	2.11

Table 4. Line index definitions

Index (1)	Bandpass (Å) (2)	Blue Pseudocontinua (Å) (3)	Red Pseudocontinua (Å) (4)	Units (5)
H β	4847.87	4876.62	4827.87	4847.87
Fe5015	4977.75	5054.00	4946.50	4977.75
Mg ₁	5069.12	5134.12	4895.12	4957.62
Mg ₂	5154.12	5196.62	4895.12	4957.62
Mg _b	5160.12	5192.62	5142.62	5161.37
Fe5270	5245.65	5285.65	5233.15	5248.15
Fe5335	5312.12	5352.12	5304.62	5315.87
Fe5406	5387.50	5415.00	5376.25	5387.50
Fe5709	5696.62	5720.37	5672.87	5696.62
NaD	5876.87	5909.35	5860.62	5875.62
[OIII]5007	4996.85	5016.85	4885.00	4935.00
				Å
				mag
				Å
				Å
				Å
				Å
				Å
				Å
				Å
				Å
				Å

Note. — The [OIII]5007 index is used to estimate the emission level in the spectra.

Table 5. Averages of Index Gradients

Index (1)	β (2)
H β	0.002±0.027
Fe5015	-0.012±0.027
Mg ₁	-0.033±0.026
Mg ₂	-0.055±0.035
Mg _b	-0.031±0.034
Fe5270	-0.016±0.025
Fe5335	-0.012±0.027
Fe5406	-0.015±0.029
Fe5709	-0.000±0.036
NaD	-0.034±0.022

Table 6. Global indices measurements

Name (1)	H β (2)	Fe5015 (3)	Mg ₁ (4)	Mg ₂ (5)	Mgb (6)	Fe5270 (7)	Fe5335 (8)	Fe5406 (9)	Fe5709 (10)	NaD (11)	[O III] (12)
NGC 7832	1.032 0.084	5.143 0.597	0.132 0.028	0.309 0.002	4.653 0.488	2.820 0.512	2.382 0.572	1.859 0.127	0.792 0.114	4.518 0.076	0.613 0.188
NGC 0050	1.375 0.015	5.533 0.217	0.137 0.011	0.303 0.002	4.688 0.078	2.963 0.392	2.738 0.218	1.610 0.066	0.642 0.192	4.573 0.170	0.767 0.077
NGC 0113	1.984 0.054	4.747 0.047	0.110 0.003	0.256 0.006	4.196 0.070	2.905 0.078	2.708 0.044	1.309 0.026	1.204 0.036	3.004 0.077	0.959 0.051
NGC 0125	1.825 0.049	4.464 0.051	...	0.153 0.005	3.199 0.059	2.620 0.054	2.110 0.029	1.979 0.026	0.883 0.037	3.403 0.099	0.568 0.061
NGC 0155	1.713 0.048	5.296 0.040	0.121 0.002	0.262 0.005	3.897 0.063	3.155 0.053	2.703 0.041	1.736 0.029	0.627 0.022	3.742 0.058	1.098 0.047
ESO 242G014	1.736 0.155	4.891 0.625	0.119 0.000	0.278 0.008	3.795 0.057	3.052 0.049	2.133 0.568	1.492 0.134	1.059 0.179	3.617 0.254	0.582 0.377
NGC 0163	1.374 0.035	3.569 0.040	0.159 0.002	0.311 0.005	4.435 0.068	2.706 0.054	2.480 0.031	1.700 0.027	0.977 0.068	4.772 0.067	0.674 0.041
NGC 0179	1.271 0.318	4.762 0.640	0.128 0.005	0.269 0.033	4.475 0.495	2.862 0.341	2.715 0.351	1.784 0.267	0.958 0.256	3.987 0.111	0.566 0.205
NGC 0193	1.160 0.200	...	0.129 0.009	0.248 0.003	4.492 0.182	2.893 0.036	2.438 0.131	1.751 0.044	1.070 0.305	4.085 0.314	0.315 0.024
MCG -01-03-018	0.892 0.043	5.761 0.041	0.120 0.034	0.244 0.006	4.731 0.074	2.617 0.061	2.322 0.034	1.546 0.024	0.797 0.041	5.253 0.097	0.952 0.059
NGC 0273	1.869 0.056	5.518 0.047	0.138 0.002	0.292 0.006	4.656 0.068	2.928 0.058	2.374 0.049	1.833 0.031	1.004 0.027	3.580 0.078	1.349 0.056
NGC 0277	...	4.913 0.891	0.135 0.022	0.272 0.007	4.258 0.049	2.643 0.485	2.291 0.028	1.592 0.134	1.122 0.112	3.657 0.581	1.397 0.327
MCG -01-03-049	1.907 0.037	4.533 0.038	0.115 0.003	0.253 0.005	3.840 0.056	2.849 0.058	2.437 0.033	1.858 0.026	1.035 0.027	3.435 0.072	0.172 0.060
IC 1609	1.988 0.044	4.673 0.690	0.120 0.007	0.263 0.002	3.888 0.242	2.637 0.335	2.471 0.129	2.017 0.113	0.963 0.106	3.534 0.193	1.120 0.106
NGC 0349	...	3.554 0.684	...	0.227 0.036	2.960 0.224	2.666 0.072	...	1.353 0.273	0.786 0.076	2.437 0.070	0.264 0.192
IC 1628	2.311 0.040	7.003 0.039	0.154 0.003	0.317 0.006	5.142 0.069	2.893 0.059	3.217 0.031	1.860 0.024	1.341 0.034	4.428 0.069	0.704 0.064
NGC 0430	1.508 0.038	6.032 0.035	0.137 0.002	0.324 0.006	4.672 0.065	3.336 0.057	2.806 0.032	2.163 0.024	1.030 0.021	4.151 0.052	0.989 0.054
NGC 0442	1.722 0.079	4.793 0.334	0.093 0.002	0.212 0.002	4.098 0.063	2.436 0.207	2.271 0.077	1.818 0.004	0.996 0.154	3.037 0.306	0.827 0.137
NGC 0448	1.595 0.056	5.299 0.046	0.130 0.003	0.266 0.006	3.757 0.073	3.121 0.061	2.503 0.035	1.550 0.026	0.992 0.035	3.958 0.075	1.516 0.052
IC 0090	1.440 0.040	5.674 0.033	0.143 0.002	0.301 0.006	4.561 0.075	3.270 0.059	2.526 0.036	1.920 0.031	1.205 0.026	5.080 0.110	0.956 0.046
NGC 0474	1.401 0.043	4.867 0.035	0.141 0.002	0.296 0.006	4.318 0.067	2.997 0.058	2.292 0.036	1.951 0.026	1.086 0.033	4.083 0.084	0.776 0.046
NGC 0502	1.086 0.037	6.214 0.056	0.078 0.004	0.271 0.006	3.818 0.071	2.692 0.070	3.245 0.044	2.101 0.033	1.146 0.039	4.606 0.088	1.911 0.058
NGC 0516	2.585	4.372	0.074	0.191	3.237	2.549	2.267	1.328	0.665	1.853	1.077

Table 6—Continued

Name (1)	H β (2)	Fe5015 (3)	Mg ₁ (4)	Mg ₂ (5)	Mgb (6)	Fe5270 (7)	Fe5335 (8)	Fe5406 (9)	Fe5709 (10)	NaD (11)	[O III] (12)
	0.071	0.053	0.003	0.005	0.064	0.059	0.037	0.026	0.024	0.050	0.054
NGC 0533	...	4.809	0.175	0.347	5.144	2.780	2.502	1.925	0.954	5.235	0.629
	...	0.429	0.000	0.013	0.282	0.351	0.097	0.168	0.268	0.055	0.007
NGC 0541	1.193	5.297	0.146	0.318	4.789	3.169	2.895	2.119	...	5.141	1.073
	0.005	0.024	0.011	0.059	0.231	0.132	0.748	0.392	...	0.025	0.195
NGC 0547	1.331	5.432	0.181	0.341	5.403	3.302	2.664	2.016	0.893	5.297	0.868
	0.121	0.838	0.001	0.001	0.247	0.447	0.160	0.289	0.028	0.112	0.171
NGC 0584	1.643	5.745	0.151	0.293	4.184	3.277	2.790	1.998	0.953	4.090	0.929
	0.127	0.245	0.007	0.007	0.228	0.139	0.130	0.081	0.098	0.104	0.047
NGC 0599	0.626	3.357	0.142	0.279	4.236	2.623	2.321	1.348	1.030	3.642	-1.023
	0.019	0.053	0.002	0.006	0.071	0.064	0.037	0.020	0.027	0.083	0.068
NGC 0596	1.765	5.745	0.120	0.241	3.620	3.021	2.634	1.919	1.021	3.153	1.069
	0.086	0.605	0.003	0.025	0.383	0.127	0.205	0.114	0.074	0.153	0.066
UGC 01169	0.579	2.555	0.113	0.172	3.440	...	1.464	0.981	0.796	2.274	0.369
	0.026	0.029	0.002	0.004	0.057	...	0.027	0.013	0.024	0.037	0.027
NGC 0641	1.587	5.440	0.131	0.292	4.393	2.876	2.763	1.760	0.913	4.064	0.896
	0.239	0.210	0.006	0.008	0.199	0.229	0.474	0.094	0.173	0.275	0.155
NGC 0636	1.738	5.985	0.144	0.292	4.400	3.113	2.968	...	1.089	4.105	1.196
	0.061	0.084	0.002	0.001	0.068	0.092	0.065	...	0.050	0.092	0.006
ESO 244G045	1.992	6.030	0.124	0.275	4.260	2.851	2.635	1.674	0.887	3.759	1.144
	0.044	0.039	0.002	0.006	0.065	0.057	0.035	0.021	0.022	0.075	0.050
IC 1729	1.296	3.821	0.122	0.251	3.857	2.965	2.443	1.827	0.859	3.239	0.137
	0.083	0.348	0.008	0.015	0.258	0.059	0.122	0.311	0.155	0.127	0.061
NGC 0682	1.899	5.160	0.122	0.284	4.454	2.951	2.640	1.755	0.725	4.280	1.115
	0.041	0.036	0.002	0.006	0.069	0.064	0.039	0.027	0.019	0.081	0.049
NGC 0686	1.944	5.720	0.156	0.297	4.426	3.189	2.912	1.986	0.780	4.185	0.852
	0.134	0.230	0.000	0.002	0.014	0.080	0.092	0.044	0.037	0.099	0.102
IC 0164	0.947	3.553	0.151	0.307	4.526	2.809	2.487	1.962	1.048	4.813	0.281
	0.098	0.138	0.002	0.009	0.158	0.213	0.404	0.283	0.179	0.321	0.240
UGC 01325	1.907	5.688	0.128	0.296	4.404	2.484	2.403	1.544	1.023	4.497	1.236
	0.038	0.038	0.002	0.005	0.062	0.054	0.038	0.024	0.032	0.078	0.041
NGC 0720	1.369	5.556	0.159	0.338	5.255	3.070	2.852	1.908	0.924	5.795	0.867
	0.079	0.622	0.026	0.009	0.205	0.106	0.227	0.166	0.017	0.201	0.280
NGC 0731	1.934	5.525	0.122	0.270	4.064	3.359	2.814	2.026	1.012	4.251	1.217
	0.044	0.044	0.003	0.006	0.069	0.065	0.035	0.027	0.026	0.082	0.049
NGC 0770	1.471	4.826	...	0.182	3.149	2.648	1.669	1.263	0.744	2.578	1.400
	0.044	0.056	...	0.005	0.062	0.060	0.033	0.020	0.037	0.089	0.050
NGC 0774	1.436	6.954	0.142	0.303	4.323	3.422	2.545	2.041	0.832	4.074	0.973
	0.048	0.039	0.003	0.006	0.063	0.065	0.034	0.028	0.030	0.058	0.064
NGC 0790	1.374	3.232	0.138	0.276	3.626	2.776	2.906	1.619	0.890	3.949	0.847
	0.041	0.039	0.002	0.006	0.072	0.051	0.049	0.024	0.021	0.077	0.042
NGC 0809	1.282	5.158	0.103	0.257	4.111	2.825	2.747	2.016	0.869	4.115	0.773
	0.037	0.040	0.003	0.006	0.068	0.061	0.032	0.026	0.018	0.085	0.047
NGC 0822	1.770	4.714	0.120	0.271	4.509	3.214	2.765	2.126	1.093	4.111	1.191
	0.050	0.039	0.002	0.006	0.070	0.064	0.032	0.027	0.021	0.077	0.042

Table 6—Continued

Name (1)	H β (2)	Fe5015 (3)	Mg ₁ (4)	Mg ₂ (5)	Mgb (6)	Fe5270 (7)	Fe5335 (8)	Fe5406 (9)	Fe5709 (10)	NaD (11)	[O III] (12)
NGC 0821	1.546	6.020	0.164	0.319	4.576	3.215	2.793	1.929	1.020	4.068	1.222
	0.061	0.332	0.006	0.005	0.052	0.125	0.075	0.078	0.023	0.079	0.079
NGC 0830	0.555	3.310	0.109	0.232	3.170	2.319	2.563	1.598	...	3.355	0.518
	0.036	0.044	0.003	0.005	0.059	0.054	0.040	0.025	...	0.064	0.051
NGC 0842	1.883	5.437	0.125	0.273	4.125	3.431	2.987	1.754	1.108	4.171	1.000
	0.047	0.037	0.003	0.006	0.066	0.065	0.042	0.025	0.028	0.087	0.054
NGC 0862	0.907	5.314	0.102	0.265	4.262	2.768	2.748	1.535	0.901	3.611	0.648
	0.039	0.042	0.003	0.006	0.065	0.059	0.038	0.019	0.032	0.058	0.058
NGC 0875	1.251	4.775	0.131	0.290	4.209	2.963	2.586	1.651	0.772	3.679	0.028
	0.013	0.917	0.002	0.009	0.124	0.072	0.109	0.132	0.080	0.128	0.028
NGC 0883	1.545	5.908	0.153	0.330	4.898	3.292	3.273	2.065	0.961	5.742	1.261
	0.040	0.034	0.002	0.006	0.080	0.060	0.038	0.027	0.020	0.085	0.038
MCG -02-07-002	1.822	5.446	0.118	0.282	4.388	3.132	2.727	1.808	1.092	4.179	1.048
	0.043	0.038	0.002	0.006	0.062	0.059	0.033	0.023	0.024	0.077	0.046
NGC 0936	1.131	4.735	0.160	0.307	4.745	2.942	2.634	1.847	0.926	3.957	0.604
	0.144	0.631	0.002	0.019	0.192	0.124	0.262	0.117	0.044	0.326	0.095
NGC 0940	2.011	4.973	0.095	0.236	4.118	3.173	2.353	1.614	0.841	3.521	0.775
	0.045	0.033	0.002	0.005	0.061	0.054	0.036	0.019	0.034	0.059	0.046
IC 0232	1.367	6.011	0.138	0.278	4.249	2.901	2.524	2.002	1.070	4.099	1.352
	0.038	0.046	0.002	0.006	0.074	0.054	0.032	0.026	0.028	0.069	0.048
NGC 0968	1.402	5.796	0.130	0.289	4.479	2.416	2.206	1.449	1.206	3.677	1.371
	0.031	0.047	0.002	0.006	0.072	0.057	0.038	0.022	0.023	0.072	0.050
NGC 0969	0.903	3.556	0.152	0.316	4.449	2.936	2.966	1.503	1.302	4.356	0.101
	0.028	0.041	0.003	0.006	0.074	0.066	0.044	0.024	0.030	0.065	0.046
NGC 0978A	1.528	3.857	0.143	0.322	4.829	3.095	2.745	2.171	0.991	4.002	0.608
	0.033	0.038	0.002	0.006	0.072	0.059	0.037	0.031	0.024	0.070	0.043
ESO 545G042	2.027	3.010	0.095	0.221	2.892	1.811	2.639	0.958	0.852	2.884	1.660
	0.057	0.047	0.002	0.006	0.094	0.068	0.029	0.015	0.019	0.049	0.041
NGC 1052	-0.962	...	0.200	0.349	5.728	3.052	2.903	2.028	0.929	6.089	-4.350
	0.019	...	0.006	0.001	0.137	0.108	0.145	0.106	0.101	0.293	0.082
IC 1858	2.145	4.586	0.112	0.252	3.332	2.462	2.034	1.385	0.897	3.988	0.720
	0.043	0.032	0.002	0.005	0.059	0.056	0.032	0.031	0.024	0.074	0.056
IC 1860	1.364	5.105	0.158	0.323	4.766	2.707	2.766	1.590	0.948	4.895	0.824
	0.106	0.169	0.007	0.008	0.199	0.157	0.353	0.099	0.146	0.198	0.261
NGC 1132	0.776	5.355	0.131	0.307	4.277	2.881	2.488	1.509	0.724	4.622	1.214
	0.033	0.042	0.002	0.005	0.063	0.061	0.036	0.020	0.022	0.069	0.048
IC 1864	1.535	...	0.133	0.283	4.245	3.043	2.377	1.736	1.022	3.975	-0.459
	0.414	...	0.001	0.006	0.020	0.041	0.551	0.209	0.128	0.172	1.772
NGC 1162	1.710	5.288	0.133	0.293	4.411	3.135	2.507	1.740	1.177	4.004	1.130
	0.206	0.243	0.010	0.011	0.633	0.202	0.085	0.027	0.029	0.257	0.049
NGC 1172	0.933	4.553	0.099	0.239	3.706	2.401	2.280	1.212	0.848	2.604	0.301
	0.071	0.044	0.002	0.006	0.065	0.059	0.040	0.018	0.024	0.073	0.077
NGC 1199	1.609	4.985	0.165	0.321	4.818	3.311	2.973	2.043	0.863	4.194	0.699
	0.119	0.626	0.007	0.005	0.135	0.364	0.130	0.043	0.037	0.723	0.436
NGC 1200	1.439	5.293	0.157	0.319	4.844	3.111	2.844	2.039	1.145	4.989	1.216

Table 6—Continued

Name (1)	H β (2)	Fe5015 (3)	Mg ₁ (4)	Mg ₂ (5)	Mgb (6)	Fe5270 (7)	Fe5335 (8)	Fe5406 (9)	Fe5709 (10)	NaD (11)	[O III] (12)
	0.251	0.644	0.010	0.016	0.350	0.177	0.265	0.230	0.062	0.252	0.599
NGC 1201	1.609	5.641	0.151	0.295	4.465	3.150	2.915	1.932	1.023	4.635	1.179
	0.127	0.086	0.004	0.020	0.115	0.117	0.281	0.103	0.001	0.272	0.017
NGC 1209	1.348	4.987	0.152	0.302	4.618	2.808	2.690	1.922	0.921	4.491	0.682
	0.151	0.144	0.025	0.043	0.307	0.163	0.130	0.202	0.237	0.264	0.082
ESO 417G021	1.637	4.611	0.147	0.294	4.348	2.919	2.493	1.389	1.021	4.542	0.600
	0.384	1.147	0.015	0.017	0.458	0.414	0.181	0.327	0.284	0.432	0.261
NGC 1297	...	5.761	0.141	0.273	4.480	...	2.733	2.098	...	4.205	0.208
	...	0.685	0.023	0.008	0.447	...	0.475	0.276	...	0.077	0.185
NGC 1298	1.962	5.720	0.113	0.259	3.625	3.414	2.767	1.904	0.837	3.918	0.923
	0.047	0.039	0.003	0.005	0.054	0.064	0.042	0.030	0.027	0.069	0.046
NGC 1315	1.245	5.066	0.096	0.224	3.056	2.934	1.743	1.454	0.779	2.425	0.737
	0.039	0.053	0.003	0.005	0.057	0.057	0.030	0.017	0.029	0.064	0.060
NGC 1332	1.336	6.198	0.213	0.390	5.785	3.460	3.231	2.286	0.994	6.236	1.160
	0.007	0.027	0.001	0.001	0.101	0.010	0.022	0.118	0.033	0.024	0.019
NGC 1331	1.890	4.835	...	0.178	2.120	2.688	1.878	1.439	1.323	1.503	1.281
	0.084	0.058	...	0.004	0.067	0.061	0.025	0.021	0.036	0.093	0.064
NGC 1336	2.572	4.581	...	0.203	3.715	2.451	1.967	1.593	0.643	2.171	0.622
	0.067	0.051	...	0.005	0.059	0.057	0.025	0.024	0.027	0.085	0.067
NGC 1339	1.293	5.207	0.160	0.291	4.753	2.875	2.724	1.651	0.920	4.158	1.155
	0.037	0.044	0.035	0.007	0.081	0.067	0.036	0.025	0.028	0.100	0.056
NGC 1344	1.979	6.353	0.141	0.296	4.197	3.236	2.810	2.046	0.976	4.910	1.383
	0.023	0.105	0.007	0.002	0.030	0.107	0.076	0.038	0.021	0.115	0.119
NGC 1351	1.711	4.653	0.123	0.244	3.948	2.737	2.488	1.728	0.943	3.280	1.168
	0.046	0.046	0.035	0.006	0.071	0.060	0.037	0.022	0.027	0.090	0.053
ESO 548G033	1.462	4.063	0.083	0.210	2.898	3.047	2.216	1.975	0.860	3.010	0.945
	0.034	0.044	0.003	0.005	0.061	0.058	0.043	0.038	0.029	0.056	0.061
NGC 1366	1.583	5.226	0.129	0.241	3.760	3.062	2.270	1.820	0.939	2.819	0.854
	0.047	0.046	0.035	0.006	0.078	0.068	0.038	0.024	0.032	0.097	0.061
NGC 1374	1.396	5.372	0.142	0.270	4.313	2.826	2.270	1.677	0.698	3.969	1.293
	0.036	0.041	0.034	0.006	0.077	0.058	0.030	0.024	0.027	0.097	0.050
ESO 358G025	...	3.497	0.032	2.804	1.760	...	0.501	1.937	-0.032
	...	0.037	0.002	0.045	0.028	...	0.022	0.048	0.047
NGC 1379	1.606	4.391	0.118	0.240	3.934	2.606	2.078	1.725	1.005	3.179	1.067
	0.158	0.829	0.001	0.004	0.026	0.050	0.029	0.193	0.059	0.147	0.011
NGC 1380	1.195	5.248	0.140	0.291	4.410	3.123	2.810	1.890	0.929	4.265	0.925
	0.102	0.672	0.024	0.020	0.094	0.013	0.145	0.056	0.132	0.122	0.280
NGC 1381	1.474	4.957	0.128	0.254	4.134	2.731	2.377	1.836	1.011	2.962	1.073
	0.043	0.047	0.035	0.006	0.072	0.064	0.034	0.027	0.027	0.087	0.057
NGC 1389	1.767	5.176	0.128	0.245	3.814	2.891	2.761	1.841	1.065	3.685	1.216
	0.043	0.049	0.035	0.006	0.071	0.066	0.038	0.025	0.031	0.094	0.053
NGC 1383	2.128	5.425	0.132	0.279	4.638	3.175	2.767	1.696	1.091	3.612	1.127
	0.049	0.045	0.002	0.007	0.086	0.067	0.043	0.025	0.031	0.077	0.041
NGC 1395	1.464	5.696	0.199	0.364	5.142	3.008	2.888	2.090	0.866	5.655	1.181
	0.130	0.288	0.008	0.006	0.072	0.120	0.029	0.143	0.013	0.133	0.092

Table 6—Continued

Name (1)	H β (2)	Fe5015 (3)	Mg ₁ (4)	Mg ₂ (5)	Mgb (6)	Fe5270 (7)	Fe5335 (8)	Fe5406 (9)	Fe5709 (10)	NaD (11)	[O III] (12)
NGC 1393	1.915 0.047	6.552 0.056	0.110 0.003	0.254 0.006	3.607 0.070	3.170 0.064	2.662 0.046	2.098 0.035	0.836 0.033	3.375 0.082	0.845 0.066
NGC 1399	1.387 0.061	6.030 0.286	0.199 0.003	0.365 0.012	5.696 0.115	3.292 0.080	2.974 0.236	2.083 0.122	0.861 0.160	6.397 0.166	1.163 0.098
NGC 1394	1.541 0.091	4.254 0.546	0.108 0.011	0.241 0.041	4.085 0.147	2.951 0.111	2.296 0.191	1.704 0.080	0.911 0.001	4.158 0.717	0.276 0.157
NGC 1404	1.423 0.059	6.028 0.142	0.175 0.007	0.336 0.018	5.193 0.057	3.242 0.091	3.022 0.084	2.003 0.063	0.966 0.058	5.408 0.228	1.155 0.043
NGC 1403	1.861 0.158	4.924 0.512	0.111 0.019	0.252 0.021	3.933 0.197	2.915 0.115	2.562 0.130	1.613 0.175	1.039 0.015	3.685 0.174	0.994 0.107
NGC 1411	1.834 0.043	4.854 0.038	0.120 0.002	0.249 0.005	3.581 0.065	2.679 0.060	2.392 0.034	1.771 0.030	1.008 0.031	3.189 0.076	0.611 0.052
NGC 1400	1.170 0.305	5.540 0.725	0.177 0.013	0.332 0.011	5.060 0.370	2.989 0.332	2.705 0.292	1.813 0.314	1.002 0.204	5.725 0.319	0.902 0.175
NGC 1407	1.401 0.015	5.928 0.243	0.191 0.004	0.359 0.013	5.488 0.316	3.470 0.065	3.020 0.065	2.175 0.018	0.916 0.097	5.878 0.219	1.259 0.025
NGC 1412	2.344 0.061	5.645 0.043	0.068 0.002	0.202 0.005	3.011 0.073	3.123 0.058	1.374 0.035	1.884 0.032	1.059 0.029	2.425 0.054	1.093 0.049
NGC 1419	1.386 0.036	5.490 0.042	0.111 0.002	0.249 0.006	3.832 0.074	2.668 0.059	2.022 0.037	1.558 0.021	0.989 0.028	2.363 0.063	1.045 0.051
NGC 1427	1.553 0.076	5.239 0.155	0.134 0.014	0.276 0.021	4.127 0.046	2.901 0.030	2.457 0.167	1.739 0.073	0.946 0.067	3.220 0.241	1.142 0.010
UGC 02836	...	2.271 0.091	0.059 0.003	0.170 0.005	2.593 0.053	2.635 0.048	1.489 0.045	1.111 0.020	0.909 0.037	3.630 0.071	-2.340 0.128
NGC 1426	1.526 0.174	5.760 0.252	0.140 0.004	0.285 0.013	4.176 0.204	3.176 0.214	2.746 0.220	1.988 0.161	0.981 0.156	3.650 0.157	1.176 0.147
NGC 1439	1.698 0.044	5.657 0.612	0.154 0.009	0.302 0.011	4.482 0.186	3.148 0.176	2.811 0.161	1.792 0.177	1.037 0.003	4.318 0.298	1.202 0.368
ESO 358G059	2.037 0.062	5.181 0.040	0.095 0.003	0.187 0.005	2.760 0.060	2.618 0.059	2.068 0.033	1.506 0.021	1.079 0.027	2.030 0.042	0.919 0.053
NGC 1453	1.038 0.026	4.419 0.034	0.165 0.002	0.325 0.005	5.149 0.064	3.383 0.051	2.586 0.029	1.744 0.022	1.073 0.023	5.240 0.073	0.231 0.044
NGC 1461	1.091 0.043	5.526 0.038	0.155 0.002	0.320 0.006	4.760 0.076	3.202 0.067	3.112 0.037	2.601 0.038	0.584 0.023	4.381 0.085	1.122 0.049
IC 2006	1.857 0.045	5.566 0.044	0.155 0.035	0.282 0.006	4.458 0.076	3.267 0.072	2.497 0.035	1.854 0.023	0.905 0.031	4.305 0.107	0.837 0.066
NGC 1521	1.688 0.092	5.842 0.347	0.144 0.003	0.304 0.003	4.460 0.115	3.320 0.131	2.729 0.110	1.852 0.125	1.095 0.031	4.576 0.148	1.131 0.067
NGC 1527	1.620 0.036	5.234 0.037	0.149 0.002	0.299 0.006	4.364 0.075	3.331 0.064	3.119 0.041	1.827 0.030	1.086 0.030	4.522 0.090	1.019 0.043
IC 2035	...	4.441 0.156	0.067 0.012	0.166 0.013	2.507 0.174	2.322 0.088	1.953 0.154	1.362 0.041	0.757 0.141	2.595 0.421	0.605 0.025
NGC 1537	1.961 0.196	5.707 0.258	0.135 0.005	0.272 0.019	4.248 0.148	3.085 0.007	2.538 0.034	1.773 0.097	1.087 0.053	3.938 0.213	1.129 0.015
NGC 1549	1.659	5.672	0.145	0.296	4.512	3.128	2.788	1.941	0.919	4.251	1.090

Table 6—Continued

Name (1)	H β (2)	Fe5015 (3)	Mg ₁ (4)	Mg ₂ (5)	Mgb (6)	Fe5270 (7)	Fe5335 (8)	Fe5406 (9)	Fe5709 (10)	NaD (11)	[O III] (12)
	0.112	0.066	0.000	0.005	0.007	0.049	0.096	0.081	0.045	0.084	0.039
NGC 1553	1.656	5.678	0.157	0.296	4.636	3.359	3.062	1.955	0.908	5.003	0.580
	0.038	0.036	0.002	0.006	0.072	0.068	0.041	0.026	0.027	0.097	0.050
NGC 1550	1.540	5.782	0.177	0.330	5.294	2.764	2.417	1.819	1.286	5.617	1.405
	0.161	0.736	0.011	0.024	0.206	0.806	0.469	0.194	0.026	0.475	0.109
NGC 1567	1.932	4.162	0.119	0.243	3.783	3.042	2.754	1.487	1.174	3.619	0.863
	0.043	0.040	0.003	0.006	0.062	0.059	0.034	0.021	0.027	0.070	0.043
NGC 1574	1.637	5.312	0.158	0.310	4.635	3.078	2.871	1.779	0.908	4.410	0.934
	0.035	0.036	0.002	0.006	0.074	0.059	0.035	0.026	0.029	0.082	0.043
NGC 1596	1.406	4.990	0.150	0.299	4.508	3.088	2.664	2.057	0.993	3.917	0.595
	0.030	0.322	0.000	0.001	0.015	0.077	0.034	0.169	0.123	0.024	0.049
NGC 1595	1.572	5.824	0.139	0.295	4.465	2.857	2.736	1.755	0.866	4.018	1.274
	0.159	0.401	0.000	0.002	0.027	0.105	0.179	0.135	0.061	0.058	0.163
NGC 1600	1.825	6.009	0.178	0.345	5.440	3.232	3.179	1.983	0.973	6.017	1.253
	0.240	0.282	0.014	0.002	0.702	0.307	0.273	0.171	0.134	0.029	0.024
ESO 084G028	1.440	5.413	0.111	0.256	3.953	2.998	2.724	1.627	0.849	3.864	1.185
	0.041	0.040	0.002	0.005	0.062	0.059	0.032	0.024	0.024	0.069	0.049
NGC 1653	1.312	4.564	0.130	0.278	4.614	3.021	2.365	1.702	0.962	4.350	0.266
	0.060	0.401	0.024	0.033	0.167	0.280	0.097	0.137	0.184	0.024	0.158
MCG -02-13-009	1.187	3.980	0.130	0.283	4.358	2.834	2.564	1.841	...	4.036	0.281
	0.200	0.488	0.004	0.002	0.194	0.142	0.104	0.262	...	0.094	0.031
IC 0395	1.038	4.314	...	0.222	4.118	3.217	3.026	1.811	1.017	4.541	0.103
	0.032	0.042	...	0.006	0.057	0.061	0.036	0.021	0.025	0.108	0.056
NGC 1713	1.117	4.228	0.154	0.299	4.487	2.689	2.371	1.904	...	4.411	0.729
	0.325	0.812	0.016	0.027	0.265	0.347	0.138	0.201	...	0.445	0.473
NGC 1700	1.808	5.988	0.144	0.301	4.159	3.178	2.781	1.972	1.049	4.610	1.190
	0.290	0.428	0.011	0.017	0.205	0.099	0.208	0.095	0.109	0.242	0.078
ESO 486G019	2.214	5.497	0.102	0.240	3.700	2.988	2.722	1.649	1.058	3.911	1.103
	0.137	0.133	0.003	0.003	0.166	0.138	0.315	0.232	0.168	0.112	0.098
NGC 1930	1.122	4.848	0.133	0.275	4.384	2.944	2.441	1.909	0.871	3.942	0.640
	0.321	0.501	0.026	0.042	0.262	0.253	0.282	0.186	0.116	0.118	0.152
NGC 1979	1.804	5.713	0.129	0.269	3.805	3.174	2.278	1.649	0.866	3.424	1.314
	0.049	0.041	0.003	0.005	0.063	0.062	0.036	0.025	0.024	0.075	0.047
ESO 423G024	1.970	5.958	0.122	0.268	3.885	3.116	2.619	1.861	1.003	3.932	1.313
	0.188	0.280	0.008	0.007	0.119	0.163	0.307	0.158	0.110	0.176	0.104
NGC 1993	1.350	4.644	0.124	0.280	4.601	2.933	0.729	3.276	0.523
	0.249	0.561	0.019	0.013	0.545	0.288	0.094	0.298	0.318
NGC 2073	1.167	4.968	0.138	0.282	4.242	2.837	2.739	1.881	1.150	4.130	0.423
	0.029	0.037	0.002	0.006	0.073	0.061	0.036	0.025	0.028	0.075	0.053
NGC 2106	1.775	5.078	0.109	0.251	3.602	2.859	2.495	1.794	0.937	3.801	0.437
	0.036	0.040	0.003	0.006	0.064	0.066	0.041	0.027	0.027	0.072	0.055
NGC 2191	2.334	6.108	0.097	0.236	3.549	2.955	2.847	1.706	0.982	3.911	0.955
	0.067	0.152	0.008	0.001	0.233	0.132	0.140	0.174	0.154	0.033	0.092
ESO 425G014	1.265	5.615	0.138	0.293	4.410	3.121	2.889	1.853	0.935	4.710	0.647
	0.032	0.804	0.009	0.007	0.157	0.008	0.052	0.239	0.013	0.240	0.282

Table 6—Continued

Name (1)	H β (2)	Fe5015 (3)	Mg ₁ (4)	Mg ₂ (5)	Mgb (6)	Fe5270 (7)	Fe5335 (8)	Fe5406 (9)	Fe5709 (10)	NaD (11)	[O III] (12)
NGC 2211	1.375 0.036	4.199 0.033	0.112 0.002	0.261 0.006	3.764 0.070	3.400 0.060	2.352 0.037	1.815 0.025	1.063 0.028	3.566 0.081	0.261 0.045
ESO 489G035	1.324 0.153	5.921 0.157	0.155 0.002	0.313 0.008	4.663 0.181	2.955 0.007	2.526 0.262	1.914 0.007	0.925 0.026	4.499 0.099	1.020 0.017
ESO 489G037	2.354 0.060	5.452 0.040	0.085 0.003	0.217 0.005	3.183 0.062	3.296 0.061	2.757 0.042	1.860 0.029	1.080 0.025	2.847 0.065	0.872 0.047
ESO 425G019	1.263 0.112	5.532 0.643	0.129 0.004	0.294 0.021	4.381 0.066	3.188 0.213	2.797 0.121	1.871 0.041	0.926 0.080	4.193 0.091	1.102 0.220
ESO 490G006	1.591 0.027	4.825 0.033	0.127 0.002	0.283 0.006	4.142 0.070	3.124 0.059	2.581 0.039	2.052 0.036	1.046 0.029	3.437 0.072	0.277 0.054
NGC 2267	1.682 0.040	4.831 0.040	0.132 0.003	0.286 0.006	4.548 0.074	3.213 0.063	2.926 0.039	2.079 0.028	1.126 0.026	3.203 0.077	1.121 0.046
NGC 2272	1.481 0.172	5.384 0.025	0.144 0.002	0.277 0.019	4.073 0.392	2.871 0.044	2.630 0.017	1.750 0.111	0.881 0.043	4.380 0.058	0.645 0.201
ESO 491G006	1.278 0.043	6.024 0.035	0.140 0.002	0.286 0.006	4.321 0.071	2.929 0.057	2.545 0.041	1.820 0.029	0.814 0.034	4.180 0.082	0.972 0.054
ESO 058G019	1.658 0.040	6.059 0.047	0.143 0.002	0.299 0.006	4.364 0.078	2.506 0.061	2.506 0.028	1.709 0.034	1.552 0.044	0.877 0.069	3.747 0.052
NGC 2325	1.016 0.035	5.204 0.032	0.153 0.002	0.309 0.005	4.479 0.068	2.895 0.056	2.638 0.033	1.870 0.025	0.940 0.024	4.530 0.071	0.386 0.050
ESO 428G011	1.623 0.018	5.154 0.333	0.129 0.005	0.269 0.016	4.134 0.277	3.094 0.005	2.562 0.150	1.799 0.247	0.856 0.247	3.522 0.421	0.840 0.135
ESO 367G008	1.410 0.038	5.486 0.039	0.151 0.002	0.299 0.005	4.050 0.069	3.159 0.062	2.275 0.032	2.114 0.031	0.734 0.029	4.818 0.080	0.376 0.058
IC 2200A	...	4.611 0.038	0.073 0.002	0.179 0.005	2.775 0.054	2.028 0.049	1.893 0.033	1.402 0.021	1.006 0.022	4.664 0.111	0.897 0.050
ESO 208G021	1.169 0.028	4.535 0.032	0.171 0.002	0.333 0.006	5.010 0.076	3.145 0.057	2.662 0.037	1.942 0.026	0.884 0.024	4.763 0.083	0.442 0.043
NGC 2502	1.376 0.078	4.297 0.332	0.180 0.015	0.328 0.012	4.921 0.002	3.349 0.102	2.887 0.113	1.711 0.220	0.879 0.013	3.569 0.128	0.332 0.277
IC 0494	1.385 0.030	4.329 0.036	0.097 0.003	0.249 0.006	4.056 0.068	2.849 0.066	2.229 0.038	1.546 0.025	1.040 0.032	4.689 0.088	0.346 0.065
UGC 04228	1.650 0.045	5.798 0.046	0.110 0.003	0.248 0.006	3.955 0.065	3.243 0.062	2.761 0.040	1.856 0.029	...	3.738 0.074	1.186 0.052
ESO 124G014	1.669 0.043	4.624 0.038	0.158 0.002	0.315 0.006	4.765 0.072	3.113 0.062	2.555 0.038	1.782 0.027	0.984 0.022	4.617 0.088	1.139 0.046
ESO 494G031	1.361 0.032	5.979 0.031	0.179 0.002	0.335 0.006	5.243 0.081	3.058 0.060	3.203 0.031	1.631 0.023	1.040 0.033	5.100 0.080	0.916 0.052
MCG -02-22-008	1.769 0.037	...	0.312 0.007	4.231 0.071	2.924 0.059	3.594 0.082	2.006 0.065
IC 0513	1.281 0.291	4.713 0.465	0.123 0.015	0.290 0.009	4.715 0.460	3.363 0.222	2.649 0.201	1.998 0.169	...	4.032 0.371	0.463 0.160
NGC 2663	1.462 0.043	5.647 0.013	0.174 0.002	0.334 0.002	4.789 0.046	2.903 0.297	2.786 0.031	1.699 0.075	0.613 0.172	4.911 0.083	1.024 0.079
ESO 563G024	2.036	5.885	0.147	0.277	3.317	2.354	2.250	2.005	0.549	3.599	1.483

Table 6—Continued

Name (1)	H β (2)	Fe5015 (3)	Mg ₁ (4)	Mg ₂ (5)	Mgb (6)	Fe5270 (7)	Fe5335 (8)	Fe5406 (9)	Fe5709 (10)	NaD (11)	[O III] (12)
	0.045	0.046	0.003	0.006	0.074	0.067	0.039	0.030	0.024	0.070	0.054
NGC 2679	2.286	4.792	0.104	0.236	3.337	2.615	2.290	1.806	1.128	3.439	1.306
	0.048	0.049	0.003	0.006	0.073	0.063	0.035	0.028	0.024	0.076	0.055
UGC 04670	2.003	5.835	0.125	0.266	3.581	2.343	2.296	2.002	0.710	4.135	1.095
	0.043	0.041	0.003	0.006	0.069	0.058	0.039	0.030	0.035	0.080	0.052
NGC 2716	2.108	6.128	0.112	0.243	3.512	3.027	2.561	1.612	1.412	3.108	0.905
	0.042	0.037	0.003	0.005	0.061	0.064	0.037	0.025	0.032	0.064	0.059
NGC 2723	1.566	5.205	0.142	0.291	3.838	2.661	2.583	1.498	0.887	4.383	1.249
	0.040	0.037	0.003	0.006	0.071	0.064	0.040	0.024	0.025	0.081	0.045
NGC 2729	1.794	5.512	0.128	0.286	4.586	2.946	2.377	1.998	0.999	3.750	0.813
	0.047	0.045	0.003	0.006	0.073	0.064	0.037	0.026	0.035	0.073	0.056
NGC 2749	1.074	3.358	0.157	0.331	5.271	3.156	2.467	1.667	0.913	5.091	0.435
	0.022	0.037	0.002	0.006	0.064	0.059	0.030	0.023	0.027	0.073	0.038
IC 2437	1.428	4.016	...	0.239	4.587	3.079	1.599	1.572	0.946	4.664	0.842
	0.041	0.049	...	0.006	0.075	0.056	0.036	0.026	0.029	0.100	0.051
NGC 2765	2.340	0.322	3.749	2.928	2.556	2.220	...	5.040	2.012
	0.065	0.005	0.055	0.083	0.036	0.036	...	0.068	0.061
NGC 2822	1.664	6.138	0.146	0.303	4.468	3.391	3.077	2.251	1.023	5.439	0.749
	0.035	0.042	0.003	0.007	0.074	0.072	0.040	0.032	0.032	0.101	0.062
NGC 2865	2.772	5.825	0.095	0.222	3.194	2.768	2.363	1.602	0.744	3.753	0.942
	0.056	0.031	0.002	0.004	0.051	0.053	0.033	0.024	0.022	0.073	0.043
ESO 498G004	2.166	4.835	0.123	0.247	3.920	2.901	2.999	1.646	0.763	3.311	1.767
	0.037	0.059	0.035	0.007	0.078	0.066	0.036	0.033	0.032	0.089	0.046
ESO 498G006	1.723	5.402	0.134	0.275	4.704	2.697	2.366	1.943	0.872	4.642	1.126
	0.044	0.045	0.035	0.006	0.070	0.058	0.037	0.024	0.025	0.087	0.056
NGC 2888	2.319	5.703	0.110	0.240	3.499	3.015	2.796	2.043	0.991	3.450	1.233
	0.052	0.044	0.003	0.005	0.063	0.065	0.036	0.026	0.029	0.071	0.048
NGC 2891	...	4.964	0.100	0.227	3.244	2.619	2.286	1.502	0.884	3.841	0.985
	...	0.178	0.005	0.014	0.063	0.122	0.192	0.149	0.057	0.132	0.061
ESO 126G014	1.178	5.421	0.168	0.324	4.252	3.205	2.740	2.030	0.889	5.758	0.267
	0.027	0.044	0.003	0.006	0.070	0.067	0.033	0.026	0.026	0.099	0.062
NGC 2911	0.518	4.456	0.162	0.312	4.640	3.118	2.210	1.639	1.017	6.927	-0.687
	0.027	0.051	0.002	0.006	0.071	0.069	0.034	0.021	0.030	0.132	0.075
NGC 2918	1.480	5.680	0.117	0.278	4.324	3.007	2.333	2.043	0.758	4.257	0.854
	0.037	0.042	0.002	0.006	0.063	0.059	0.032	0.028	0.026	0.076	0.055
NGC 2945	0.387	3.478	0.125	0.265	4.478	2.642	2.574	1.626	1.055	3.334	-0.875
	0.022	0.045	0.002	0.007	0.082	0.059	0.038	0.026	0.025	0.076	0.069
IC 0552	1.849	4.779	0.149	0.290	4.593	3.358	2.842	1.480	0.905	4.564	1.124
	0.039	0.044	0.002	0.006	0.074	0.063	0.031	0.021	0.022	0.076	0.049
IC 0555	2.007	4.379	0.127	0.281	4.262	2.642	2.550	1.564	1.101	4.198	1.014
	0.044	0.040	0.003	0.006	0.068	0.060	0.038	0.026	0.021	0.079	0.049
NGC 2974	1.010	4.601	0.152	0.301	5.086	3.197	2.965	1.960	1.032	4.832	-0.347
	0.214	0.489	0.011	0.014	0.332	0.319	0.372	0.216	0.118	0.404	0.198
NGC 2984	2.059	4.937	0.131	0.276	4.309	2.532	1.806	1.336	0.567	3.956	1.505
	0.037	0.049	0.002	0.006	0.069	0.058	0.032	0.022	0.029	0.066	0.051

Table 6—Continued

Name (1)	H β (2)	Fe5015 (3)	Mg ₁ (4)	Mg ₂ (5)	Mgb (6)	Fe5270 (7)	Fe5335 (8)	Fe5406 (9)	Fe5709 (10)	NaD (11)	[O III] (12)
NGC 2983	2.062 0.047	5.553 0.051	0.141 0.035	0.272 0.007	4.304 0.071	2.803 0.066	3.051 0.045	2.162 0.026	1.293 0.037	3.816 0.098	1.183 0.068
NGC 2986	1.394 0.031	5.891 0.037	0.177 0.002	0.347 0.006	5.252 0.067	3.292 0.053	3.014 0.032	2.138 0.024	0.997 0.030	5.718 0.080	1.135 0.038
UGC 05226	1.790 0.046	4.985 0.045	0.103 0.003	0.260 0.006	3.931 0.079	2.912 0.070	2.654 0.041	2.242 0.039	0.999 0.038	3.671 0.070	1.371 0.049
ESO 434G040	-1.387 0.375	-14.404 1.176	0.151 0.001	0.261 0.003	4.103 0.310	2.867 0.236	2.889 0.268	1.777 0.107	0.956 0.206	3.737 0.245	-30.181 2.676
NGC 3022	1.206 0.014	4.854 1.104	0.135 0.001	0.296 0.006	4.512 0.486	2.935 0.328	2.943 0.225	1.567 0.246	0.790 0.035	4.384 0.174	1.254 0.004
NGC 3042	1.792 0.034	5.808 0.039	0.129 0.003	0.274 0.006	3.869 0.063	2.992 0.067	2.554 0.035	1.419 0.021	1.099 0.025	5.470 0.101	0.853 0.057
ESO 499G013	1.720 0.038	4.529 0.043	0.131 0.035	0.244 0.006	3.781 0.070	2.999 0.061	2.673 0.041	1.551 0.022	1.165 0.030	4.127 0.096	0.749 0.051
NGC 3051	1.924 0.037	2.795 0.045	0.148 0.035	0.269 0.006	4.746 0.072	2.235 0.055	2.514 0.030	1.768 0.022	0.834 0.032	3.369 0.091	-0.764 0.058
NGC 3056	1.217 0.081	3.204 0.211	0.067 0.002	0.178 0.005	2.567 0.167	2.600 0.137	2.235 0.129	1.522 0.178	0.926 0.018	1.619 0.021	-0.816 0.012
IC 2526	1.631 0.038	4.699 0.038	0.142 0.003	0.288 0.006	4.113 0.068	2.976 0.064	2.917 0.036	1.651 0.026	1.013 0.023	3.884 0.077	0.742 0.052
NGC 3078	1.369 0.034	4.638 0.036	0.161 0.002	0.324 0.006	5.161 0.070	3.021 0.051	3.274 0.035	2.209 0.024	0.932 0.022	5.321 0.078	0.422 0.049
NGC 3082	1.324 0.031	5.289 0.037	0.134 0.003	0.286 0.006	4.330 0.072	3.099 0.063	2.692 0.036	1.760 0.024	0.835 0.021	4.295 0.074	0.877 0.048
NGC 3085	1.609 0.043	4.866 0.038	0.128 0.002	0.276 0.006	4.071 0.062	2.948 0.059	2.734 0.034	1.698 0.026	1.154 0.027	3.836 0.074	0.953 0.045
NGC 3091	1.331 0.027	5.935 0.037	0.178 0.002	0.347 0.005	4.973 0.068	3.309 0.053	3.014 0.032	1.984 0.022	0.894 0.023	5.575 0.072	1.180 0.041
NGC 3090	1.344 0.025	6.231 0.037	0.158 0.002	0.330 0.005	4.941 0.064	3.071 0.065	2.672 0.031	1.623 0.022	0.753 0.037	5.435 0.078	0.695 0.048
NGC 3096	2.007 0.051	5.140 0.041	0.121 0.003	0.284 0.006	4.400 0.074	3.330 0.062	3.040 0.042	2.039 0.028	0.917 0.025	3.962 0.081	1.146 0.057
NGC 3100	0.531 0.027	3.721 0.064	0.170 0.003	0.321 0.007	4.770 0.073	2.907 0.063	2.734 0.037	1.747 0.028	0.782 0.029	5.146 0.089	-1.354 0.090
NGC 3115	1.601 0.066	6.458 0.221	0.162 0.007	0.328 0.006	5.159 0.174	3.515 0.097	3.335 0.155	2.256 0.122	1.055 0.058	5.772 0.192	1.238 0.079
ESO 316G034	0.972 0.037	3.749 0.042	0.141 0.002	0.300 0.005	4.349 0.064	2.546 0.053	2.159 0.022	1.869 0.027	0.822 0.026	4.830 0.080	1.144 0.038
NGC 3142	1.416 0.098	5.971 0.871	0.126 0.009	0.275 0.019	4.325 0.290	2.958 0.095	2.804 0.093	1.777 0.134	0.960 0.022	4.574 0.214	1.316 0.075
IC 2552	1.485 0.043	4.882 0.038	0.141 0.002	0.290 0.006	4.167 0.072	3.168 0.063	2.747 0.037	1.901 0.027	0.906 0.030	4.141 0.079	0.977 0.046
ESO 316G046	1.327 0.039	5.075 0.042	0.130 0.003	0.270 0.006	4.021 0.070	3.159 0.067	2.852 0.039	1.635 0.024	1.230 0.028	3.846 0.077	0.847 0.058
ESO 500G018	0.936	5.011	0.120	0.244	3.525	2.053	2.831	1.962	1.034	3.761	0.496

Table 6—Continued

Name (1)	H β (2)	Fe5015 (3)	Mg ₁ (4)	Mg ₂ (5)	Mgb (6)	Fe5270 (7)	Fe5335 (8)	Fe5406 (9)	Fe5709 (10)	NaD (11)	[O III] (12)
	0.019	0.036	0.003	0.006	0.063	0.056	0.035	0.025	0.024	0.063	0.059
ESO 567G052	1.560	4.178	0.108	0.261	3.973	2.584	2.300	1.241	0.968	2.836	0.621
	0.047	0.039	0.002	0.006	0.074	0.056	0.034	0.026	0.022	0.064	0.055
NGC 3209	1.484	4.992	0.153	0.316	4.745	3.236	2.930	1.833	0.866	5.278	1.036
	0.031	0.036	0.002	0.006	0.069	0.055	0.028	0.022	0.019	0.067	0.041
NGC 3224	2.128	5.210	0.117	0.250	3.612	2.879	2.463	1.826	0.982	3.630	1.138
	0.052	0.044	0.003	0.006	0.070	0.063	0.034	0.025	0.025	0.072	0.047
ESO 317G021	1.759	3.588	0.115	0.256	3.741	2.867	2.306	1.477	0.597	2.699	0.904
	0.054	0.035	0.003	0.006	0.065	0.065	0.038	0.023	0.028	0.060	0.047
ESO 263G033	1.045	5.257	0.128	0.269	4.783	2.779	3.006	2.027	0.890	4.240	0.590
	0.048	0.045	0.003	0.007	0.077	0.069	0.040	0.025	0.035	0.096	0.060
ESO 436G027	1.698	4.375	0.123	0.245	3.714	2.819	2.211	1.677	0.932	3.647	0.029
	0.028	0.034	0.002	0.005	0.053	0.055	0.038	0.021	0.020	0.069	0.054
NGC 3273	1.379	5.714	0.166	0.323	4.748	3.191	2.799	1.496	0.867	4.609	1.068
	0.031	0.034	0.002	0.006	0.073	0.058	0.034	0.019	0.020	0.072	0.046
IC 2586	1.419	5.638	0.144	0.284	4.862	3.529	3.215	2.123	1.055	5.080	0.896
	0.034	0.043	0.035	0.006	0.068	0.055	0.036	0.020	0.024	0.094	0.052
IC 2587	1.773	5.923	0.130	0.258	3.880	2.889	2.664	1.748	0.906	3.875	0.994
	0.030	0.040	0.003	0.006	0.066	0.072	0.040	0.027	0.029	0.067	0.051
ESO 263G048	1.295	6.022	0.213	0.377	4.285	3.043	2.604	1.731	0.551	5.745	1.316
	0.034	0.048	0.003	0.006	0.065	0.064	0.030	0.025	0.023	0.090	0.053
ESO 501G003	1.299	5.889	0.112	0.245	4.290	3.142	2.730	1.702	1.004	3.907	1.322
	0.174	0.769	0.012	0.007	0.258	0.103	0.437	0.203	0.126	0.649	0.049
NGC 3282	1.505	4.982	0.125	0.266	3.889	2.832	2.839	1.607	1.015	4.791	0.697
	0.034	0.039	0.003	0.006	0.074	0.068	0.042	0.026	0.032	0.097	0.066
MCG -01-27-015	1.341	4.981	0.141	0.298	4.718	2.588	2.752	1.922	0.986	4.570	1.038
	0.003	0.136	0.003	0.001	0.169	0.037	0.190	0.174	0.222	0.139	0.076
MCG -01-27-018	0.995	5.268	0.161	0.318	4.713	2.712	2.816	1.505	0.541	4.762	1.126
	0.028	0.040	0.002	0.006	0.067	0.055	0.035	0.021	0.021	0.065	0.045
ESO 501G025	1.538	5.900	...	0.231	3.684	3.104	2.337	1.968	1.371	3.633	1.455
	0.041	0.056	...	0.006	0.068	0.070	0.044	0.026	0.038	0.114	0.059
NGC 3302	1.391	4.572	0.197	0.339	4.600	3.181	2.938	1.625	0.896	4.685	0.259
	0.034	0.033	0.002	0.006	0.067	0.064	0.033	0.019	0.024	0.080	0.045
NGC 3305	1.785	4.760	0.135	0.275	5.021	2.613	2.386	1.421	0.878	4.881	1.353
	0.032	0.050	0.034	0.006	0.072	0.056	0.027	0.020	0.023	0.100	0.048
NGC 3300	1.515	4.513	0.115	0.261	4.049	3.003	2.607	1.657	1.228	3.604	1.222
	0.043	0.043	0.003	0.006	0.063	0.065	0.044	0.026	0.033	0.076	0.044
NGC 3308	1.563	6.082	0.157	0.324	4.828	3.234	2.668	1.838	1.179	4.603	1.333
	0.041	0.046	0.002	0.006	0.074	0.061	0.036	0.026	0.035	0.079	0.048
NGC 3311	1.429	4.048	0.173	0.356	5.222	2.548	3.022	1.483	1.239	5.736	1.249
	0.034	0.047	0.003	0.007	0.081	0.065	0.038	0.028	0.025	0.089	0.037
ESO 437G015	2.478	5.133	2.697	2.500	2.066	1.650	0.948	3.214	1.186
	0.053	0.050	0.055	0.052	0.027	0.020	0.028	0.102	0.054
NGC 3316	1.552	5.433	0.115	0.253	3.969	3.269	2.724	2.096	1.140	3.974	1.276
	0.142	0.369	0.007	0.027	0.333	0.251	0.183	0.020	0.013	0.220	0.027

Table 6—Continued

Name (1)	H β (2)	Fe5015 (3)	Mg ₁ (4)	Mg ₂ (5)	Mgb (6)	Fe5270 (7)	Fe5335 (8)	Fe5406 (9)	Fe5709 (10)	NaD (11)	[O III] (12)
ESO 501G056	1.566 0.029	5.255 0.044	...	0.210 0.007	3.254 0.104	2.888 0.074	2.171 0.033	1.709 0.027	0.748 0.035	4.311 0.103	1.199 0.061
ESO 437G021	2.088 0.077	4.121 0.161	0.113 0.001	0.247 0.005	4.071 0.155	3.091 0.121	2.345 0.086	1.545 0.322	0.962 0.092	3.665 0.142	0.746 0.309
NGC 3325	1.939 0.046	4.243 0.043	0.109 0.002	0.243 0.006	3.384 0.068	2.834 0.064	2.310 0.035	1.587 0.023	0.958 0.023	3.400 0.069	1.234 0.041
NGC 3335	1.012 0.032	3.878 0.036	0.112 0.002	0.262 0.005	4.052 0.064	2.650 0.059	2.454 0.035	1.456 0.019	1.168 0.028	4.047 0.073	0.224 0.048
NGC 3332	0.783 0.027	4.312 0.036	0.127 0.002	0.282 0.006	4.608 0.065	2.667 0.056	2.412 0.031	1.885 0.025	0.933 0.022	3.951 0.063	0.148 0.059
[R89] 461	0.124	...	2.358	1.825	0.161
	0.022	...	0.051	0.420	0.231
ESO 437G038	1.271 0.027	4.311 0.051	0.141 0.003	0.298 0.006	4.651 0.070	2.756 0.073	2.654 0.044	1.587 0.029	0.740 0.030	4.131 0.082	0.823 0.046
ESO 437G045	1.745 0.046	5.194 0.039	0.112 0.003	0.263 0.006	4.110 0.072	3.400 0.066	3.150 0.038	1.986 0.027	0.953 0.028	3.733 0.074	0.744 0.056
ESO 376G009	1.647 0.043	4.835 0.042	0.126 0.003	0.265 0.006	3.723 0.068	3.122 0.065	2.424 0.040	1.949 0.029	1.225 0.027	3.375 0.069	1.283 0.051
IC 0642	1.028 0.043	3.988 0.041	0.116 0.003	0.273 0.006	4.359 0.068	2.807 0.058	3.062 0.034	1.859 0.025	0.742 0.026	3.522 0.068	-0.178 0.058
ESO 569G012	1.198 0.026	4.530 0.045	2.350 0.052	1.885 0.028	1.268 0.018	1.038 0.030	2.797 0.103	0.632 0.058
NGC 3412	2.024 0.048	5.234 0.040	0.098 0.003	0.238 0.006	3.527 0.064	3.004 0.065	2.669 0.037	1.866 0.032	0.920 0.030	3.018 0.067	1.186 0.051
NGC 3483	1.320 0.169	4.749 0.639	0.127 0.013	0.284 0.009	4.224 0.209	2.968 0.246	2.481 0.182	1.727 0.166	1.009 0.099	4.234 0.283	0.766 0.159
NGC 3522	1.379 0.034	4.244 0.037	0.095 0.002	0.219 0.005	3.280 0.063	2.671 0.061	2.273 0.031	1.543 0.025	0.917 0.028	2.055 0.056	0.302 0.057
MCG -03-28-037	1.100 0.018	4.294 0.035	0.152 0.002	0.309 0.006	4.622 0.072	3.272 0.062	2.782 0.037	1.622 0.026	1.011 0.027	4.608 0.074	0.182 0.053
NGC 3546	0.583 0.040	5.840 0.050	0.122 0.035	0.258 0.007	4.860 0.077	3.266 0.058	3.421 0.039	1.780 0.024	1.064 0.030	3.970 0.094	0.767 0.064
NGC 3557	1.409 0.023	6.053 0.498	0.143 0.002	0.311 0.007	4.807 0.165	3.221 0.053	2.892 0.066	2.026 0.294	0.927 0.074	5.640 0.349	1.279 0.027
NGC 3564	1.449 0.046	5.184 0.043	0.150 0.003	0.309 0.006	4.533 0.072	3.059 0.065	2.877 0.036	1.895 0.028	0.883 0.024	3.765 0.067	1.110 0.049
NGC 3585	1.578 0.031	6.351 0.269	0.172 0.000	0.332 0.001	4.941 0.008	3.181 0.276	3.245 0.051	2.177 0.006	0.950 0.032	4.833 0.038	1.134 0.046
NGC 3591	1.894 0.043	5.014 0.053	...	0.183 0.005	3.444 0.058	2.662 0.056	2.483 0.041	1.747 0.025	1.074 0.027	3.532 0.102	0.580 0.069
ESO 377G029	1.324 0.034	5.557 0.038	0.150 0.002	0.310 0.006	4.726 0.072	2.662 0.058	2.450 0.030	1.604 0.024	0.774 0.022	4.536 0.070	1.147 0.046
NGC 3598	0.949 0.053	5.210 1.178	0.104 0.015	0.269 0.024	4.670 0.831	2.816 0.200	2.774 0.105	2.102 0.432	...	4.224 0.084	0.836 0.342
NGC 3599	2.225	4.429	0.086	0.211	3.339	3.048	2.764	1.660	1.231	3.209	-0.116

Table 6—Continued

Name (1)	H β (2)	Fe5015 (3)	Mg ₁ (4)	Mg ₂ (5)	Mgb (6)	Fe5270 (7)	Fe5335 (8)	Fe5406 (9)	Fe5709 (10)	NaD (11)	[O III] (12)
	0.047	0.043	0.003	0.006	0.065	0.068	0.037	0.024	0.034	0.064	0.071
NGC 3605	1.995	4.958	0.093	0.219	3.425	3.207	2.659	1.591	1.135	3.556	1.057
	0.049	0.046	0.003	0.006	0.074	0.068	0.040	0.022	0.023	0.062	0.059
NGC 3617	1.835	5.304	0.115	0.246	3.534	2.609	2.434	1.734	0.844	3.429	1.183
	0.045	0.039	0.003	0.006	0.070	0.062	0.036	0.028	0.025	0.074	0.049
NGC 3615	1.359	5.654	0.141	0.305	4.486	3.247	2.087	1.757	0.956	4.470	1.264
	0.037	0.042	0.002	0.005	0.062	0.055	0.034	0.022	0.022	0.068	0.041
NGC 3636	2.490	3.181	3.364	2.459	1.645	...	2.688	-0.023
	0.054	0.066	0.097	0.066	0.030	...	0.073	0.052
IC 2764	1.155	5.409	0.095	0.224	3.603	3.296	2.745	...	1.058	1.999	0.169
	0.323	0.847	0.008	0.004	0.246	0.804	0.229	...	0.196	0.128	0.395
NGC 3706	1.631	5.977	0.167	0.335	4.731	3.429	2.961	1.999	1.007	5.386	1.204
	0.035	0.034	0.002	0.005	0.061	0.054	0.035	0.023	0.022	0.070	0.038
NGC 3768	1.482	5.979	0.127	0.279	3.845	3.048	2.640	1.668	0.916	4.436	1.444
	0.038	0.046	0.002	0.006	0.070	0.058	0.038	0.021	0.026	0.070	0.045
NGC 3778	1.392	5.422	0.149	0.314	4.711	2.854	2.722	1.752	1.080	4.019	1.023
	0.040	0.039	0.002	0.006	0.069	0.053	0.038	0.024	0.022	0.066	0.051
NGC 3805	1.207	4.651	0.152	0.307	4.303	3.368	2.737	1.826	0.835	5.208	0.705
	0.022	0.033	0.002	0.006	0.069	0.059	0.031	0.024	0.024	0.078	0.042
NGC 3818	1.296	5.493	0.163	0.287	4.581	3.096	2.538	1.648	0.910	4.018	1.030
	0.031	0.046	0.035	0.006	0.073	0.061	0.029	0.025	0.028	0.104	0.060
NGC 3837	1.161	5.040	0.159	0.313	4.457	2.277	2.202	1.881	0.944	4.783	0.967
	0.031	0.035	0.002	0.006	0.073	0.057	0.034	0.026	0.022	0.070	0.041
NGC 3886	1.499	4.878	0.142	0.307	4.415	3.219	2.578	1.667	0.806	4.666	1.091
	0.037	0.038	0.002	0.006	0.068	0.060	0.031	0.021	0.022	0.071	0.042
ESO 378G020	2.542	5.838	0.064	0.184	2.967	2.502	2.517	1.661	0.813	3.950	1.185
	0.058	0.040	0.002	0.005	0.057	0.062	0.034	0.024	0.031	0.087	0.054
NGC 3892	1.874	5.801	0.108	0.270	4.213	3.236	2.637	1.711	1.376	3.494	1.216
	0.051	0.045	0.003	0.006	0.069	0.072	0.045	0.026	0.033	0.075	0.051
NGC 3904	1.578	5.577	0.150	0.304	4.687	2.970	2.821	1.902	0.941	4.211	1.194
	0.168	0.406	0.017	0.024	0.372	0.405	0.202	0.112	0.072	0.117	0.106
NGC 3919	1.046	5.487	0.172	0.348	5.209	2.778	2.812	1.626	0.781	6.186	0.862
	0.026	0.040	0.002	0.006	0.076	0.064	0.037	0.020	0.025	0.088	0.044
NGC 3923	1.623	6.332	0.171	0.341	4.987	3.288	2.975	2.180	0.974	5.924	1.197
	0.138	0.500	0.005	0.004	0.139	0.131	0.169	0.114	0.164	0.347	0.085
NGC 3954	1.841	5.146	0.113	0.262	3.801	3.015	2.729	1.803	1.200	4.141	1.333
	0.042	0.039	0.002	0.005	0.064	0.067	0.040	0.022	0.019	0.070	0.040
NGC 3962	1.076	5.066	0.156	0.323	5.094	3.209	2.836	...	1.068	5.359	0.311
	0.031	0.034	0.002	0.006	0.070	0.057	0.030	...	0.032	0.089	0.049
ESO 440G037	1.378	4.168	0.094	0.213	3.507	2.575	2.159	1.736	0.956	1.871	0.516
	0.046	0.037	0.002	0.005	0.062	0.065	0.032	0.023	0.023	0.057	0.051
NGC 4033	2.041	5.568	0.103	0.246	3.728	2.826	2.818	1.696	0.997	3.130	1.098
	0.047	0.037	0.003	0.006	0.066	0.065	0.041	0.027	0.030	0.068	0.053
ESO 440G038	2.236	5.405	0.091	0.226	3.266	3.072	2.330	1.746	1.016	2.908	1.238
	0.102	0.313	0.003	0.008	0.095	0.296	0.229	0.114	0.046	0.220	0.198

Table 6—Continued

Name (1)	H β (2)	Fe5015 (3)	Mg ₁ (4)	Mg ₂ (5)	Mgb (6)	Fe5270 (7)	Fe5335 (8)	Fe5406 (9)	Fe5709 (10)	NaD (11)	[O III] (12)
NGC 4078	1.572 0.043	5.299 0.035	0.139 0.002	0.293 0.006	4.520 0.069	2.771 0.062	2.421 0.031	1.575 0.025	0.860 0.026	4.417 0.076	0.900 0.047
NGC 4191	1.543 0.041	3.518 0.042	0.117 0.002	0.259 0.006	4.091 0.078	3.169 0.070	2.289 0.038	1.776 0.032	1.092 0.029	3.607 0.074	0.416 0.054
NGC 4215	1.815 0.044	6.477 0.041	0.112 0.003	0.254 0.006	3.803 0.074	3.016 0.056	2.639 0.035	1.850 0.029	1.037 0.025	4.189 0.077	1.416 0.060
NGC 4233	1.601 0.034	5.365 0.029	0.141 0.002	0.299 0.006	4.715 0.070	3.243 0.062	2.763 0.034	1.967 0.025	0.946 0.024	4.682 0.076	0.654 0.048
NGC 4239	2.377 0.056	4.784 0.038	0.068 0.003	0.197 0.005	3.127 0.060	2.586 0.065	2.530 0.034	1.488 0.021	0.776 0.019	2.658 0.037	0.644 0.052
NGC 4240	...	5.198 0.174	0.096 0.009	0.228 0.007	3.616 0.235	2.756 0.128	2.547 0.210	1.500 0.112	1.031 0.097	3.018 0.053	0.506 0.141
NGC 4261	1.244 0.027	5.329 0.032	0.171 0.002	0.344 0.006	5.502 0.071	3.408 0.051	2.673 0.029	2.046 0.022	1.444 0.086	5.987 0.075	0.739 0.038
NGC 4270	2.006 0.045	5.068 0.044	0.105 0.003	0.262 0.006	4.555 0.069	3.013 0.062	2.847 0.040	1.670 0.022	1.058 0.029	3.647 0.062	0.950 0.048
NGC 4318	1.431 0.042	4.841 0.038	0.089 0.003	0.215 0.005	3.199 0.062	3.001 0.059	2.526 0.037	1.816 0.025	0.896 0.027	2.325 0.053	0.961 0.049
NGC 4339	1.573 0.043	6.316 0.043	0.127 0.003	0.272 0.007	4.464 0.082	2.976 0.071	2.914 0.038	1.748 0.027	1.202 0.029	4.112 0.080	1.347 0.053
IC 3289	1.342 0.037	5.266 0.044	0.166 0.003	0.322 0.006	4.565 0.071	2.845 0.066	2.827 0.036	2.054 0.027	0.970 0.021	4.973 0.089	1.143 0.044
NGC 4374	1.001 0.217	5.088 0.330	0.158 0.007	0.320 0.006	5.193 0.078	3.158 0.039	2.840 0.203	1.973 0.015	0.903 0.010	5.043 0.269	0.636 0.078
NGC 4373	1.609 0.037	5.649 0.038	0.154 0.002	0.309 0.005	4.542 0.064	3.226 0.056	2.686 0.035	1.728 0.025	1.115 0.024	4.386 0.071	1.115 0.042
NGC 4379	1.659 0.039	4.846 0.040	0.103 0.003	0.243 0.006	4.128 0.073	2.815 0.057	2.581 0.038	1.819 0.025	1.111 0.028	3.438 0.069	1.074 0.044
NGC 4373A	0.640 0.022	4.210 0.034	0.132 0.002	0.263 0.006	3.973 0.068	3.026 0.056	2.353 0.027	1.516 0.021	0.957 0.027	4.314 0.080	0.448 0.048
NGC 4404	0.879 0.038	4.579 0.030	0.150 0.002	0.300 0.006	4.396 0.071	2.464 0.062	2.518 0.030	1.875 0.024	1.054 0.027	4.366 0.075	-0.168 0.054
NGC 4417	1.685 0.192	5.371 0.083	0.131 0.002	0.276 0.015	4.235 0.271	2.974 0.169	2.445 0.376	1.770 0.136	0.901 0.225	3.749 0.461	1.076 0.056
NGC 4472	1.363 0.391	6.404 0.066	0.190 0.007	0.329 0.000	5.574 0.379	3.241 0.279	3.183 0.018	2.165 0.035	1.207 0.123	5.331 0.260	1.256 0.167
NGC 4474	2.447 0.048	5.659 0.046	0.085 0.003	0.245 0.006	3.984 0.071	2.922 0.066	2.680 0.039	1.835 0.027	1.471 0.026	2.464 0.066	1.089 0.054
NGC 4486	-0.688 0.037	2.838 0.053	0.207 0.035	0.332 0.006	6.173 0.073	2.794 0.053	2.152 0.019	1.904 0.015	1.048 0.018	4.961 0.072	-1.054 0.070
NGC 4489	2.103 0.058	5.921 0.043	0.060 0.003	0.204 0.005	3.469 0.060	2.875 0.064	2.616 0.038	1.879 0.032	1.372 0.029	3.057 0.060	1.260 0.054
NGC 4515	1.783 0.052	4.865 0.043	0.098 0.003	0.220 0.006	3.444 0.068	2.519 0.061	2.191 0.036	1.491 0.021	1.157 0.029	2.193 0.051	1.178 0.053
NGC 4546	0.988	4.786	0.172	0.323	4.860	3.037	2.902	1.794	0.985	6.437	-0.368

Table 6—Continued

Name (1)	H β (2)	Fe5015 (3)	Mg ₁ (4)	Mg ₂ (5)	Mgb (6)	Fe5270 (7)	Fe5335 (8)	Fe5406 (9)	Fe5709 (10)	NaD (11)	[O III] (12)
	0.025	0.046	0.003	0.006	0.072	0.064	0.036	0.024	0.025	0.117	0.070
NGC 4550	1.638	4.485	0.105	0.233	3.607	2.928	2.383	1.773	0.939	3.751	0.113
	0.037	0.038	0.003	0.005	0.064	0.062	0.039	0.026	0.025	0.060	0.064
NGC 4551	1.702	5.431	0.118	0.277	4.504	3.176	2.810	1.946	0.965	3.548	1.292
	0.046	0.040	0.002	0.006	0.075	0.061	0.038	0.034	0.027	0.078	0.049
NGC 4553	1.683	5.812	0.145	0.301	4.254	3.062	3.170	1.889	1.050	4.400	0.879
	0.038	0.037	0.003	0.006	0.069	0.078	0.042	0.027	0.035	0.084	0.056
ESO 574G012	2.095	6.277	0.103	0.287	3.851	2.713	2.567	2.000	0.644	3.930	1.169
	0.052	0.036	0.003	0.005	0.060	0.066	0.044	0.037	0.025	0.079	0.042
UGC 07813	1.446	6.829	0.131	0.285	4.673	2.995	2.298	1.320	0.867	4.377	1.428
	0.041	0.035	0.002	0.006	0.063	0.058	0.028	0.020	0.025	0.073	0.049
NGC 4603C	2.328	6.685	0.112	0.274	4.117	2.910	3.024	2.344	1.301	4.037	1.528
	0.052	0.053	0.003	0.006	0.073	0.065	0.039	0.032	0.029	0.075	0.062
ESO 322G051	0.705	6.868	0.155	0.350	4.560	2.253	2.785	2.400	0.943	4.705	0.791
	0.047	0.036	0.003	0.006	0.073	0.063	0.033	0.036	0.030	0.077	0.070
NGC 4612	2.096	6.032	0.074	0.220	3.187	3.035	2.833	1.699	1.018	3.280	1.107
	0.052	0.044	0.003	0.006	0.064	0.065	0.041	0.022	0.028	0.071	0.057
NGC 4645A	0.909	3.442	0.162	0.301	3.458	2.404	3.001	1.465	1.090	4.514	0.094
	0.048	0.056	0.003	0.006	0.068	0.066	0.036	0.035	0.026	0.088	0.066
NGC 4645B	1.451	5.126	0.162	0.309	4.357	3.171	2.626	2.026	0.884	4.663	1.229
	0.044	0.047	0.003	0.006	0.077	0.065	0.042	0.025	0.026	0.088	0.047
NGC 4649	1.299	6.164	0.188	0.364	5.918	3.425	3.389	2.160	0.763	6.490	0.986
	0.031	0.035	0.002	0.005	0.064	0.048	0.031	0.021	0.016	0.079	0.038
NGC 4645	1.468	5.360	0.155	0.309	4.533	3.161	2.783	2.013	0.943	4.249	0.676
	0.034	0.036	0.002	0.005	0.065	0.068	0.036	0.029	0.033	0.070	0.051
NGC 4685	2.766	4.724	0.065	0.184	2.727	2.569	2.138	1.595	0.857	3.267	0.956
	0.059	0.035	0.002	0.004	0.047	0.055	0.028	0.025	0.019	0.070	0.044
NGC 4683	1.330	5.507	0.137	0.305	4.487	2.729	2.746	1.208	1.169	4.257	1.095
	0.035	0.038	0.003	0.006	0.076	0.064	0.038	0.019	0.032	0.070	0.051
ESO 507G014	1.826	5.350	0.101	0.261	3.837	2.988	2.705	1.888	1.145	3.895	1.197
	0.046	0.040	0.003	0.006	0.068	0.068	0.039	0.025	0.029	0.075	0.055
NGC 4694	2.929	3.306	0.027	0.101	1.840	1.931	1.560	1.029	0.610	2.072	0.135
	0.046	0.032	0.002	0.003	0.039	0.035	0.020	0.016	0.023	0.051	0.047
NGC 4697	1.509	5.577	0.129	0.281	4.389	3.361	2.852	1.941	0.861	4.482	1.115
	0.063	0.320	0.021	0.014	0.231	0.147	0.140	0.114	0.185	0.145	0.125
NGC 4696	0.920	5.539	0.190	0.356	5.344	2.328	2.231	1.812	0.811	5.452	0.487
	0.024	0.035	0.002	0.006	0.070	0.049	0.033	0.021	0.017	0.070	0.037
NGC 4714	1.326	5.334	0.130	0.276	4.426	2.671	2.780	1.750	1.337	4.369	0.879
	0.031	0.043	0.035	0.006	0.068	0.053	0.034	0.022	0.029	0.097	0.053
ESO 507G021	0.945	4.171	0.160	0.311	4.488	3.327	2.749	1.909	1.102	4.572	-0.243
	0.025	0.037	0.003	0.006	0.078	0.058	0.036	0.026	0.025	0.080	0.063
ESO 507G024	2.144	5.960	...	0.191	3.227	3.277	2.035	1.599	1.085	2.848	1.346
	0.064	0.052	...	0.005	0.058	0.051	0.032	0.027	0.027	0.083	0.065
ESO 507G025	0.951	4.467	0.156	0.305	4.320	2.941	2.339	1.521	1.093	4.646	0.480
	0.025	0.040	0.002	0.005	0.064	0.054	0.031	0.023	0.028	0.072	0.046

Table 6—Continued

Name (1)	H β (2)	Fe5015 (3)	Mg ₁ (4)	Mg ₂ (5)	Mgb (6)	Fe5270 (7)	Fe5335 (8)	Fe5406 (9)	Fe5709 (10)	NaD (11)	[O III] (12)
ESO 507G027	1.621 0.044	5.501 0.053	… 0.127	0.239 0.006	3.860 0.076	3.416 0.067	2.510 0.034	1.855 0.023	0.965 0.040	4.238 0.098	1.262 0.065
NGC 4739	1.447 0.038	5.556 0.044	0.127 0.003	0.248 0.006	4.317 0.078	2.405 0.058	2.672 0.035	1.614 0.029	0.874 0.028	2.727 0.066	0.997 0.058
NGC 4730	1.472 0.260	5.561 0.341	0.159 0.012	0.320 0.006	4.945 0.217	2.981 0.218	2.733 0.403	1.972 0.133	0.878 0.161	5.091 0.267	1.003 0.083
NGC 4742	… …	5.194 0.034	0.070 0.002	0.176 0.004	2.604 0.051	2.386 0.053	2.212 0.030	1.548 0.023	0.840 0.023	2.780 0.065	1.001 0.050
NGC 4756	1.299 0.033	4.355 0.037	0.147 0.002	0.311 0.006	4.467 0.068	2.947 0.061	2.879 0.030	1.734 0.021	0.953 0.023	4.620 0.079	1.053 0.040
NGC 4760	0.993 0.031	5.374 0.036	0.159 0.002	0.311 0.006	5.199 0.079	3.189 0.047	2.519 0.032	1.366 0.020	0.875 0.026	4.532 0.068	0.781 0.048
NGC 4767	1.662 0.037	5.821 0.035	0.162 0.002	0.326 0.005	4.274 0.068	3.272 0.060	2.566 0.037	1.880 0.026	0.993 0.026	4.846 0.077	1.213 0.042
IC 3896	1.694 0.041	5.839 0.038	0.186 0.002	0.330 0.006	4.464 0.070	3.085 0.059	2.703 0.035	1.917 0.025	0.748 0.022	4.992 0.079	1.260 0.041
NGC 4825	0.266 0.024	4.594 0.036	0.162 0.002	0.334 0.005	4.969 0.065	2.687 0.052	2.131 0.027	1.784 0.022	0.902 0.025	4.940 0.070	-0.218 0.049
NGC 4830	1.241 0.082	4.680 0.886	0.135 0.005	0.287 0.001	4.382 0.212	2.917 0.083	2.169 0.431	1.783 0.171	0.946 0.185	3.646 0.072	0.708 0.125
NGC 4855	2.004 0.042	5.692 0.036	0.114 0.002	0.253 0.005	3.920 0.061	2.825 0.054	2.218 0.028	1.677 0.025	1.008 0.028	3.656 0.070	0.836 0.052
MCG -01-33-074	1.359 0.048	2.816 0.040	0.092 0.003	0.237 0.006	3.920 0.071	2.946 0.068	2.708 0.040	1.394 0.021	1.195 0.026	2.706 0.055	0.188 0.062
ESO 443G039	1.909 0.042	4.204 0.042	0.131 0.003	0.252 0.006	3.565 0.063	2.687 0.063	2.862 0.041	1.900 0.028	1.063 0.028	3.693 0.080	1.169 0.040
NGC 4933A	1.213 0.038	4.968 0.043	0.114 0.003	0.241 0.006	3.772 0.061	1.819 0.078	2.495 0.033	1.490 0.025	0.931 0.022	4.879 0.112	0.245 0.065
NGC 4936	0.655 0.022	4.461 0.048	0.176 0.002	0.321 0.006	4.944 0.075	3.199 0.057	3.032 0.035	2.212 0.029	0.950 0.021	5.471 0.080	-0.319 0.062
ESO 443G053	1.509 0.035	5.067 0.042	0.154 0.002	0.336 0.006	4.571 0.081	2.587 0.064	2.266 0.029	1.698 0.025	0.821 0.031	4.404 0.082	0.977 0.050
NGC 4958	1.475 0.062	4.744 0.303	0.133 0.014	0.273 0.013	4.285 0.206	3.154 0.112	2.901 0.101	1.963 0.169	1.140 0.042	4.064 0.214	0.389 0.161
IC 4180	1.569 0.028	4.728 0.040	0.091 0.003	0.205 0.005	2.995 0.060	2.676 0.059	2.347 0.039	1.717 0.030	0.983 0.022	2.948 0.056	0.844 0.052
ESO 508G008	1.026 0.091	6.554 0.259	0.168 0.003	0.329 0.006	4.591 0.309	3.064 0.066	2.436 0.068	1.818 0.082	0.737 0.044	4.975 0.179	1.095 0.344
NGC 4989	1.344 0.024	6.425 0.037	0.134 0.003	0.293 0.006	4.233 0.059	2.923 0.062	2.891 0.043	1.923 0.027	0.992 0.029	5.242 0.082	0.582 0.060
NGC 4993	1.259 0.040	6.150 0.038	0.140 0.003	0.267 0.006	3.898 0.071	2.994 0.055	2.146 0.039	1.917 0.027	0.529 0.023	4.178 0.085	0.667 0.061
NGC 4997	2.451 0.047	5.842 0.040	0.107 0.003	0.258 0.006	3.594 0.069	2.903 0.066	2.378 0.033	1.714 0.033	0.841 0.028	4.116 0.087	1.292 0.049
ESO 323G092	1.458	4.451	0.136	0.274	3.609	2.341	2.934	1.355	1.149	3.715	0.978

Table 6—Continued

Name (1)	H β (2)	Fe5015 (3)	Mg ₁ (4)	Mg ₂ (5)	Mgb (6)	Fe5270 (7)	Fe5335 (8)	Fe5406 (9)	Fe5709 (10)	NaD (11)	[O III] (12)
	0.038	0.044	0.003	0.006	0.064	0.067	0.036	0.025	0.021	0.071	0.047
NGC 5011	1.442	5.878	0.165	0.314	4.095	3.059	2.619	1.691	0.844	4.649	1.214
	0.030	0.038	0.002	0.005	0.064	0.058	0.035	0.024	0.021	0.069	0.038
NGC 5017	1.613	...	0.131	0.273	4.246	3.302	2.733	1.970	0.848	3.683	2.168
	0.042	...	0.002	0.006	0.066	0.058	0.039	0.026	0.025	0.069	0.310
NGC 5028	1.847	6.009	0.152	0.308	4.991	3.090	3.270	1.327	0.743	5.070	1.334
	0.039	0.041	0.002	0.005	0.065	0.054	0.028	0.014	0.019	0.064	0.038
NGC 5044	0.371	4.305	0.170	0.322	5.753	2.825	2.474	1.786	0.677	5.325	0.023
	0.028	0.036	0.002	0.007	0.079	0.056	0.033	0.023	0.019	0.085	0.048
NGC 5048	1.433	4.770	0.118	0.265	4.207	3.226	2.465	1.915	1.052	3.245	0.659
	0.022	0.185	0.013	0.007	0.288	0.913	0.230	0.324	0.128	0.155	0.270
NGC 5049	1.599	5.452	0.122	0.268	4.085	2.755	2.269	1.799	1.045	3.518	1.012
	0.046	0.033	0.002	0.006	0.071	0.059	0.036	0.024	0.028	0.070	0.053
ESO 382G034	1.579	4.503	0.097	0.243	3.771	2.996	2.624	1.722	1.098	2.851	0.282
	0.044	0.035	0.003	0.006	0.064	0.063	0.035	0.026	0.028	0.064	0.062
NGC 5061	2.267	6.016	0.147	0.290	4.088	3.086	2.888	1.898	0.803	5.052	1.259
	0.047	0.037	0.002	0.005	0.063	0.058	0.035	0.025	0.027	0.084	0.041
NGC 5062	1.324	5.839	0.186	0.347	5.486	3.419	3.426	2.175	0.941	6.076	0.990
	0.031	0.033	0.002	0.006	0.070	0.056	0.029	0.022	0.017	0.072	0.045
ESO 576G030	1.297	3.281	0.131	0.263	3.829	2.899	2.680	1.618	0.829	3.351	-0.605
	0.043	0.048	0.003	0.006	0.071	0.063	0.036	0.022	0.027	0.076	0.077
NGC 5077	2.458	4.510	0.169	0.328	5.457	3.223	2.947	2.148	0.804	5.888	-0.356
	0.096	0.044	0.002	0.006	0.070	0.054	0.032	0.024	0.025	0.089	0.076
NGC 5087	1.558	5.478	0.179	0.337	5.069	3.347	3.279	2.119	0.858	5.510	1.016
	0.225	0.745	0.002	0.004	0.220	0.029	0.082	0.134	0.030	0.102	0.183
NGC 5102	...	2.882	0.016	0.077	...	1.778	1.249	1.077	0.624	2.204	0.320
	...	0.025	0.002	0.003	...	0.036	0.021	0.017	0.017	0.036	0.035
NGC 5111	1.548	6.370	0.163	0.317	5.399	2.575	3.137	2.169	0.922	5.478	1.414
	0.041	0.045	0.002	0.007	0.076	0.060	0.037	0.031	0.032	0.077	0.052
ESO 576G076	2.213	4.526	0.098	0.248	3.734	2.736	1.993	1.748	0.818	3.143	1.352
	0.049	0.048	0.003	0.005	0.060	0.067	0.032	0.030	0.031	0.058	0.056
NGC 5193	1.439	5.179	0.143	0.301	4.470	2.956	2.288	1.914	0.961	4.461	1.259
	0.177	0.810	0.010	0.006	0.231	0.256	0.299	0.166	0.144	0.025	0.222
NGC 5203	1.451	4.645	0.130	0.298	4.695	2.981	2.668	1.790	1.033	4.430	1.058
	0.034	0.110	0.007	0.017	0.027	0.448	0.396	0.264	0.123	0.028	0.003
NGC 5206	3.034	4.101	0.036	0.127	1.582	2.287	1.813	1.031	0.937	1.855	0.718
	0.068	0.036	0.002	0.004	0.039	0.050	0.033	0.019	0.027	0.039	0.049
IC 4296	1.509	5.778	0.180	0.354	5.327	3.271	2.953	2.185	1.006	5.591	0.941
	0.344	0.472	0.009	0.013	0.274	0.315	0.507	0.388	0.102	0.293	0.182
MCG -01-35-007	1.720	5.531	0.111	0.259	4.103	2.903	2.544	1.732	0.956	4.159	0.952
	0.041	0.040	0.003	0.006	0.064	0.065	0.035	0.024	0.032	0.085	0.051
IC 4310	1.340	5.608	0.141	0.290	4.173	2.911	2.570	1.793	0.903	4.148	0.602
	0.032	0.041	0.002	0.006	0.070	0.067	0.033	0.029	0.028	0.086	0.061
MCG -05-32-074	1.839	4.434	0.122	0.291	4.660	2.917	2.884	2.062	1.001	3.628	0.953
	0.056	0.130	0.003	0.009	0.213	0.525	0.267	0.072	0.236	0.349	0.076

Table 6—Continued

Name (1)	H β (2)	Fe5015 (3)	Mg ₁ (4)	Mg ₂ (5)	Mgb (6)	Fe5270 (7)	Fe5335 (8)	Fe5406 (9)	Fe5709 (10)	NaD (11)	[O III] (12)
ESO 509G108	1.167 0.037	5.127 0.044	0.151 0.002	0.305 0.006	4.480 0.069	2.975 0.057	1.974 0.025	1.873 0.026	0.896 0.024	5.109 0.074	1.303 0.046
ESO 445G028	...	4.807	0.141	0.293	4.585	3.055	2.583	1.685	0.717	5.035	0.565
IC 4329	...	0.198	0.015	0.053	0.055	0.243	0.163	0.345	0.112	0.101	0.267
IC 4329	1.377 0.186	5.609 1.679	0.146 0.016	0.306 0.032	5.218 0.424	3.092 0.281	2.657 0.331	2.006 0.410	...	5.183 0.191	1.027 0.204
ESO 445G049	1.737 0.033	4.243 0.040	0.124 0.002	0.273 0.006	4.485 0.076	3.112 0.065	2.121 0.030	1.427 0.019	1.068 0.023	5.170 0.090	1.062 0.040
NGC 5304	1.379 0.038	4.509 0.037	0.130 0.002	0.286 0.006	4.413 0.067	2.297 0.062	2.268 0.036	1.759 0.021	1.199 0.032	3.446 0.060	0.095 0.068
NGC 5330	...	5.382	0.146	0.303	4.470	2.578	3.029	1.808	0.932	4.113	1.351
NGC 5343	...	0.426	0.006	0.002	0.017	0.086	0.345	0.498	0.250	0.174	0.040
NGC 5343	1.389 0.043	4.713 0.035	0.120 0.002	0.247 0.005	3.171 0.067	2.636 0.063	2.351 0.035	1.717 0.025	0.995 0.024	3.019 0.069	0.718 0.051
ESO 510G009	1.019 0.057	5.584 0.497	0.166 0.010	0.336 0.002	5.272 0.107	3.140 0.701	3.301 0.375	2.103 0.104	0.844 0.188	5.880 0.130	0.812 0.180
ESO 445G075	-3.705 0.173	...	0.113 0.003	0.229 0.006	4.206 0.071	1.911 0.058	2.493 0.038	1.537 0.021	0.685 0.025	3.394 0.066	-3.712 0.181
ESO 384G013	1.503 0.030	4.742 0.035	0.059 0.003	0.183 0.005	3.183 0.051	2.467 0.057	2.731 0.040	1.486 0.027	1.260 0.032	4.030 0.070	0.627 0.053
IC 4350	1.513 0.028	5.659 0.036	0.153 0.003	0.319 0.006	4.735 0.064	3.420 0.061	2.953 0.037	1.734 0.022	1.030 0.028	5.360 0.077	0.422 0.056
ESO 384G019	1.837 0.048	5.980 0.051	...	0.215 0.006	3.793 0.069	2.449 0.067	3.125 0.041	1.842 0.031	1.250 0.029	3.801 0.091	0.988 0.062
UGC 08872	1.423 0.132	5.239 0.230	0.080 0.003	0.212 0.003	3.688 0.337	2.426 0.172	2.524 0.050	1.627 0.042	1.021 0.116	3.977 0.172	0.657 0.063
ESO 384G021	1.869 0.044	5.771 0.038	0.105 0.003	0.253 0.006	3.744 0.072	2.885 0.065	2.542 0.036	1.306 0.026	0.943 0.033	...	1.234 0.052
ESO 221G020	1.974 0.051	5.224 0.042	0.119 0.003	0.263 0.006	3.596 0.067	2.988 0.068	2.366 0.043	1.994 0.031	0.643 0.026	4.819 0.113	0.809 0.052
ESO 384G023	1.206 0.026	5.257 0.049	0.135 0.003	0.208 0.006	3.828 0.064	2.781 0.065	3.127 0.041	1.877 0.024	1.024 0.024	2.537 0.066	1.069 0.054
NGC 5397	1.435 0.036	4.949 0.049	0.139 0.034	0.273 0.006	4.700 0.063	2.982 0.058	2.329 0.029	1.732 0.021	0.980 0.042	3.608 0.094	1.244 0.050
NGC 5424	1.153 0.035	4.223 0.040	0.119 0.002	0.275 0.006	4.947 0.070	3.032 0.057	2.471 0.036	1.996 0.027	0.644 0.025	3.895 0.071	0.639 0.049
NGC 5419	1.600 0.322	5.637 0.345	0.174 0.008	0.335 0.009	5.153 0.274	3.169 0.169	2.916 0.443	1.853 0.179	1.065 0.108	5.605 0.351	1.124 0.087
ESO 510G054	1.866 0.043	6.545 0.042	0.125 0.002	0.260 0.005	3.992 0.064	2.798 0.059	2.315 0.032	1.694 0.025	0.766 0.023	3.714 0.066	1.480 0.055
IC 4374	-0.375 0.032	2.753 0.062	0.180 0.002	0.344 0.007	5.566 0.076	1.955 0.057	2.556 0.033	2.065 0.028	0.830 0.022	5.615 0.087	-1.696 0.074
ESO 510G071	1.510 0.029	5.312 0.036	0.162 0.002	0.330 0.005	4.492 0.067	2.365 0.065	2.668 0.030	2.049 0.024	0.857 0.017	4.948 0.077	1.106 0.042
NGC 5493	2.141	5.989	0.106	0.241	3.510	3.009	2.529	1.807	0.880	3.645	1.246

Table 6—Continued

Name (1)	H β (2)	Fe5015 (3)	Mg ₁ (4)	Mg ₂ (5)	Mgb (6)	Fe5270 (7)	Fe5335 (8)	Fe5406 (9)	Fe5709 (10)	NaD (11)	[O III] (12)
	0.082	0.558	0.000	0.007	0.121	0.032	0.042	0.025	0.063	0.068	0.171
NGC 5507	1.325	5.250	0.165	0.333	5.316	2.866	2.320	1.833	0.906	5.086	0.746
	0.028	0.040	0.002	0.007	0.081	0.063	0.033	0.026	0.028	0.087	0.050
NGC 5516	2.115	5.436	0.123	0.268	3.943	3.325	2.687	1.678	0.971	3.543	1.383
	0.048	0.045	0.003	0.006	0.068	0.062	0.042	0.025	0.033	0.077	0.054
ESO 221G037	...	4.999	0.091	0.211	3.467	2.758	2.202	1.566	1.052	3.395	0.912
	...	0.037	0.002	0.005	0.053	0.056	0.032	0.021	0.026	0.070	0.050
ESO 579G017	1.392	3.285	0.098	0.231	3.061	2.214	2.305	1.302	0.840	3.198	0.002
	0.027	0.053	0.003	0.005	0.070	0.053	0.037	0.023	0.025	0.061	0.055
IC 0999	1.509	4.809	0.098	0.246	4.001	2.860	2.026	1.280	1.016	3.217	0.711
	0.041	0.031	0.002	0.005	0.056	0.067	0.034	0.018	0.030	0.071	0.054
NGC 5576	1.928	5.369	0.116	0.243	3.777	2.853	2.374	1.672	...	3.151	1.189
	0.052	0.260	0.004	0.010	0.303	0.097	0.460	0.071	...	0.593	0.005
NGC 5583	1.470	4.758	0.084	0.214	3.676	2.671	1.900	1.792	1.039	2.460	0.575
	0.034	0.033	0.002	0.005	0.064	0.061	0.032	0.026	0.026	0.053	0.054
IC 4421	1.444	5.580	0.146	0.307	4.602	2.862	2.149	2.101	0.828	4.414	1.403
	0.127	0.620	0.001	0.002	0.158	0.277	0.099	0.298	0.067	0.052	0.081
NGC 5628	0.800	3.757	0.163	0.338	4.591	2.862	2.326	2.206	0.936	5.089	0.052
	0.032	0.041	0.002	0.006	0.073	0.057	0.033	0.027	0.021	0.088	0.057
UGC 09288	1.989	5.090	...	0.198	3.405	2.841	2.546	1.559	1.019	3.189	0.639
	0.319	0.962	...	0.030	0.639	0.807	0.043	0.180	0.160	0.701	0.138
NGC 5626	1.286	4.464	0.138	0.298	4.302	3.104	2.125	1.593	0.867	4.513	0.676
	0.040	0.036	0.002	0.006	0.063	0.060	0.025	0.028	0.024	0.074	0.059
NGC 5638	1.471	5.541	0.134	0.298	4.640	2.892	2.869	1.913	0.955	4.328	1.049
	0.041	0.036	0.002	0.006	0.074	0.053	0.039	0.026	0.028	0.080	0.049
ESO 447G030	1.958	5.488	0.111	0.258	3.762	3.029	2.647	1.663	0.843	3.680	1.274
	0.040	0.041	0.003	0.006	0.075	0.064	0.037	0.023	0.027	0.083	0.050
ESO 447G031	2.432	3.862	0.067	0.172	2.360	2.793	2.125	2.014	0.872	2.970	0.569
	0.049	0.034	0.002	0.005	0.055	0.062	0.038	0.030	0.027	0.070	0.050
NGC 5726	1.602	6.050	...	0.232	3.635	2.764	2.436	1.781	1.125	4.013	1.124
	0.046	0.050	...	0.005	0.058	0.067	0.032	0.029	0.035	0.094	0.059
ESO 512G019	0.934	5.104	0.142	0.300	4.750	3.231	2.855	1.799	1.204	4.262	0.529
	0.027	0.035	0.003	0.006	0.075	0.068	0.035	0.023	0.023	0.080	0.049
NGC 5761	1.210	5.569	0.144	0.297	3.997	2.722	2.925	1.708	0.746	4.290	0.845
	0.052	1.001	0.001	0.003	0.251	0.679	0.124	0.425	0.186	0.020	0.073
NGC 5770	2.709	5.577	0.091	0.228	3.359	2.880	2.355	1.522	0.973	2.522	1.001
	0.053	0.041	0.003	0.006	0.068	0.068	0.039	0.023	0.027	0.074	0.059
ESO 386G038	1.796	4.410	0.073	0.201	2.961	2.050	2.194	1.344	0.973	3.796	0.075
	0.038	0.040	0.002	0.005	0.060	0.058	0.035	0.024	0.022	0.067	0.063
NGC 5791	1.537	5.832	0.152	0.315	4.813	3.228	2.933	2.125	0.959	5.016	1.083
	0.162	0.073	0.002	0.007	0.278	0.170	0.077	0.147	0.024	0.321	0.115
NGC 5796	1.359	5.529	0.176	0.342	4.989	3.160	2.460	1.930	0.844	5.931	1.083
	0.034	0.038	0.002	0.006	0.068	0.062	0.030	0.025	0.019	0.082	0.044
NGC 5813	...	5.209	0.150	0.312	5.043	2.568	2.658	1.723	0.852	4.946	0.933
	...	0.587	0.020	0.019	0.340	0.408	0.187	0.295	0.170	0.191	0.430

Table 6—Continued

Name (1)	H β (2)	Fe5015 (3)	Mg ₁ (4)	Mg ₂ (5)	Mgb (6)	Fe5270 (7)	Fe5335 (8)	Fe5406 (9)	Fe5709 (10)	NaD (11)	[O III] (12)
NGC 5831	1.744	5.790	0.134	0.293	4.234	3.303	2.921	1.926	0.995	4.199	1.099
	0.058	0.960	0.013	0.017	0.281	0.330	0.391	0.326	0.129	0.188	0.121
NGC 5846	0.966	5.677	0.171	0.329	5.205	3.306	3.029	2.052	0.878	5.130	0.690
	0.029	0.036	0.002	0.006	0.077	0.054	0.035	0.024	0.021	0.083	0.048
NGC 5858	1.701	4.201	0.124	0.276	3.912	3.233	2.608	1.806	0.724	3.810	0.342
	0.049	0.035	0.003	0.006	0.065	0.064	0.035	0.028	0.030	0.071	0.043
NGC 5869	1.713	5.872	0.128	0.288	4.492	3.283	2.308	1.829	1.377	4.539	1.177
	0.040	0.038	0.002	0.006	0.075	0.053	0.031	0.027	0.098	0.080	0.045
ESO 387G016	1.299	5.479	0.150	0.302	4.489	3.098	2.755	2.141	1.218	3.914	0.996
	0.039	0.038	0.002	0.006	0.070	0.059	0.038	0.034	0.026	0.079	0.055
NGC 5898	1.458	5.059	0.156	0.322	4.653	3.603	2.657	1.929	0.942	4.915	0.665
	0.289	0.565	0.018	0.021	0.249	0.283	0.469	0.307	0.202	0.158	0.267
NGC 5903	1.403	5.087	0.142	0.299	4.496	3.089	2.639	2.028	0.934	4.450	0.591
	0.117	0.499	0.005	0.005	0.166	0.223	0.188	0.210	0.189	0.365	0.095
NGC 5928	1.793	5.039	0.130	0.272	3.970	3.369	2.581	1.708	1.155	4.235	1.174
	0.037	0.044	0.003	0.006	0.063	0.066	0.035	0.021	0.030	0.069	0.050
NGC 6017	1.846	4.681	0.087	0.214	3.433	2.575	2.340	1.520	0.882	3.161	0.292
	0.152	0.870	0.009	0.008	0.205	0.267	0.233	0.223	0.173	0.230	0.245
NGC 6172	2.287	4.649	0.076	0.200	2.942	2.240	2.112	1.688	0.879	3.904	0.672
	0.030	0.792	0.014	0.002	0.396	0.108	0.030	0.100	0.034	0.080	0.045
ESO 137G024	1.846	5.218	0.156	0.309	5.353	2.937	2.207	2.199	0.806	5.103	1.275
	0.046	0.048	0.002	0.006	0.071	0.059	0.028	0.029	0.027	0.068	0.042
ESO 137G036	1.873	4.932	0.127	0.279	3.913	3.197	2.169	1.837	0.818	3.438	0.787
	0.068	0.038	0.003	0.006	0.072	0.069	0.031	0.024	0.029	0.071	0.051
ESO 137G044	1.344	4.702	0.169	0.345	6.044	3.705	3.860	2.604	1.063	6.167	0.635
	0.029	0.034	0.002	0.006	0.073	0.054	0.029	0.023	0.025	0.064	0.037
NGC 6364	1.583	5.461	0.116	0.263	...	2.755	2.351	1.679	0.690	5.013	1.372
	0.031	0.041	0.003	0.008	...	0.060	0.027	0.024	0.032	0.081	0.042
UGC 10864	...	4.051	0.050	0.140	2.064	2.119	1.764	1.044	0.771	3.773	0.595
	...	0.036	0.002	0.004	0.044	0.052	0.030	0.021	0.019	0.096	0.045
NGC 6375	1.236	4.668	0.145	0.299	4.480	3.066	2.061	1.750	0.897	4.563	0.657
	0.033	0.037	0.002	0.006	0.075	0.060	0.032	0.027	0.037	0.078	0.053
ESO 139G005	1.583	6.343	0.099	0.246	4.659	2.679	2.506	1.603	0.809	3.414	0.374
	0.036	0.041	0.003	0.006	0.067	0.060	0.032	0.027	0.029	0.064	0.064
NGC 6442	1.458	5.683	0.147	0.300	4.729	2.999	2.800	1.652	0.884	4.686	1.009
	0.039	0.039	0.003	0.006	0.067	0.057	0.035	0.022	0.020	0.073	0.059
NGC 6495	1.241	5.722	0.169	0.337	4.840	3.213	2.608	1.744	0.921	5.255	1.423
	0.038	0.045	0.002	0.006	0.077	0.061	0.036	0.023	0.023	0.089	0.052
UGC 11082	1.329	4.404	0.138	0.291	4.385	2.708	2.630	1.579	1.038	4.159	0.395
	0.024	0.033	0.003	0.006	0.070	0.055	0.035	0.025	0.029	0.073	0.043
NGC 6548	1.654	5.586	0.141	0.292	4.121	3.203	2.825	1.903	0.864	4.263	1.193
	0.036	0.042	0.003	0.006	0.072	0.065	0.040	0.025	0.025	0.079	0.048
NGC 6577	1.553	6.419	0.146	0.291	4.573	2.832	3.389	2.028	1.093	4.437	0.920
	0.040	0.038	0.002	0.005	0.062	0.051	0.030	0.023	0.022	0.068	0.057
NGC 6587	1.220	5.294	0.158	0.332	5.066	2.733	2.156	1.742	0.972	4.449	1.164

Table 6—Continued

Name (1)	H β (2)	Fe5015 (3)	Mg ₁ (4)	Mg ₂ (5)	Mgb (6)	Fe5270 (7)	Fe5335 (8)	Fe5406 (9)	Fe5709 (10)	NaD (11)	[O III] (12)
	0.033	0.033	0.002	0.005	0.067	0.051	0.025	0.021	0.016	0.061	0.037
ESO 182G007	...	5.231	...	0.165	2.954	2.790	2.322	1.601	0.878	3.588	1.094
	...	0.048	...	0.005	0.060	0.058	0.030	0.024	0.034	0.109	0.054
NGC 6614	...	4.207	0.149	0.305	4.942	3.073	3.097	1.788	0.917	5.334	-0.910
	...	0.051	0.003	0.006	0.068	0.061	0.036	0.022	0.026	0.098	0.074
IC 4704	1.590	5.351	0.181	0.339	4.893	3.380	2.609	1.960	1.068	4.995	1.154
	0.015	0.142	0.001	0.003	0.147	0.113	0.189	0.109	0.111	0.132	0.049
IC 4731	1.700	5.397	0.123	0.297	4.185	2.990	2.422	1.987	1.250	4.814	1.266
	0.036	0.046	0.002	0.006	0.065	0.063	0.030	0.028	0.032	0.085	0.052
NGC 6673	1.664	5.884	0.155	0.308	4.256	3.161	2.823	1.886	0.951	3.908	1.208
	0.048	0.016	0.002	0.002	0.024	0.064	0.026	0.028	0.031	0.043	0.053
ESO 141G003	1.770	5.092	0.155	0.318	4.825	3.205	2.873	1.682	0.625	4.771	1.294
	0.032	0.041	0.002	0.006	0.069	0.060	0.028	0.022	0.017	0.079	0.037
NGC 6684	1.924	6.868	0.137	0.228	3.790	3.307	2.342	2.124	...	3.083	2.029
	0.044	0.054	0.003	0.007	0.081	0.070	0.045	0.030	...	0.079	0.053
NGC 6706	1.783	4.999	0.100	0.249	3.447	2.891	2.713	1.784	1.177	3.522	1.147
	0.041	0.044	0.003	0.005	0.050	0.055	0.034	0.031	0.025	0.052	0.043
IC 4796	2.095	5.796	0.108	0.258	3.471	2.973	2.624	1.678	0.862	3.557	1.157
	0.053	0.040	0.003	0.006	0.065	0.067	0.041	0.026	0.025	0.073	0.053
NGC 6721	1.416	5.603	0.156	0.327	5.057	2.945	2.684	2.046	1.020	5.276	1.033
	0.262	0.586	0.008	0.013	0.338	0.189	0.437	0.289	0.119	0.233	0.155
NGC 6725	1.851	5.301	0.117	0.265	4.057	2.920	2.145	1.525	0.776	3.370	0.944
	0.050	0.042	0.002	0.006	0.070	0.064	0.038	0.021	0.025	0.073	0.052
ESO 231G017	2.746	5.712	...	0.205	3.414	3.143	2.674	1.834	0.726	4.245	1.179
	0.054	0.051	...	0.005	0.063	0.065	0.033	0.025	0.030	0.108	0.059
ESO 282G010	1.601	4.769	0.144	0.304	4.845	3.198	2.617	1.891	0.462	4.827	0.186
	0.026	0.036	0.002	0.006	0.064	0.056	0.034	0.025	0.024	0.092	0.050
ESO 282G024	1.127	6.604	0.164	0.323	5.002	3.240	2.887	1.885	0.725	4.823	1.119
	0.032	0.040	0.002	0.006	0.072	0.058	0.026	0.019	0.020	0.072	0.049
ESO 282G028	1.057	4.477	0.108	0.236	3.566	3.023	2.764	1.850	1.077	3.878	0.063
	0.028	0.032	0.003	0.005	0.064	0.052	0.036	0.022	0.028	0.077	0.053
ESO 283G020	1.448	5.746	0.107	0.260	3.806	2.756	2.453	1.815	0.609	3.235	0.830
	0.030	0.038	0.002	0.006	0.063	0.054	0.034	0.027	0.023	0.072	0.052
ESO 142G049	1.034	4.447	0.147	0.313	4.884	2.975	3.202	1.647	0.907	4.878	0.903
	0.047	0.038	0.003	0.007	0.074	0.060	0.032	0.024	0.024	0.079	0.043
IC 4913	2.173	4.617	...	0.229	3.705	2.773	2.358	1.459	1.017	3.366	0.910
	0.038	0.054	...	0.006	0.070	0.062	0.035	0.025	0.031	0.102	0.050
NGC 6841	1.411	5.823	0.161	0.331	5.038	3.064	2.879	1.808	0.641	5.358	1.260
	0.235	0.838	0.015	0.007	0.366	0.387	0.206	0.241	0.139	0.295	0.182
IC 4931	1.598	5.565	0.155	0.326	5.170	2.858	3.119	1.677	0.958	5.040	1.141
	0.070	0.414	0.003	0.007	0.387	0.188	0.257	0.311	0.085	0.104	0.178
NGC 6850	1.600	4.649	0.113	0.243	3.408	2.930	2.621	1.813	0.842	...	0.313
	0.036	0.038	0.003	0.005	0.059	0.056	0.040	0.024	0.027	...	0.051
NGC 6851	1.801	6.356	0.148	0.301	4.499	3.395	2.783	1.899	1.072	4.591	1.338
	0.049	0.043	0.003	0.006	0.063	0.060	0.035	0.024	0.022	0.069	0.049

Table 6—Continued

Name (1)	H β (2)	Fe5015 (3)	Mg ₁ (4)	Mg ₂ (5)	Mgb (6)	Fe5270 (7)	Fe5335 (8)	Fe5406 (9)	Fe5709 (10)	NaD (11)	[O III] (12)
IC 4943	2.057	5.297	0.126	0.277	4.015	2.783	2.407	1.851	0.891	3.584	1.522
	0.192	0.402	0.013	0.003	0.051	0.112	0.093	0.055	0.014	0.113	0.635
NGC 6849	1.410	4.382	0.149	0.290	4.553	2.687	3.269	1.787	...	4.527	0.801
	0.029	0.033	0.002	0.006	0.073	0.067	0.038	0.022	...	0.066	0.042
NGC 6861	1.263	6.552	0.210	0.383	6.328	3.630	3.592	2.491	0.892	7.136	0.937
	0.159	0.186	0.011	0.014	0.254	0.305	0.454	0.310	0.099	0.152	0.084
NGC 6868	0.989	5.269	0.179	0.346	5.251	3.173	2.839	1.944	0.945	5.505	0.312
	0.177	0.390	0.013	0.013	0.272	0.168	0.228	0.245	0.153	0.227	0.127
IC 1317	2.499	...	0.061	0.199	2.943	2.617	2.269	1.406	1.364	2.836	0.863
	0.294	...	0.013	0.007	0.077	0.070	0.123	0.213	0.277	0.220	0.176
NGC 6903	1.436	5.534	0.182	0.338	4.549	2.918	2.499	1.543	...	4.968	1.228
	0.084	0.449	0.009	0.021	0.219	0.220	0.181	0.292	...	0.153	0.119
NGC 6909	2.174	5.208	0.085	0.223	3.616	2.948	2.319	1.703	0.881	2.638	0.964
	0.195	0.158	0.001	0.000	0.324	0.295	0.157	0.166	0.126	0.179	0.092
NGC 6924	1.380	5.429	0.165	0.321	4.732	3.062	...	1.334	0.766	4.104	1.297
	0.044	0.043	0.003	0.007	0.066	0.054	...	0.024	0.033	0.081	0.051
ESO 341G013	1.642	5.456	0.117	0.265	3.889	2.686	2.272	1.649	0.900	4.019	0.851
	0.041	0.041	0.002	0.006	0.064	0.067	0.038	0.027	0.022	0.073	0.051
NGC 6958	1.577	4.319	0.132	0.277	4.057	2.878	2.437	1.718	0.973	3.601	-0.192
	0.191	0.485	0.016	0.021	0.241	0.311	0.137	0.111	0.085	0.211	0.149
ESO 107G004	2.159	6.172	0.118	0.262	3.847	3.106	2.847	2.102	0.966	4.245	1.190
	0.048	0.040	0.003	0.006	0.065	0.063	0.038	0.026	0.026	0.079	0.054
ESO 235G049	1.195	4.309	0.149	0.321	5.422	3.347	3.104	2.162	1.143	4.890	0.387
	0.040	0.036	0.003	0.007	0.081	0.065	0.037	0.025	0.029	0.073	0.044
ESO 235G051	1.851	5.677	0.072	0.196	2.711	3.289	2.516	1.966	...	2.515	1.096
	0.393	0.444	0.013	0.023	0.297	0.082	0.474	0.132	...	0.004	0.090
ESO 286G049	1.059	4.987	0.160	0.324	5.306	3.632	3.185	1.759	0.949	5.274	0.425
	0.037	0.043	0.003	0.006	0.070	0.067	0.039	0.024	0.023	0.084	0.063
ESO 286G050	2.707	4.313	0.052	0.157	2.327	2.115	1.668	1.489	0.750	1.782	-0.094
	0.327	0.443	0.003	0.000	0.020	0.002	0.159	0.074	0.031	0.076	0.334
NGC 7014	1.147	5.261	0.183	0.356	5.345	3.248	2.905	2.076	0.914	6.267	1.159
	0.059	0.190	0.001	0.003	0.053	0.056	0.089	0.108	0.083	0.044	0.083
NGC 7029	...	5.360	0.141	0.285	4.205	3.074	2.228	1.826	...	3.580	0.981
	...	0.185	0.004	0.001	0.192	0.148	0.300	0.157	...	0.220	0.059
NGC 7049	1.124	5.207	0.171	0.339	5.210	3.560	3.355	1.916	0.993	5.697	0.841
	0.225	0.717	0.008	0.008	0.237	0.184	0.399	0.139	0.176	0.111	0.278
NGC 7075	1.470	4.470	0.173	0.343	5.422	...	2.542	1.533	1.158	4.777	1.101
	0.038	0.045	0.002	0.006	0.076	...	0.030	0.025	0.021	0.066	0.058
NGC 7079	1.819	4.630	0.098	0.246	3.978	2.949	2.557	1.736	0.876	3.240	0.509
	0.039	0.035	0.002	0.005	0.061	0.058	0.033	0.023	0.024	0.059	0.051
NGC 7097	0.379	4.306	0.159	0.308	4.966	3.116	2.565	1.781	0.882	4.944	-0.464
	0.012	0.033	0.007	0.004	0.001	0.131	0.423	0.061	0.026	0.052	0.241
NGC 7144	1.589	5.730	0.154	0.297	4.506	2.900	2.685	1.966	0.878	4.124	1.129
	0.024	0.086	0.002	0.001	0.050	0.061	0.061	0.015	0.019	0.063	0.018
NGC 7145	1.777	5.236	0.125	0.261	3.820	2.988	2.635	1.774	0.860	3.391	0.908

Table 6—Continued

Name (1)	H β (2)	Fe5015 (3)	Mg ₁ (4)	Mg ₂ (5)	Mgb (6)	Fe5270 (7)	Fe5335 (8)	Fe5406 (9)	Fe5709 (10)	NaD (11)	[O III] (12)
	0.025	0.025	0.002	0.001	0.010	0.154	0.042	0.013	0.020	0.113	0.293
ESO 466G026	1.405	4.433	0.119	0.274	4.424	2.457	2.628	1.844	1.151	4.204	0.748
	0.035	0.037	0.003	0.006	0.069	0.057	0.035	0.024	0.021	0.069	0.043
NGC 7173	1.470	5.503	0.167	0.329	4.824	2.850	2.542	1.800	0.922	4.543	1.093
	0.107	0.139	0.009	0.011	0.121	0.203	0.176	0.046	0.043	0.173	0.059
NGC 7176	1.300	5.583	0.187	0.352	5.101	3.099	2.763	1.920	0.933	5.016	1.037
	0.051	0.109	0.006	0.006	0.147	0.134	0.123	0.055	0.062	0.293	0.007
NGC 7185	1.865	5.080	0.091	0.220	3.589	2.530	2.281	1.527	0.931	2.436	0.838
	0.124	0.346	0.011	0.009	0.052	0.141	0.278	0.261	0.136	0.186	0.142
IC 5157	1.637	4.873	0.154	0.310	4.732	2.983	2.550	1.798	0.909	4.992	1.068
	0.032	0.042	0.002	0.006	0.074	0.063	0.030	0.021	0.022	0.080	0.040
NGC 7196	1.444	5.893	0.179	0.342	5.257	3.102	2.949	2.208	0.968	5.053	0.986
	0.188	0.031	0.008	0.006	0.333	0.181	0.205	0.163	0.092	0.275	0.033
NGC 7192	1.530	5.487	0.140	0.294	4.442	3.212	2.812	1.955	0.997	4.251	0.810
	0.038	0.013	0.001	0.001	0.083	0.145	0.033	0.115	0.041	0.173	0.031
ESO 467G037	1.802	4.971	0.133	0.288	4.934	2.933	3.172	1.614	0.901	4.492	0.918
	0.035	0.038	0.002	0.005	0.062	0.057	0.029	0.019	0.025	0.069	0.039
MCG -01-57-004	0.536	3.541	...	0.212	3.611	3.066	2.561	1.327	0.976	3.576	0.701
	0.023	0.049	...	0.005	0.061	0.067	0.034	0.023	0.034	0.094	0.049
ESO 533G025	1.557	5.600	0.126	0.281	4.292	3.250	2.537	1.950	1.192	4.051	0.871
	0.040	0.037	0.003	0.006	0.076	0.061	0.042	0.026	0.034	0.078	0.053
IC 1445	1.755	6.253	0.123	0.276	3.652	3.123	2.634	1.311	0.799	3.251	1.556
	0.049	0.046	0.003	0.005	0.062	0.066	0.036	0.021	0.027	0.073	0.048
NGC 7280	2.143	5.545	0.099	0.232	3.543	2.894	2.475	1.586	1.080	3.849	0.725
	0.123	0.418	0.004	0.001	0.274	0.305	0.572	0.173	0.046	0.231	0.236
NGC 7302	1.883	5.137	0.113	0.256	4.078	3.041	2.695	1.813	1.071	3.720	1.012
	0.004	0.065	0.013	0.010	0.111	0.035	0.255	0.245	0.007	0.269	0.143
NGC 7351	2.828	3.754	0.066	0.156	2.666	2.299	2.587	1.272	0.738	2.329	0.118
	0.047	0.042	0.003	0.005	0.049	0.052	0.038	0.017	0.024	0.041	0.050
NGC 7359	2.382	5.159	0.084	0.221	3.332	3.068	2.511	1.644	0.969	3.483	0.646
	0.566	0.668	0.008	0.008	0.215	0.207	0.037	0.044	0.072	0.000	0.102
NGC 7365	2.210	5.138	0.084	0.208	3.106	2.758	2.494	1.753	0.860	2.638	1.087
	0.048	0.041	0.003	0.005	0.064	0.063	0.034	0.027	0.030	0.064	0.049
NGC 7391	1.366	5.397	0.184	0.348	4.877	2.871	2.418	1.922	0.968	5.110	0.933
	0.033	0.038	0.002	0.006	0.065	0.065	0.031	0.023	0.018	0.079	0.043
NGC 7404	1.859	5.274	0.065	0.185	3.005	2.696	2.442	1.656	1.077	1.817	1.297
	0.067	0.046	0.003	0.005	0.066	0.065	0.035	0.025	0.025	0.053	0.055
IC 5267B	1.965	4.823	0.079	0.171	2.320	2.783	1.889	1.466	0.763	2.042	1.306
	0.050	0.049	0.002	0.004	0.054	0.062	0.036	0.021	0.030	0.030	0.042
IC 1459	0.720	5.375	0.200	0.367	5.587	3.487	3.262	2.141	1.002	6.255	0.107
	0.088	0.197	0.002	0.004	0.213	0.100	0.052	0.015	0.092	0.251	0.133
NGC 7454	1.936	5.243	0.079	0.212	3.502	2.880	2.518	1.667	1.080	2.751	1.034
	0.054	0.033	0.002	0.005	0.067	0.057	0.033	0.026	0.087	0.057	0.052
NGC 7458	1.345	5.380	0.134	0.300	3.951	2.833	2.907	2.048	0.924	4.956	1.362
	0.040	0.048	0.003	0.006	0.066	0.064	0.043	0.028	0.025	0.075	0.044

Table 6—Continued

Name (1)	H β (2)	Fe5015 (3)	Mg ₁ (4)	Mg ₂ (5)	Mgb (6)	Fe5270 (7)	Fe5335 (8)	Fe5406 (9)	Fe5709 (10)	NaD (11)	[O III] (12)
NGC 7507	1.554 0.146	6.135 0.310	0.173 0.010	0.339 0.011	5.073 0.092	3.332 0.155	3.038 0.159	2.080 0.123	0.979 0.088	5.576 0.162	1.296 0.097
NGC 7562	1.545 0.034	6.069 0.044	0.162 0.002	0.325 0.006	4.773 0.069	3.165 0.057	2.748 0.030	1.675 0.021	0.880 0.021	4.744 0.071	1.336 0.047
NGC 7576	2.267 0.050	5.231 0.042	0.089 0.003	0.217 0.005	2.999 0.061	2.991 0.060	2.557 0.036	1.833 0.031	1.281 0.033	3.310 0.076	0.902 0.053
NGC 7600	2.311 0.041	5.126 1.422	0.088 0.002	0.229 0.010	3.372 0.046	2.476 0.712	2.333 0.198	1.416 0.136	1.022 0.137	3.257 0.063	0.985 0.275
UGC 12515	1.410 0.051	4.049 0.034	0.127 0.003	0.280 0.006	4.441 0.081	3.299 0.056	3.061 0.034	2.019 0.027	1.014 0.030	5.015 0.077	0.555 0.046
NGC 7619	1.435 0.037	5.426 0.044	0.163 0.034	0.301 0.006	5.181 0.070	3.349 0.055	2.990 0.028	1.847 0.018	1.221 0.023	5.463 0.092	1.127 0.049
NGC 7626	1.429 0.070	5.778 0.579	0.172 0.008	0.330 0.022	4.999 0.248	2.921 0.399	2.222 0.480	1.800 0.000	0.865 0.156	5.282 0.034	1.092 0.298
IC 1492	1.512 0.041	4.787 0.038	0.146 0.002	0.313 0.006	4.379 0.069	3.006 0.058	3.035 0.035	1.948 0.027	1.041 0.027	4.475 0.075	1.148 0.040
IC 5328	1.582 0.141	5.360 0.827	0.153 0.008	0.313 0.005	4.370 0.083	3.247 0.208	2.933 0.380	1.812 0.089	0.915 0.117	4.328 0.124	0.994 0.251
NGC 7778	1.632 0.046	5.173 0.039	0.158 0.002	0.313 0.006	4.561 0.073	3.156 0.061	2.319 0.031	1.878 0.024	0.914 0.033	4.968 0.080	1.120 0.048
UGC 12840	1.980 0.036	4.847 0.048	0.094 0.003	0.248 0.006	3.838 0.068	2.292 0.061	2.276 0.035	2.098 0.032	0.936 0.041	3.519 0.073	0.740 0.057
NGC 7785	1.514 0.057	4.487 1.008	0.151 0.018	0.319 0.025	4.969 0.554	2.925 0.249	2.728 0.422	1.943 0.057	0.944 0.024	4.832 0.447	0.939 0.216
NGC 7796	1.400 0.020	5.429 0.411	0.177 0.006	0.350 0.000	5.063 0.036	3.123 0.017	2.548 0.149	1.716 0.003	0.939 0.062	5.466 0.127	0.922 0.029
NGC 7805	1.994 0.055	5.258 0.040	0.104 0.003	0.280 0.006	4.294 0.070	3.698 0.073	2.547 0.044	1.799 0.028	0.895 0.031	4.366 0.081	1.014 0.050

Note. — The index [O III] in column (12) refers to the line of [O III] λ 5007.

Table 7. Fractional error statistics based on multiple observations ($N > 2$).

Index (1)	Average (2)	Median (3)	Lower quartile (4)	Upper quartile (5)
H β	0.103±0.071	0.085	0.044	0.151
Fe5015	0.085±0.059	0.074	0.037	0.123
Mg ₁	0.062±0.051	0.048	0.023	0.093
Mg ₂	0.036±0.034	0.025	0.010	0.055
Mg b	0.046±0.031	0.045	0.020	0.063
Fe5270	0.071±0.053	0.053	0.038	0.096
Fe5335	0.081±0.054	0.071	0.042	0.117
Fe5406	0.087±0.055	0.076	0.052	0.115
Fe5709	0.112±0.071	0.103	0.048	0.162
NaD	0.045±0.035	0.037	0.022	0.058

Note. — The values quoted in the table refer to the distribution of final fractional errors distribution. This is done combining several measurements for the same galaxy on different occasions or with distinct setups.

Table 8. Comparison between our galaxies indices measurements and the literature.

Index (1)	N_{gal} (2)	$\langle \delta I \rangle$ (3)	t (4)
Trager et al. (1998)			
H β	83	-0.030±0.331	0.42
Fe5015	85	0.031±0.728	0.24
Mg ₁	89	-0.000±0.016	0.06
Mg ₂	89	0.000±0.021	0.06
Mgb	88	-0.001±0.426	0.01
Fe5270	90	-0.020±0.389	0.33
Fe5335	90	0.060±0.415	1.01
Fe5406	83	-0.001±0.377	0.03
Fe5709	78	0.021±0.259	0.63
NaD	90	0.248±0.434	1.55
Trager et al. (2000a)			
H β	22	0.088±0.154	0.94
Mgb	24	-0.204±0.239	1.20
Fe5270	24	-0.158±0.180	3.15
Fe5335	24	-0.028±0.237	0.43
Denicoló et al. (2005)			
H β	31	0.028±0.282	0.16
Fe5015	30	0.036±0.709	0.19
Mg ₁	30	-0.008±0.017	0.99
Mg ₂	30	-0.003±0.018	0.29
Mgb	33	-0.314±0.601	1.59
Fe5270	32	0.113±0.268	1.44
Fe5335	33	0.241±0.479	2.22
Fe5406	32	-0.130±0.254	2.16
Fe5709	31	-0.124±0.250	2.58
NaD	30	-0.012±0.362	0.04
Sánchez-Blázquez et al. (2006)			
H β	20	0.131±0.228	1.44
Fe5015	22	-0.406±0.536	2.59
Mgb	22	-0.411±0.329	1.78
Fe5270	22	-0.108±0.231	1.44
Fe5335	22	-0.043±0.281	0.49
Wegner et al. (2003)			
Mg ₂	418	-0.001±0.024	0.42

Table 9. Mean values of mass indicators.

Sample	N_{gal}	$\langle \log \sigma_0 \rangle$ (km s $^{-1}$)	Skewness	Kurtosis	$\langle \log M_e \rangle$ (M $_{\odot}$)	Skewness	Kurtosis
(1)	(2)	(3)	(4)	(5)	(6)	(7)	(8)
E Total	226	2.30±0.15	-0.38	1.92	10.79±0.52	-0.32	0.86
S0 Total	230	2.21±0.18	-0.43	1.02	10.51±0.59	-0.06	0.01
E LD	49	2.28±0.13	-0.38	3.24	10.73±0.49	-0.45	1.97
E MD	116	2.32±0.12	-0.12	-0.07	10.85±0.43	0.14	-0.11
E HD	61	2.27±0.20	-0.87	0.20	10.72±0.67	-0.77	-0.45
S0 LD	71	2.22±0.15	-0.09	1.12	10.52±0.52	-0.02	-0.55
S0 MD	98	2.21±0.18	-0.72	1.80	10.53±0.58	-0.19	0.53
S0 HD	61	2.18±0.20	-0.44	-0.35	10.46±0.69	-0.06	-0.52

Table 10. Probabilities of Kolmogorov-Smirnov test between distributions of mass indicators.

Sample	$\log \sigma_0$ (%)	$\log M_e$ (%)
S0 - E	0	0
E: LD - HD	8	9
S0: LD - HD	9	40

Table 11. Coefficients of the $I' - \log \sigma_0$ linear fits for different morphological types.

Index	A	B	N_{gal}	r_s	t
Elliptical galaxies					
H β	0.146±0.014	-0.038±0.006	231	-0.36	-5.82
Fe5015	0.040±0.010	0.017±0.004	234	0.23	3.68
Mg ₁	-0.146±0.021	0.124±0.009	231	0.65	12.92
Mg ₂	-0.175±0.026	0.202±0.011	237	0.72	16.11
Mgb	-0.131±0.016	0.126±0.007	238	0.74	17.11
Fe5270	0.028±0.007	0.025±0.003	237	0.42	7.11
Fe5335	0.003±0.008	0.031±0.004	236	0.44	7.42
Fe5406	0.022±0.008	0.023±0.004	235	0.32	5.21
Fe5709	0.044±0.007	-0.000±0.003	230	0.00	0.03
NaD	-0.276±0.023	0.188±0.010	238	0.76	17.98
Lenticular galaxies					
H β	0.177±0.013	-0.051±0.006	238	-0.51	-9.04
Fe5015	0.049±0.009	0.012±0.004	246	0.13	2.03
Mg ₁	-0.175±0.018	0.135±0.008	230	0.71	15.25
Mg ₂	-0.171±0.028	0.197±0.013	247	0.68	14.49
Mgb	-0.102±0.015	0.111±0.007	245	0.69	14.80
Fe5270	0.047±0.007	0.016±0.003	248	0.23	3.76
Fe5335	0.020±0.008	0.024±0.004	247	0.27	4.41
Fe5406	0.025±0.009	0.021±0.004	246	0.21	3.34
Fe5709	0.048±0.006	-0.001±0.003	239	-0.08	-1.30
NaD	-0.177±0.017	0.144±0.008	247	0.72	16.09

Table 12. Results from the $I' - \log \sigma_0$ linear fits for different environments.

Index	A	B	N_{gal}	r_s	t
Low Density					
H β	0.212±0.023	-0.067±0.010	123	-0.45	-5.53
Fe5015	0.033±0.016	0.018±0.007	124	0.17	1.87
Mg ₁	-0.167±0.033	0.130±0.014	117	0.61	8.23
Mg ₂	-0.200±0.046	0.208±0.020	125	0.63	9.05
Mgb	-0.148±0.024	0.131±0.010	124	0.72	11.31
Fe5270	0.036±0.013	0.021±0.006	125	0.23	2.62
Fe5335	0.017±0.014	0.024±0.006	123	0.30	3.51
Fe5406	0.016±0.014	0.025±0.006	124	0.26	2.92
Fe5709	0.042±0.010	0.001±0.004	118	0.01	0.08
NaD	-0.168±0.031	0.139±0.014	126	0.64	9.32
Medium Density					
H β	0.163±0.014	-0.045±0.006	226	-0.43	-7.13
Fe5015	0.037±0.010	0.018±0.004	232	0.24	3.83
Mg ₁	-0.185±0.019	0.141±0.008	226	0.72	15.73
Mg ₂	-0.211±0.028	0.217±0.012	235	0.76	17.90
Mgb	-0.139±0.015	0.128±0.007	235	0.77	18.38
Fe5270	0.031±0.007	0.023±0.003	235	0.38	6.31
Fe5335	0.001±0.008	0.032±0.004	235	0.39	6.53
Fe5406	0.015±0.009	0.026±0.004	233	0.30	4.73
Fe5709	0.044±0.007	0.000±0.003	230	-0.03	-0.46
NaD	-0.251±0.021	0.177±0.009	234	0.76	17.61
High Density					
H β	0.156±0.013	-0.042±0.006	120	-0.56	-7.43
Fe5015	0.053±0.010	0.011±0.004	124	0.21	2.43
Mg ₁	-0.159±0.020	0.131±0.009	118	0.78	13.59
Mg ₂	-0.153±0.029	0.194±0.013	124	0.79	14.31
Mgb	-0.095±0.018	0.112±0.008	124	0.77	13.23
Fe5270	0.049±0.008	0.015±0.004	125	0.37	4.49
Fe5335	0.029±0.009	0.020±0.004	125	0.33	3.84
Fe5406	0.034±0.009	0.018±0.004	124	0.33	3.91
Fe5709	0.054±0.008	-0.004±0.004	121	-0.17	-1.88
NaD	-0.202±0.022	0.157±0.010	125	0.83	16.34

Table 13. Correlation test for the $I' - \log \sigma_0$ residuals versus H β' for different morphologies.

Index	S0		E	
	r_s	t	r_s	t
Fe5015	0.166	2.566	0.322	5.105
Mg ₁	-0.252	-3.843	-0.241	-3.723
Mg ₂	-0.258	-4.089	-0.183	-2.812
Mgb	-0.258	-4.082	-0.285	-4.505
Fe5270	-0.019	-0.296	0.157	2.395
Fe5335	-0.070	-1.068	0.087	1.321
Fe5406	0.044	0.672	-0.006	-0.089
Fe5709	-0.007	-0.107	0.099	1.487
NaD	-0.137	-2.117	-0.189	-2.915

Table 14. Correlation test for the $I' - \log \sigma_0$ residuals versus $H\beta'$ for different environments.

Index	LD		MD		HD	
	r_s	t	r_s	t	r_s	t
Fe5015	0.311	3.571	0.230	3.507	0.144	1.575
Mg ₁	-0.251	-2.744	-0.274	-4.185	-0.242	-2.631
Mg ₂	-0.175	-1.951	-0.307	-4.818	-0.135	-1.469
Mgb	-0.323	-3.725	-0.301	-4.723	-0.115	-1.263
Fe5270	0.044	0.480	0.051	0.756	0.118	1.288
Fe5335	0.098	1.073	-0.081	-1.209	0.026	0.282
Fe5406	0.015	0.163	0.022	0.327	0.032	0.343
Fe5709	0.070	0.744	-0.007	-0.098	0.145	1.566
NaD	-0.045	-0.495	-0.238	-3.649	-0.044	-0.476